2-57000/5R-3239

F-8 OBLIQUE WING STRUCTURAL FEASIBILITY STUDY

By E. Koltko, A. Katz, M. A. Geli, W. D. Smith
R. Lauridia, C. T. Overstreet, C. Klapprott
T. F. Orr, C. L. Jobe, F. G. Wyatt

November 1975

Prepared under Contract NAS4-2266 by

VOUGHT SYSTEMS DIVISION
LTV AEROSPACE CORPORATION
Dallas, Texas

for

FLIGHT RESEARCH CENTER
NATIONAL AERONAUTICS AND SPACE ADMINISTRATION

ABSTRACT

The structural feasibility of fitting an F-8 aircraft with a rotating oblique wing is studied and confirmed. Requirements for a follow-on program are established and scheduled. The requirements include the study and analysis of the flying qualities of the modified aircraft, the design and fabrication of prototype hardware, and the modification of the two-place NTF-8A aircraft to the oblique wing configuration.

TABLE OF CONTENTS

TABLE OF CONTENTS (CONTINUED)

TABLE OF CONTENTS (CONTINUED)

TABLE OF CONTENTS (CONTINUED)

TABLE OF CONTENTS (CONCLUDED)

LIST OF FIGURES

LIST OF FIGURES (CONTINUED)

LIST OF FIGURES (CONTINUED)

LIST OF FIGURES (CONTINUED)

LIST OF TABLES

LIST OF TABLES (CONTINUED)

F-8 OBLIQUE WING STRUCTURAL FEASIBILITY STUDY

By E. Koltko, A. Katz, M. A. Bell, W. D. Smith,
R. Lauridia, C. T. Overstreet, C. Klapprott,
T. F. Orr, C. L. Jobe, F. G. Wyatt

1.0 SUMMARY

This report is submitted as part of the requirements of NASA contract NAS4-2266. It describes a study of the structural and systems feasibility of fitting an F-8 airplane with a rotating oblique wing. It also sets forth a follow-on program to design and fabricate the hardware and perform the modification on the two place F-8 (NTF-8A) aircraft.

The study confirms the structural feasibility of the project, develops a design concept and shows it to be safe from the point of view of static load and of aeroelastic stability. A proposed follow-on program is presented in three phases as follows:

Phase I - Engineering Validation

Phase II - Engineering Design

Phase III - Tooling, Fabrication and Modification of F-8

A proposed schedule for the three phases is presented to provide the anticipated time span for each phase and for the total program to installed hardware. A final phase to encompass ground and flight tests will be required to demonstrate the oblique wing concept on the flying aircraft. This final phase, however, was not defined as part of the study program.

2.0 INTRODUCTION

The concept of an oblique wing airplane shows promise for efficient transonic and supersonic operations. An important step in proving this concept is to produce a full scale manned prototype aircraft capable of operating in the transonic and supersonic speed range. The purpose of this study is to verify the structural feasibility of producing such a prototype by fitting a rotating oblique wing on an F-8 aircraft.

The F-8 is well suited for the prototype modification program because of its high wing configuration and three point wing attach arrangement. The wing is easily removed from its cavity, in which the new wing and pivot mechanism can be located.

The study is a demonstration of structural and systems feasibility. The proposed prototype is analyzed for a strength, aeroelastic stability and limited fatigue life. Clearance and arrangement of control systems are also considered. Stability and control, control surface geometry and deflection, control laws, control augmentation, and aeroelastic problems related to control surfaces were not studied. All of these subjects have to be addressed before the prototype can be designed. The tasks involved are defined and spelled out as Phase I (Engineering Validation) of the follow-on program presented in Section 5.2.

The loads analysis of this study is restricted to a single design point. The point called for by the contract is Mach 0.98 at 6.1×10^3m (20×10^3 ft) with a skew angle of $\frac{\pi}{4}$ (45^o). Because of the difficulty of calculating near Mach one, the aerodynamics loads were actually obtained at Mach 0.90 at the same dynamic pressure.

Symmetric maneuver loads of +3g and -1g are studied as well as a condition of maximum roll acceleration which maximizes the moment through the pivot. The study of a single Mach number - altitude combination is deemed sufficient for the purpose of structural feasibility demonstration; other conditions will have to be addressed in the design stage including several sweep angles and takeoff and landing conditions. The task of defining these conditions is included in the study stage of the follow on program, Phase I, Section 5.2.1. The task of analyzing these conditions is included in the design stage of the follow on program, Phase II, Section 5.2.2.

The result of the study is a concept for a new wing, a pivot, a skewing mechanism, control systems that operate through the pivot, and a wing support assembly that attaches in the F-8 wing cavity. This concept is described in Section 3 and analyzed in Section 4. Further detail on the concept is included in drawings 78-002817 through 78-002822 which are furnished separately, as Exhibit A. The concept is firm enough to serve as the basis for a budgetary cost estimate and for the schedule for fabrication as presented in Section 5.

The completed study shows that installing a rotating oblique wing onto an F-8 is feasible, it outlines a concept for doing so, and defines the necessary time and effort required to prepare the aircraft for subsequent ground and flight testing.

2.1 Conventions

Two basic coordinate systems are employed throughout the report:

(a) Airplane system, in which:

The x axis is parallel to the airplane longitudinal axis.
The y axis is perpendicular to the fuselage plane of symmetry.
The z axis is perpendicular to both the x, and y axes.

(b) Wing system in which the axes are parallel to the airplane axes with the wing unskewed. The wing coordinate axes are fixed to the wing and rotate with the wing as it is skewed.

The two coordinate systems as used for design purposes are defined in Figures 3.3-1 and 3.3-2. Descriptive locations are referred to in the text as stations, butt lines, and water lines, which are defined as follows:

Fuselage Station - airplane system x coordinate in inches - positive aft.
Butt Line - absolute value of airplane system y coordinate in inches
Water Line - airplane system z coordinate in inches - positive up.
Wing Station - wing system x coordinate in inches - positive aft.
Wing Butt Line - absolute value of wing system y coordinate in inches.
Wing Water Line - wing system z coordinate in inches - positive up.

In the analytic work, the origins of the airplane coordinates and of the wing coordinates are chosen to coincide with the pivot. The y coordinate is measured positive toward the left. Together with x positive aft, and z positive up, this makes a left hand system.

The design specifies a right wing forward skew, so that positive y correspond to the aft wing and negative y to the forward wing.

Notations throughout the report are conventional. Wherever necessary, they are explained as they occur.

3.0 CONCEPT

3.1 General Assumptions

3.1.1 Configuration

(a) The 2-place F-8 (NTF-8A) aircraft will be used

(b) Wing geometry is

(1) Area 23.23 m^2 (250 ft^2)

(2) Span 15.24 m (50 ft)

(3) Planform: straight tapered with taper ratio .4 and 40% chord line straight

(4) Airfoil section: NACA 3612 at root, NACA 3606 at tip and straight surface generator interpolation in between. (Increase in tip thickness may be required for control system installation). The wing planform shown in drawing 78-002820 and in Figure 3.3-3 shows rounded tips for manufacturing cost estimating purposes.

(c) Maximum sweep angle is $\frac{\pi}{3}$ (60^o).

(d) Wing incidence of up to .05 (3^o) will be considered. However, the present study assumes zero incidence.

(e) Wing will contain no fuel.

(f) No lights to be fitted on wing (day operation only).

3.1.2 Performance

Projected performance of the prototype is

(a) Normal load of -1g to +3g (symmetric).

(b) Maximum Mach number 1.4

(c) Maximum equivalent airspeed 870 km/hr (470 knots)

(d) Obtainable roll rate of at least 0.5 rad/s

The analysis of the present study is limited to

(e) Mach number of 0.98 at 6.1 x 10^3m (20 x 10^3 ft)

3.1.3 Ground Rules

(a) Structural strength: A factor of safety of 2.0 applies to all newly designed structure, no structural testing required. A factor of safety of 1.5 is to be maintained for tested F-8 structure.

(b) Fatigue: A minimum of 200 flight hours.

(c) Flutter and divergence: a margin of 20% in equivalent airspeed to be maintained.

3.2 Wing Pivot Concept

Two concepts were evaluated for pivoting the wing: the turntable concept and the cantilevered post bearing concept. The one selected as the most feasible is the turntable concept which employes a large diameter bearing. This bearing attaches to the wing structure and to the fuselage structure.

3.2.1 Turntable Concept

The concept proposed for pivoting the wing is the turntable concept as shown by Figure 3.2-1. This concept utilizes a large diameter ball bearing and was selected for the following reasons:

- Structurally superior wing load paths into fuselage.
- Large number of wing attach bolts and the inner and outer race aspect of the bearing provides for structural redundancy between the wing and fuselage.
- Low risk involved in use of a proven bearing for turntable application.
- Very limited free play in bearing ball/race interface and the large bearing diameter provides for acceptable wing tip deflections. The plane of the bearing is an easy reference for wing location. Shimming is possible to vary wing location.
- Provides maximum space for controls and systems routing from the fuselage and thru the wing center.
- Smaller wing pivot actuator required.
- Wing pivot support structure is lighter and less expensive.

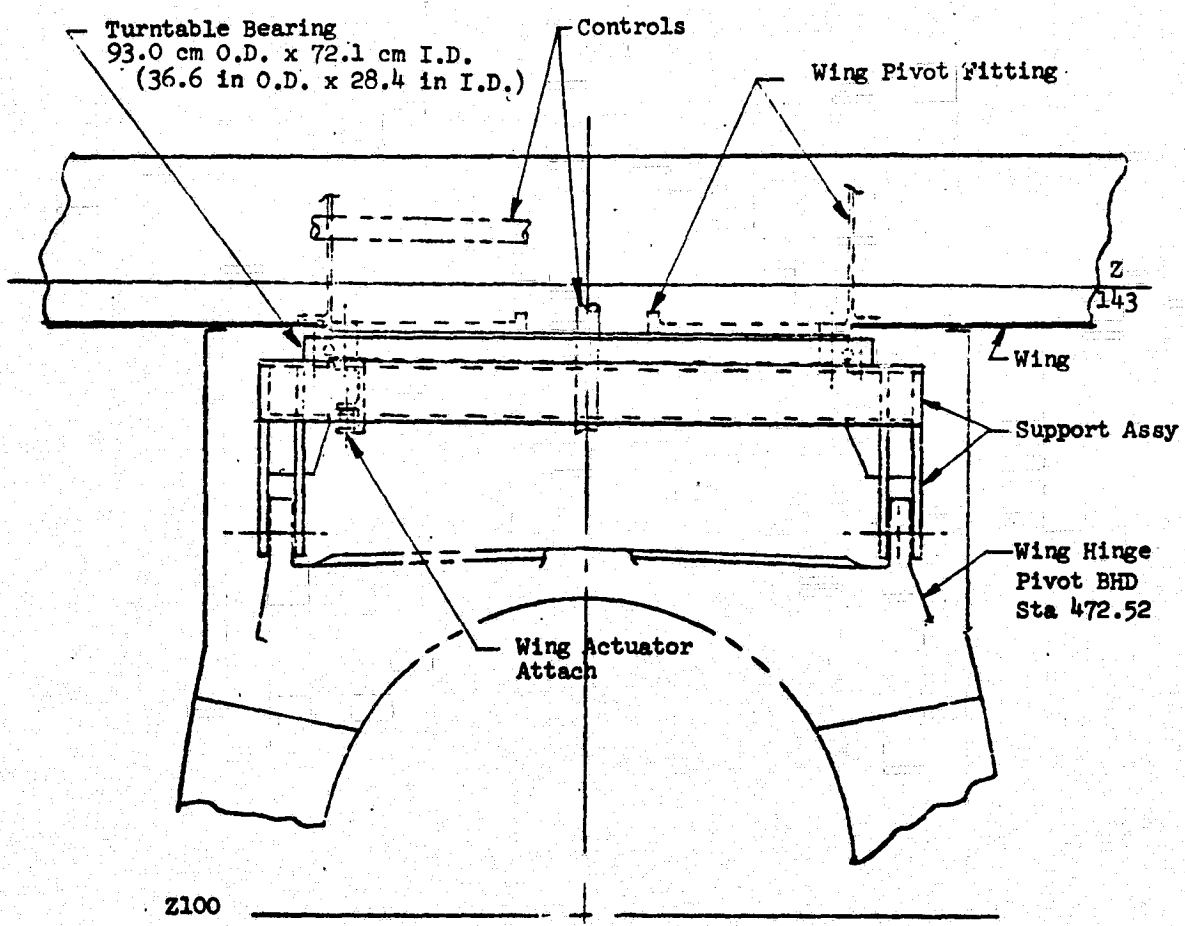

View Looking Aft

FIG. 3.2-1 Turntable Concept

3.2.1.1 General Description

A large diameter ball bearing (O.D. = 93.0 cm (36.6 in.)) is the structural interface between the wing and the fuselage. The bearing inner race attaches to the wing and the outer race attaches to a bearing support structure. The description of the wing support structure is presented in Figure 3.2-1 and Section 3.4.

3.2.1.2 Detailed Description

The bearing is a 4130 alloy steel turntable ball bearing manufactured by Keene Corp., Kaydon Bearing Division, Muskegon, Michigan, Part No. S325 (Reference 1). The bearing has an O.D. of 93.0 cm (36.6 in.), I.D. of 72.1 cm (28.4 in.), thickness of 6.35 cm (2.50 in.) and weighs approximately 110 kg (240 lb.)

The inner race of the bearing is bolted to the wing center fitting with 32 1.43 cm(9/16 in.) diameter bolts. The outer race is bolted to the bearing support fitting with 28 1.43 cm(9/16 in.) diameter bolts.

3.2.2 Cantilevered Post Bearing Concept

Figures 3.2-2 and 3.2-3 represent cantilevered post bearing pivot concepts which were evaluated as a part of the contract requirements. Basically, the post is an integral extension of the wing pivot fitting, machined from 17-4 stainless steel.

The wing post extends down into, and pivots about, a stainless steel support fitting which reacts and distributes a major portion of the wing loads to the fuselage attach lugs at F.S. 472.52. The support fitting contains a bearing in which the post rotates. Figure 3.2-2 depicts a post 28 cm (11 in) in diameter and 6.4 mm (.25 in.) wall thickness supported by a non-metallic bearing which could be constructed of glass fiber reinforced "Delrin" acetal resins, glass fiber reinforced nylons, or teflon. Figure 3.2-3 depicts a support fitting with two roller bearings. This configuration requires a larger diameter post (approximately 38 cm (15 in.) diameter) to accommodate the bearing requirements. In both cases the lower end of the post is retained in the bearing with a ring fitting with an integral lug for attaching the pivot actuator. Controls and systems routing is accomplished through the center of the post. This concept is feasible but it was not selected for the following reasons:

- Structural load paths not desirable.
- No structural redundancy aspect of the post (horizontal crack in post could result in loss of the aircraft).
- High risk involved in use of non-metallic bearing without back up test data. Two vertically stacked roller bearings have no significant advantages over a single turntable bearing.

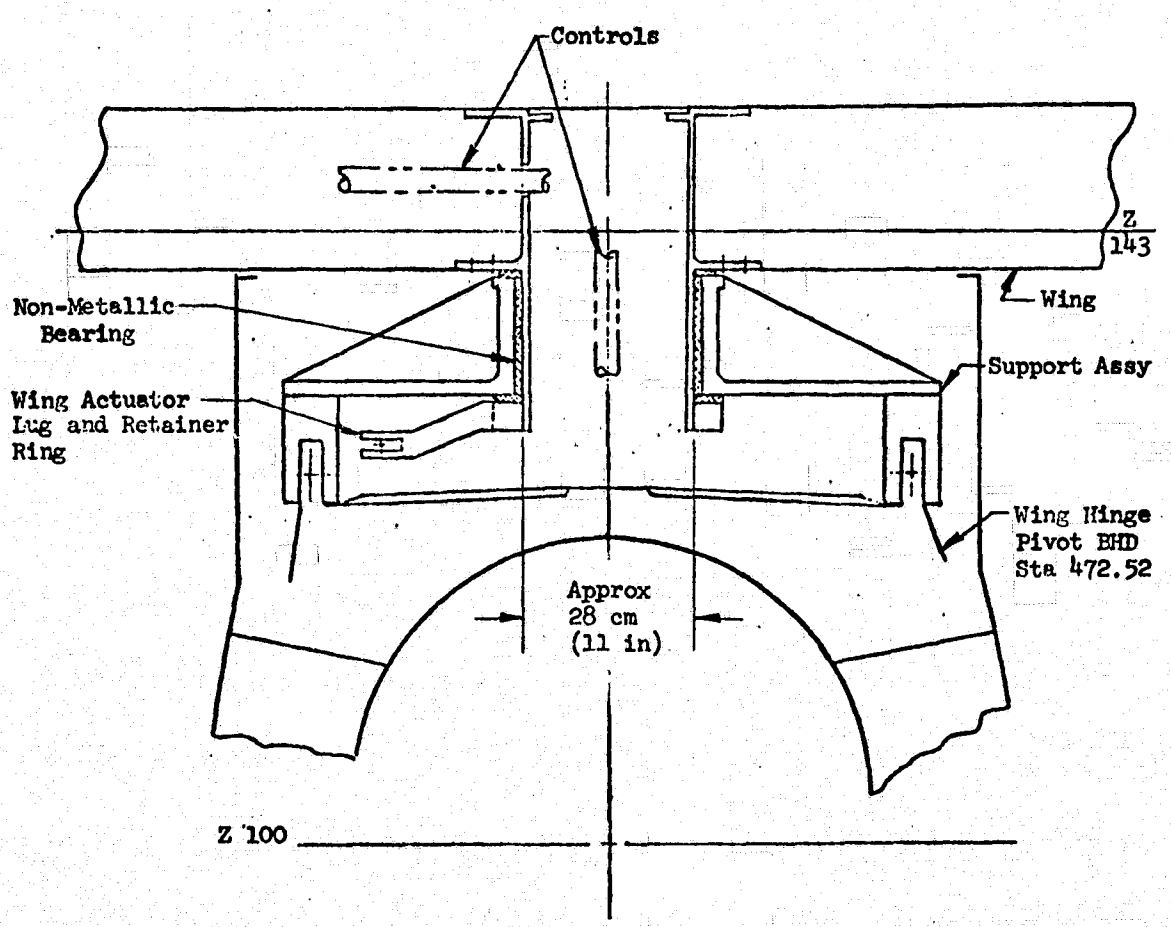

View Looking AFT

Fig. 3.2-2 Cantilever Post Concept
(Non-Metallic Bearing)

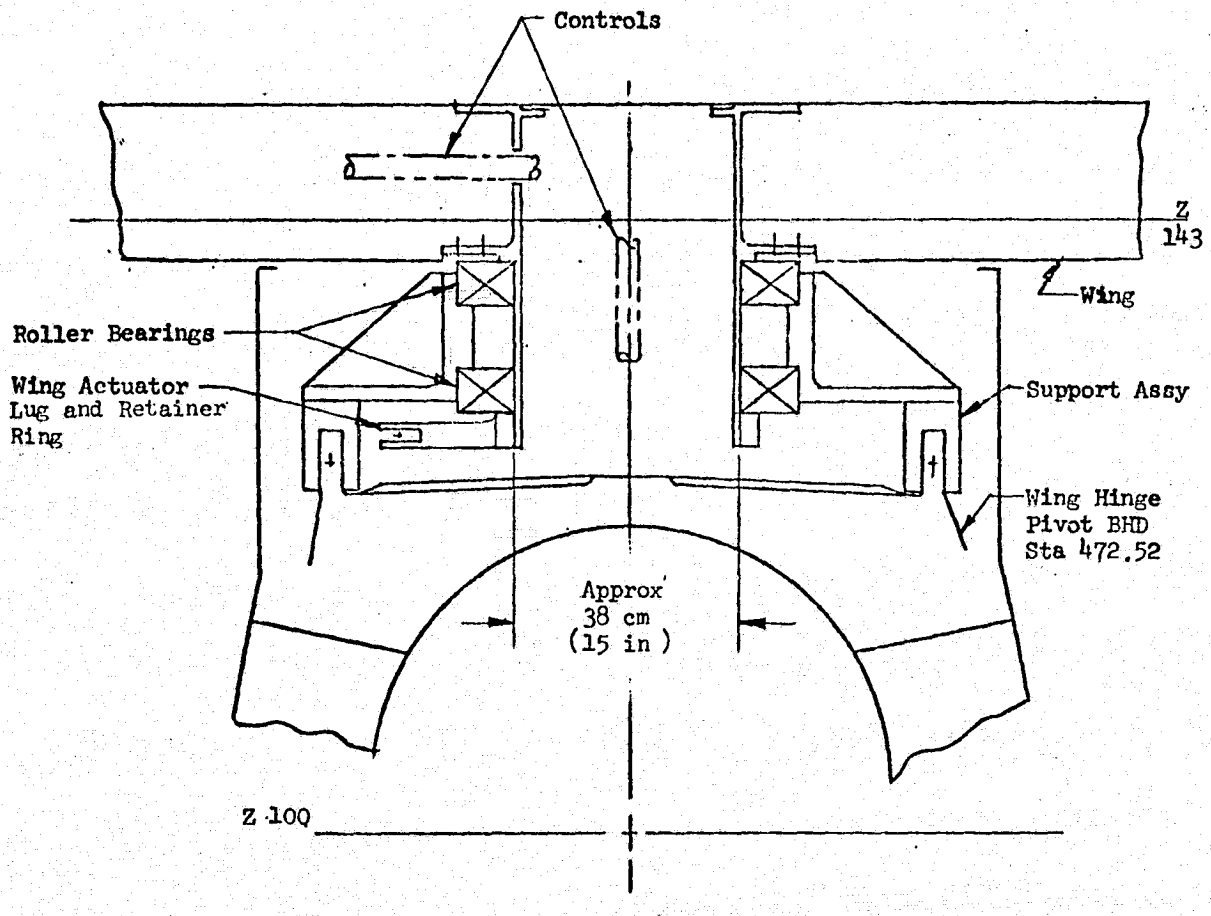

View Looking AFT

Fig. 3.2-3 Cantilever Post Concept
(Roller Bearings)

- o Rigid tolerance control between the post diameter and angularity and the bearing bore would be required to obtain desirable wing tip location limits. There are no adjustment provisions such as shimming.

- o Limited space provisions for controls and systems routing.

- o Larger wing pivot actuator would be required than for a turntable.

- o Wing pivot support structure would be heavier and more costly.

- o Structural tests would be necessary to establish safety-of-flight integrity of the combinations of detail parts.

3.3 Wing

3.3.1 Wing Location

Three wing station and pivot locations were evaluated. The wing waterline for each configuration was set to provide a clearance between the wing and fuselage with the wing rotated to the $\pi/3$ (60°) position. Configuration III was selected for more detailed study and is the recommended configuration.

Configuration I - 50% Chord pivot at fuselage station 454 (normal gross weight center of gravity, landing gear down for basic single-place aircraft). This was the configuration of the NASA Ames Research Center wind tunnel model.

The wing waterline location for this configuration was controlled by the forward fuselage on the two-place aircraft and by the aft fuselage dorsal fairing on the single place aircraft.

The configuration was judged undesirable because significant rework of fuselage structure was indicated in order to provide structurally adequate forward reaction points for the wing loads.

Configuration II - 50% Chord pivot at fuselage station 472.5 (Wing pivot bulkhead).

Relocating the wing aft to this fuselage station allows the wing load to be structurally reacted at the existing forward fuselage reaction points with no appreciable modification to fuselage structure.

The wing waterline location for this configuration was controlled by the aft fuselage dorsal fairing for both the two-place and the single-place aircraft.

This configuration was judged undesirable because it provided an inefficient structural arrangement of the primary wing structure.

Configuration III - 40% Chord pivot at fuselage station 463.53. The unskewed wing position is identical with configuration II, however, the pivot is further forward (by 10% of the root chord). Figures 3.3-1 and 3.3-2 depict this configuration for the two-place aircraft.

Relocation of the pivot point to the 40% chord provides an efficient structural arrangement for the primary wing structure and maintains the improved conditions of configuration II at the existing forward fuselage reaction points.

The wing water line location for this configuration was controlled by the aft fuselage dorsal fairing for both the two-place and the single-place aircraft.

3.3.2 Wing Structure

The wing configuration resulting from this study is symmetric right and left. It consists of a main structural torque box, a fixed leading edge structure, a fixed trailing edge structure, wing tips and control surfaces. The study did not specifically address control surface requirements; therefore, the plain trailing edge flaps and ailerons assumed by the study are conceptual for preliminary evaluation. The structural arrangement is depicted in drawing 78-002820 and in Figure 3.3-3.

Main Torque Box Structure

The main torque box is a three cell structure from the 20% Chord to the 60% Chord of the wing. The structure consists of mechanically attached machine tapered steel skins, four spars, twelve ribs and a major pivot fitting for attaching the wing to the wing support structure. The pivot fitting, spars and ribs are steel weldments. Access to wing systems components (Controls, Electrical and Hydraulic) in the pivot area is available through a structural panel attached to the upper surface of the pivot fitting.

Fixed Leading Edge Structure

The fixed leading edge is located forward of the 20% wing chord. The compound contour areas at the centerline and adjacent to the wing tip are fiber-glass structures. The rest of the leading edge is conventional aluminum sheet metal structure.

Fixed Trailing Edge Structure

The fixed trailing edge is located aft of the 60% wing chord. This structure includes hinge ribs to support the control surfaces and houses the systems components necessitated by them. Access to the systems components is from the upper surface in the portion of the wing over the fuselage - and from the lower surface in the portion of the wing outboard of the fuselage.

Preliminary evaluation indicates the current wing thickness is marginal for housing the aileron actuators and related components. Some

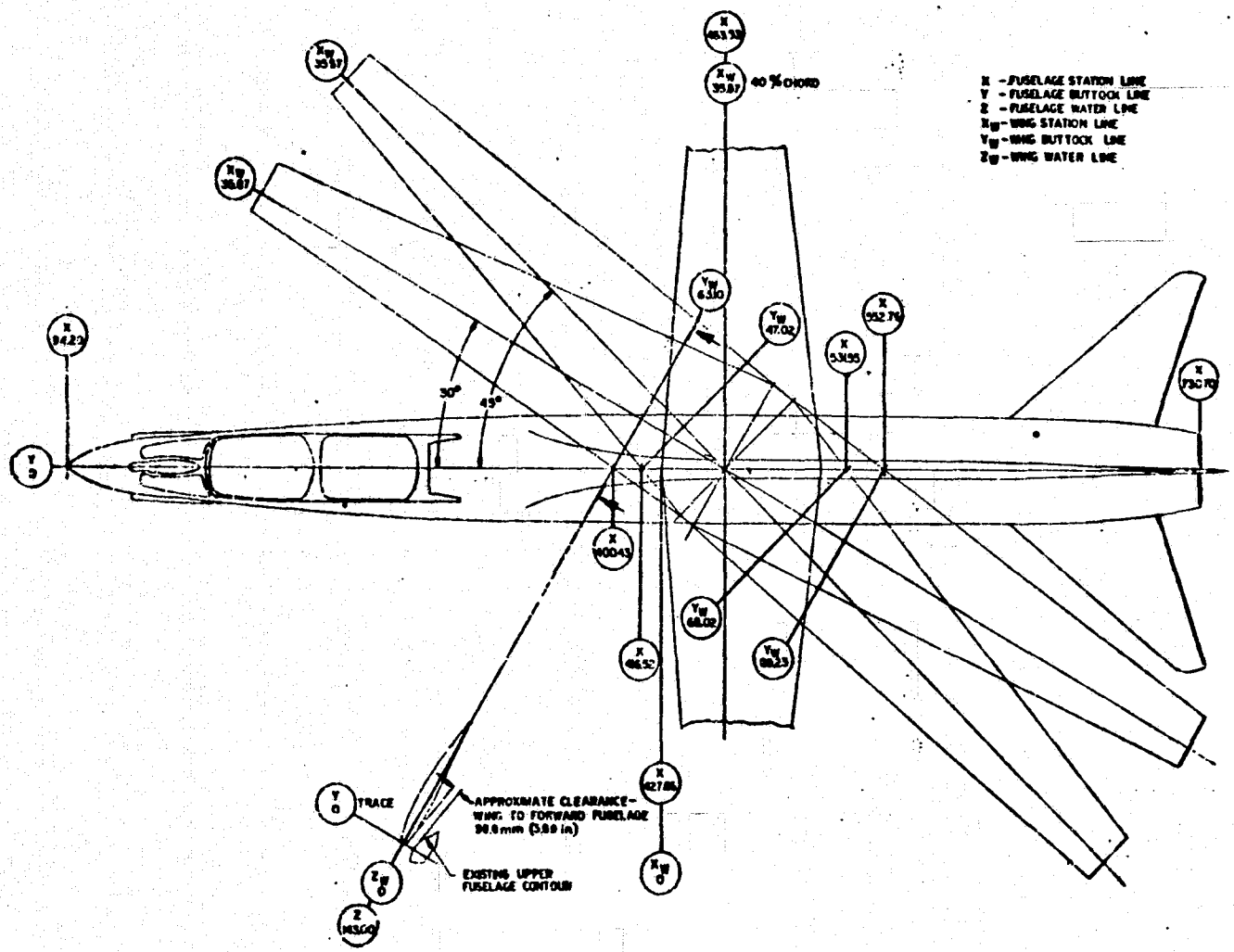

FIGURE 3.3-1 - Wing Location - Plan View

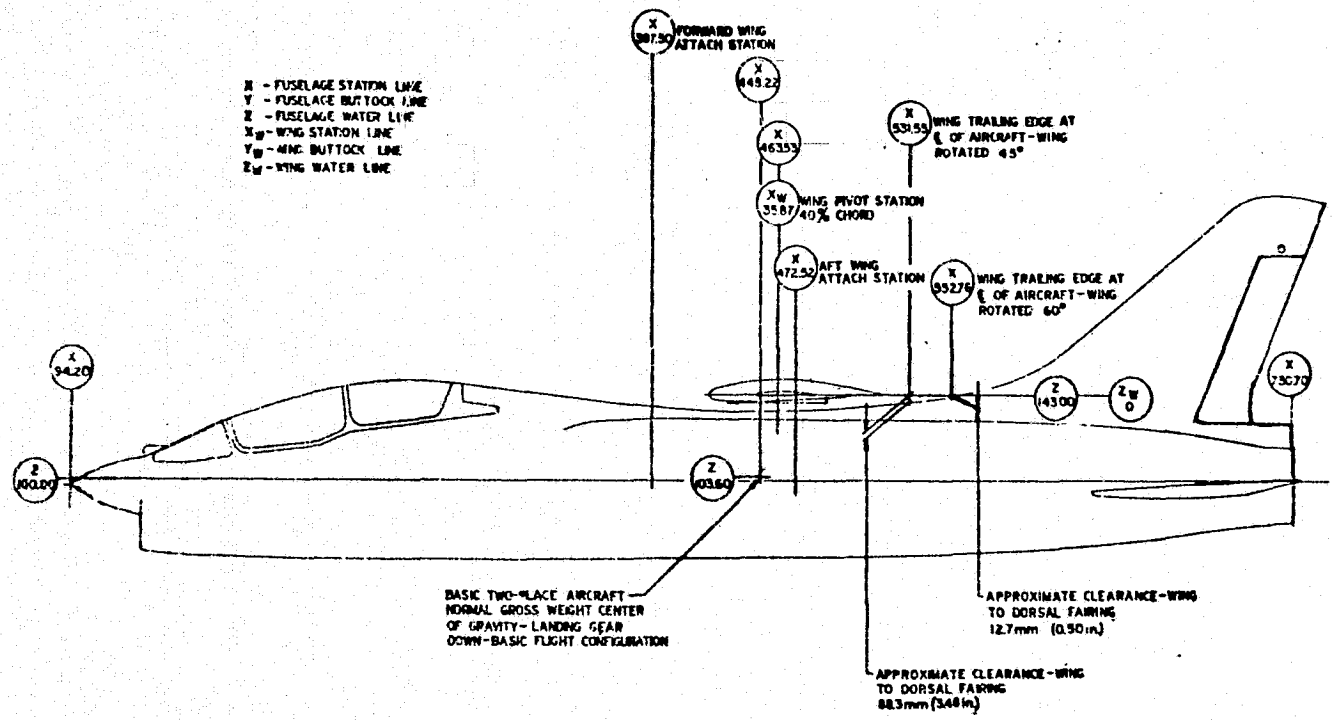

FIGURE 3.3-2 - Wing Location - Profile View.

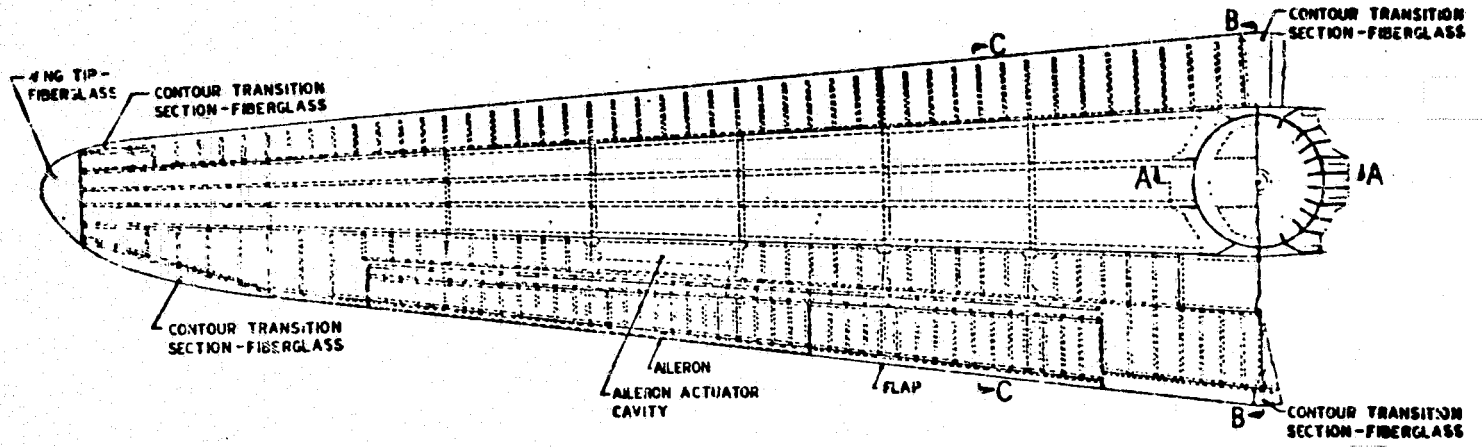

Note: Left wing shown, right wing opposite.

FIGURE 3.3-3 - Wing Structural Arrangement

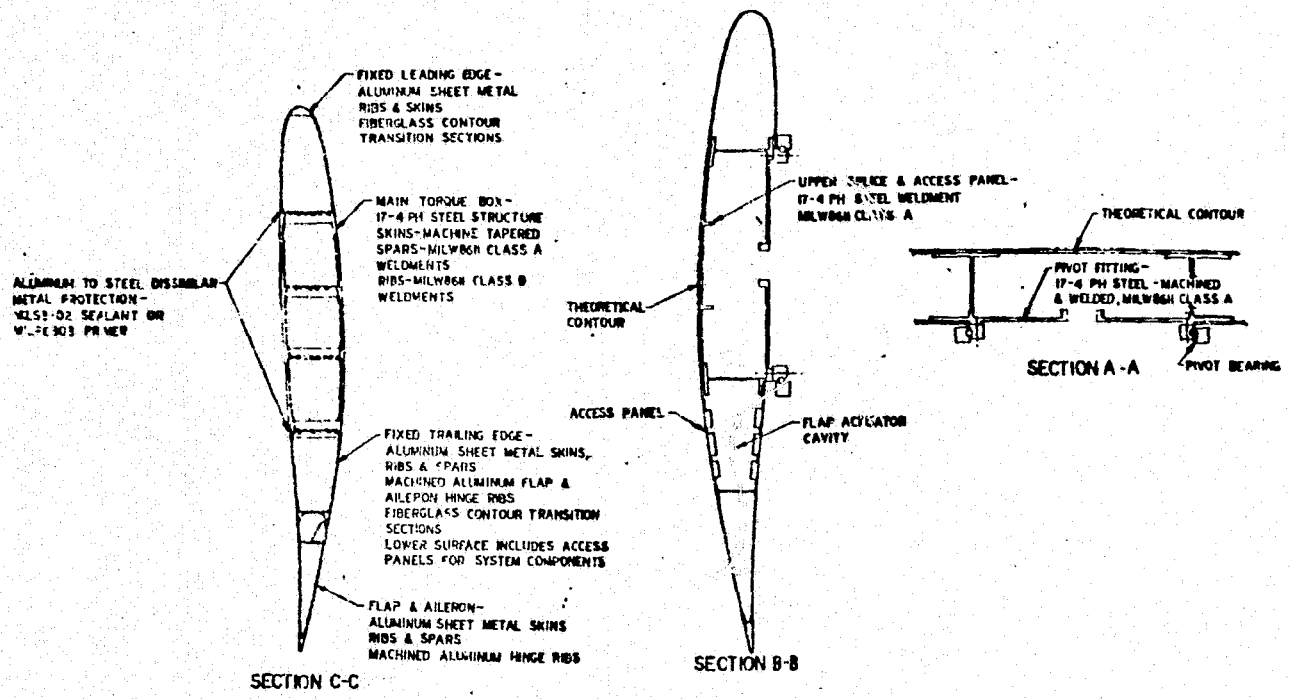

FIGURE 3.3-3(concluded) - Wing Structural Arrangement

increase in the wing tip thickness ratio over the current 6% may be necessary when control surface requirements are established and an aileron actuator is selected. This evaluation would be conducted in the proposed Design Phase of the follow-on program.

The compound contour areas at centerline and adjacent to the wing tip are fiber-glass structures. The rest of the trailing edge is conventional aluminum sheet metal structure with machined aluminum hinge ribs for the control surfaces.

Wing Tip

The wing tip is fiber-glass structure.

Control Surfaces

The control surfaces are conventional aluminum sheet metal structure with machined aluminum hinge fittings.

3.4 Fuselage Design

3.4.1 General Description

The outer race of the bearing bolts onto the wing support structure. The support structure (Figure 3.4-1) attaches to the existing fuselage aft LH and RH wing attach lugs at F.S. 472.5. A major portion of the wing loads is reacted at these lugs. The bearing support structure extends forward to F.S. 397.5 where it attaches to a truss assembly. This joint is a spherical bearing to insure that no moments are reacted by the fuselage at the forward attach points. Vertical loads only are reacted at this joint and are equally distributed by the truss assembly.

The bearing support assembly has an integral lug located at F.S. 412 to anchor the wing pivot actuator. The truss assembly attaches to new, LH and RH, fittings located on the upper longerons at F.S. 397.5.

A fairing is required to provide an aerodynamic cover below the wing and over the fuselage cavity and fair into the pivot bearing.

3.4.2 Detailed Description

See drawing 78-002821 or Figure 3.4-1 for the wing support structure.

(a) Bearing Support Assembly

The bearing support assembly is a weldment of 17-4 stainless steel utilizing 1.27 cm (.50 in.) thick plate. The LH and RH side of the steel weldment have integral double lugs which attach to the existing fuselage wing attach lugs at F.S. 472.5. Lugs are also provided at F.S. 412.0 to support the pivot actuator. The forward end of the support assembly is at F.S. 396.0. A spherical bearing is used at this location to attach to the truss fitting

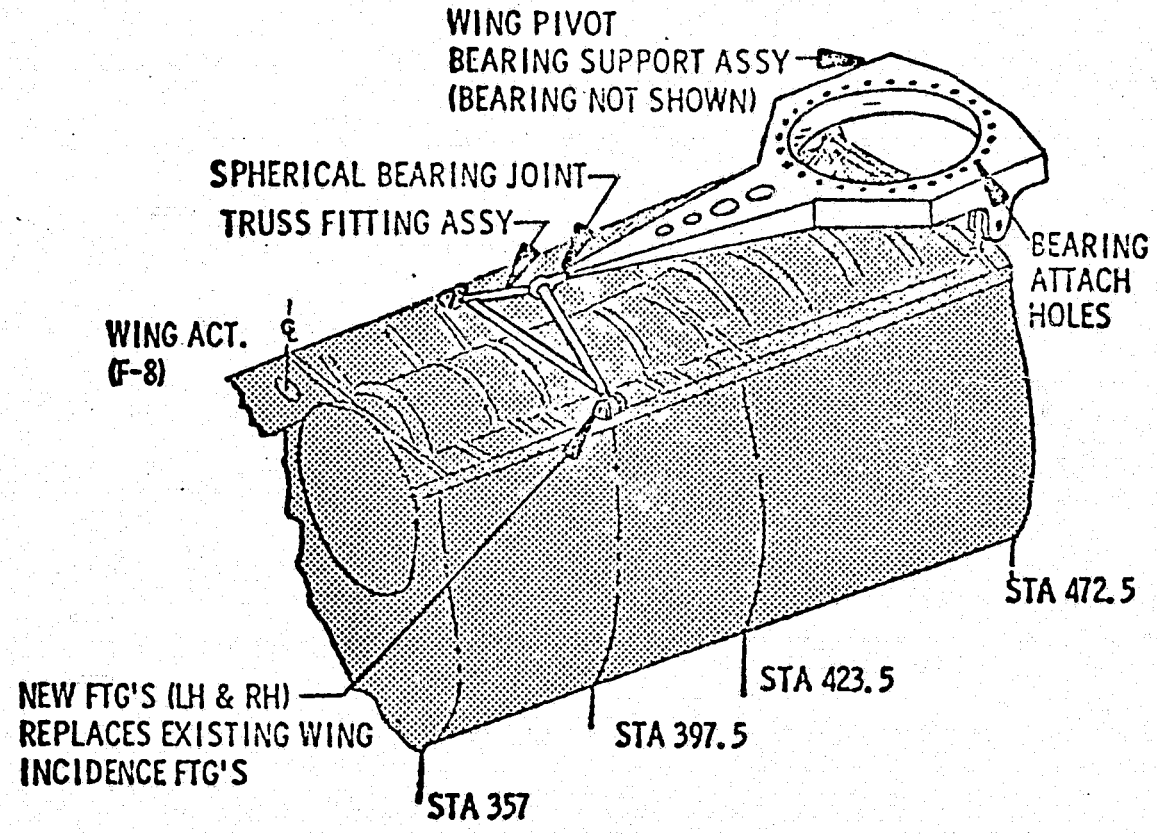

FIG. 3.4-1 WING SUPPORT STRUCTURE
FOR TURNTABLE CONCEPT

assembly.

(b) Truss Fitting Assembly

The truss fitting assembly is a 4130 steel weldment. The two diagonal truss members are identical parts and consist of a tube 3.81 cm (1.5 in.) O.D. with a 6.35 mm (.25 in.) wall thickness. A machined fitting is welded into each end for attaching to the bearing support assembly and the fuselage fittings.

The horizontal truss member is a tube 3.81 cm (1.5 in.) O.D. with a 6.35 mm (.25 in.) thick wall. It is welded at each end to the diagonal members. Gussets of 6.35 mm (.25 in.) thick sheet are welded in the two corners.

(c) Truss Attach Fittings

Two new fittings (one LH, one RH) are required at F.S. 397.5 to replace the existing CV15-410563 LH and the CV15-410658 RH wing incidence fittings located on the upper longerons. The new fittings are machined from 7075 aluminum and are similar to the existing fittings except for the double lug in lieu of the threaded bolt hole. The lugs are used for attaching the truss assembly.

(d) Fairing, Wing Pivot

The wing pivot fairing is a non-structural member which covers the existing fuselage cavity and fairs in the wing/fuselage pivot area. The fairing originates at F.S. 347 and extends aft to F.S. 560 (approximately) and fairs into the dorsal.

Four access doors are required for access into the wing pivot area.

(e) Aircraft Modification

The following fuselage items are to be removed from the 2-Place F-8 to accommodate the wing pivot support structure and fairing.

(1) CV15-520067 Fairing

(2) CV15-520055 Door Installation

(3) CV15-410563-1 Fitting Assy (LH) and CV15-410658-1 Fitting Assy (RH)

3.5 Systems

3.5.1 Design Criteria

Control system definition for the F-8 oblique wing airplane was established from the limited study requirements of NAS4-2266 and general

assumptions for other control system tasks presumed necessary for the eventual complete airplane modification.

Since the study did not address control surface requirements, the aileron and flap control systems shown in the wing are conceptual configurations for preliminary evaluation and budgetary pricing only - see drawing 78-002822.

The control systems, as defined, are considered a feasible approach for prototyping the 2-Place F-8 airplane. However, the configurations are not considered as being firm, should subsequent control system requirements dictate the need for changes. There is enough flexibility in areas of high cost items such as the proposed wing position and T.E. flap linear actuators to consider other design approaches should lower cost "off-the-shelf" units be found available.

3.5.2 General Assumptions

- o Existing dualized controls in aft cockpit for unaffected systems will be retained.
- o New cockpit requirements will be dualized.
- o Existing longitudinal control system will require no modification.
- o Wing surface controls will consist of a two-position LH and RH T.E. flap and an F-8 type LH and RH drooping aileron.
- o Existing lateral control system in fuselage will require no modification other than for interfacing with controls in wing and reworking feel system back to original F-8 configuration.
- o Existing rudder surface deflections and feel system characteristics will require modification (new surface deflections will not exceed existing available limits).

3.5.3 General Description

Wing Position Control System

The wing position control system is a mechanical-hydraulic control system used to rotate and hold the wing in a skewed position. Movement of a control handle on the LH console transmits a signal through a combination cable-pushrod system to a servo valve to direct utility pressure to a hydraulic actuator. An electric drive is incorporated within the actuator assembly to allow use of an alternate power source.

Wing Trailing Edge Flap Control System

The wing trailing edge flap control system is a mechanical-hydraulic control system used to position the flaps in either the down position for

takeoff and landing or the up position for the cruise condition. Movement of a control handle on the LH console transmits a signal through a combination cable-pushrod system to a remotely located valve to direct utility pressure to a hydraulic actuator. An electric drive is incorporated within the actuator assembly to provide an alternate power source.

Lateral Control System

The lateral control system is similar to the existing F-8 lateral control system in theory of operation except roll control will be achieved by ailerons only (no spoilers). Aileron cruise and takeoff/landing neutral positions will be sequenced to flap operation. The existing F-8 stick deflection and feel force characteristics will be retained. The aileron input signal will be transmitted from the fuselage into the wing by a swivel pushrod at the wing pivot hinge line. Flexible hydraulic hoses and electrical wire will route into the wing through the pivot bearing. Aileron control surface location, deflection and hinge moment requirements will be established during follow-on investigations.

Directional Control System

The directional control system is basically similar to that of the existing airplane; however, there are some significant modifications. The exact extent of the modifications is dependent upon future flying quality investigations. For preliminary evaluation and budgetary pricing only, the directional control system modification for the oblique wing airplane is proposed as being similar to that performed on the NASA supercritical wing test aircraft. The modification consists of reworking the existing control system to change operational rudder surface deflections, feel force gradients, and cruise condition stops/feel engagement actuation.

Automatic Flight Control System

Automatic UHT-wing position and aileron-rudder-wing position interconnect provisions will be added to the automatic flight control system.

3.5.4 Detailed Description

The detailed description is stated in terms of the changes to the present NTF-8A airplane that are necessary to adapt the systems to the oblique wing requirements.

3.5.4.1 Wing Position Actuation System

Install ball screw hydraulic/electric linear actuator. Normal operation will be hydraulic wherein the actuator will operate as a positioning power servo with its ram position output proportional to a manual control lever position input. An electric motor with integral brake driving the screw jack through a clutch and gear train will provide alternate power source capability. A hydraulic shutoff and bypass valve will be provided to release hydraulic constraint when the actuator is required to operate in the

electric mode. The power transfer clutch will be a spring-engage, pressure-release unit located between the screw jack and the electric drive assembly. The actuator will be attached to the bearing support assembly and to a bracket on the inner race of the wing pivot bearing. - See drawing 78-002822

Install a wing position control switch in the fwd and aft cockpits to enable wing hold or rotation and energize the hydraulic shut-off and bypass valve.

Replace the wing down lock/wing incidence handle installation in the fwd and aft cockpits with a flap actuation/wing position handle installation wherein the wing position handle will interface with the existing wing incidence system routing. The handle installation will contain a friction wheel or detents or some other device in order to prevent inadvertent movement of the wing pivot handle. The aft cockpit handle installation will not duplicate the fwd cockpit handle installation with respect to friction wheel or detents. (Ref 3.5.4.2.4 for additional handle definition.)

Modify existing wing incidence cable system for operating the wing position actuator manual hydraulic servo valve. The cable system will be routed aft (instead of down to wing incidence valve) from LH side of F.S. 312.8 bhd where it will be converted into a pushrod system connecting to the servo valve mechanism.

Route utility hydraulic system plumbing and electrical system network to wing position actuator with wire routing to the wing position control normal/emergency switch in fwd and aft cockpits.

Install a wing position potentiometer at the wing pivot area.

Install a wing position indicator in the fwd and aft cockpits.

3.5.4.2 Wing Trailing Edge Flap System

Install ballscrew hydraulic/electric linear actuator. The actuator will be similar to the wing rotation actuator in function except there will be dual rams operating on a single screw and a hydraulic two-position valve will be located remote from the actuator. The actuator will contain position monitors. The actuator will be installed in the wing on W.B.L.O. and a station plane just aft of the wing structural box. - See Drawing 78-002822.

Install a flap position control switch in the fwd and aft cockpits to enable flap hold or rotation and energize the hydraulic shut-off and bypass valve.

Install wing flap linkage routing from flap actuator outboard to LH and RH T.E. flaps - See Drawing 78-002822.

Replace wing down lock handle (ref 3.5.4.1) with two-position flap handle which will interface with the existing wing down lock system routing. The handle design will be such that the flap handle must be placed

in the flap up position before the wing position handle can rotate to skew the wing, and the wing position handle must be in the wing un-skewed position before the flap handle can move to the flap down position. The handle will also operate the aileron c/c stops. (Ref 3.5.4.3.2)

Install a flap position indicator in the fwd and aft cockpits.

Modify the existing wing down lock cable system for operating the wing T.E. flap actuator valve. The cable system will either be routed down from where it presently attaches to the wing incidence cylinder to the flap valve (existing wing fold valve) or aft to a flap valve located in the existing wing cavity area.

Route utility hydraulic system plumbing and electrical system network to flap actuator with wire routing to the flap control normal/emergency switch and a flap position indicator in fwd and aft cockpits.

3.5.4.3 Lateral Control System

Rework existing feel package into, or replace with, a conventional F-8 feel package.

Reinstall conventional F-8 type cruise configuration (c/c) stops in the forward cockpit (presently exists in feel package of 2-Place F-8). The installation will consist of a new hybrid swivel assembly with mass balance, conventional F-8 stop assembly and springs, and an actuating cable assembly routing from the stop assembly to the forward flap handle assembly.

Modify the lateral control system linkage downstream of the existing feel and trim package. The modification will consist of routing linkage up through the wing pivot hinge line into the wing and out to the LH and RH aileron P.C. packages. The wing linkage will be similar to that in the existing F-8 wing, including aileron-rudder interconnect potentiometers and an aileron neutral position switch. Additional linkage will connect between the aileron signal linkage and the flap linkage to droop the ailerons in conjunction with drooping the flaps. - See drawing 78-002822.

Route P.C. 1 and P.C. 2 hydraulic system plumbing into the wing and out to the aileron P.C. actuators.

3.5.4.4 Directional Control System

Modify fwd cockpit pedals installation to allow increased pedal travel in cruise configuration (c/c).

Replace existing c/c stops cable installation with new installation which will consist of a new cable assembly operated by a hydraulic actuator located in the dorsal which is sequenced to the landing gear operation.

Replace existing c/c stops/feel assembly with new assembly to change feel force gradients and allow increased surface travel in c/c.

Modify linkage in rudder P.C. package and install A-7 rudder P.C. valve in place of existing valve.

3.5.4.5 Automatic Flight Control System

Install aileron-rudder-wing position interconnect potentiometer in wing pivot area.

Install UHT-wing position interconnect potentiometer in wing pivot area.

4.0 ENGINEERING ANALYSIS

4.1 Aerodynamics

Many aerodynamic considerations must be evaluated to establish an Oblique Wing design suitable for installation on the F-8 airplane. An analysis of specific design concepts must be made to establish a configuration which will exhibit proper flying qualities and also achieve the desired performance characteristics. The present study does not address these items. The aerodynamic effort under the contract was limited to the determination of rigid spanwise loadings on the Oblique Wing for one flight condition and a comparison of the integrated value of those loadings to wind tunnel data obtained for a similar configuration. The load distributions result in forces which are in agreement with the magnitude and trends with angle of attack of the wind tunnel data. These trends are also in agreement with work done under separate contract by Boeing on an Oblique Wing transport configuration.

4.1.1 Span Load Determination

Structural design loads were required to meet the contract design conditions of 0.98 Mach at 20,000 feet for the wing skewed $\pi/4$ (45°) to the longitudinal axis. Since no experimental wing pressure data were available from which to establish spanwise load distributions, a theoretical solution was made using finite element lifting surface methods. At a Mach number of 0.98, shock systems will be imbedded in the flow and a rigid theoretical solution would be complex. Since one of the purposes of the Oblique Wing is to minimize the shock strength, it is assumed these effects will be minimal, thus a solution at Mach 0.90 should provide reliable distributions for the structural evaluation. This assumption is supported by the experimental data obtained from NASA for a comarable wing configuration. Comparisons of these experimental data with the theoretical solution are made in the sections which follow.

The theoretical solution for spanwise and chordwise aerodynamic loadings was made using 150 finite panels to simulate the total skewed wing. For this configuration, the following simplifying assumptions were made.

(a) Wing is composed of three interdependent connected panels.

(b) Wing tips are streamwise and have an equivalent planform area.

(c) No body simulation.

(d) No wing thickness distribution.

Since no plane of symmetry exists for a wing pivoted along the midchord, it was necessary to subdivide the wing into three panels; the exposed left and right panels and a section over the fuselage which joins the

leading and trailing edges of the exposed panels. The assumption of streamwise tips is required for any finite element solution to assure that the trailing vortex from any element does not impinge on any other element. A sketch of the basic wing and assumed planform is shown in Figure 4.1-1.

The wing and pivot design are primarily affected by wing bending and torsional loads which act on the exposed wing panels. These loads, for a given flight condition, are not significantly affected by the fuselage either due to an induced loading on the wing or by a reduction in wing load which is transferred to the fuselage.

The wing and pivot design are primarily affected by wing bending and torsional loads which act on the exposed wing panels. These loads, for a given flight condition, are not significantly affected by the fuselage either due to an induced loading on the wing or by a reduction in wing load which is transferred to the fuselage.

Wing chordwise thickness distribution was not simulated for the theoretical solution since this affects only the local panel loading and does not influence the lift forces which establish bending or torsion values.

These assumptions were made based on experience with the theoretical method and previous comparisons with experimental results. The data as calculated for the Oblique Wing were then compared to experimental NASA data. No real deficiencies were present in the results. Solutions were also made for the camber effect, however since it was not possible to incorporate these distributions for zero angle of attack in the Structural Loads routine, AIRLOD, these data are not presented.

Spanwise distributions of aerodynamic loading and center of pressure were determined due to angle of attack and aileron deflection. All distributions are for the rigid wing.

4.1.2 Additional Lift

The distribution of aerodynamic lift due to angle of attack and the point of application of that force is presented in Figures 4.1-2 and 4.1-3. The additional lift is presented as a sectional normal force coefficient multiplied by the local section chord measured in a streamwise direction. The symbols indicate the number of spanwise locations for which a solution is made. For each spanwise point, ten chordwise divisions are used for the calculation. Data are presented for one degree angle of attack. Values for specific angles of attack are obtained by multiplying the $c_n c$ values by the given angle of attack. C.P. values of Figure 4.1-3 are presented as a fraction of local streamwise chord, x/c, and are constant for any angle of attack. The data are presented for the wing pivot located at 0.50 of the wing root chord. This was the wing location used for the theoretical

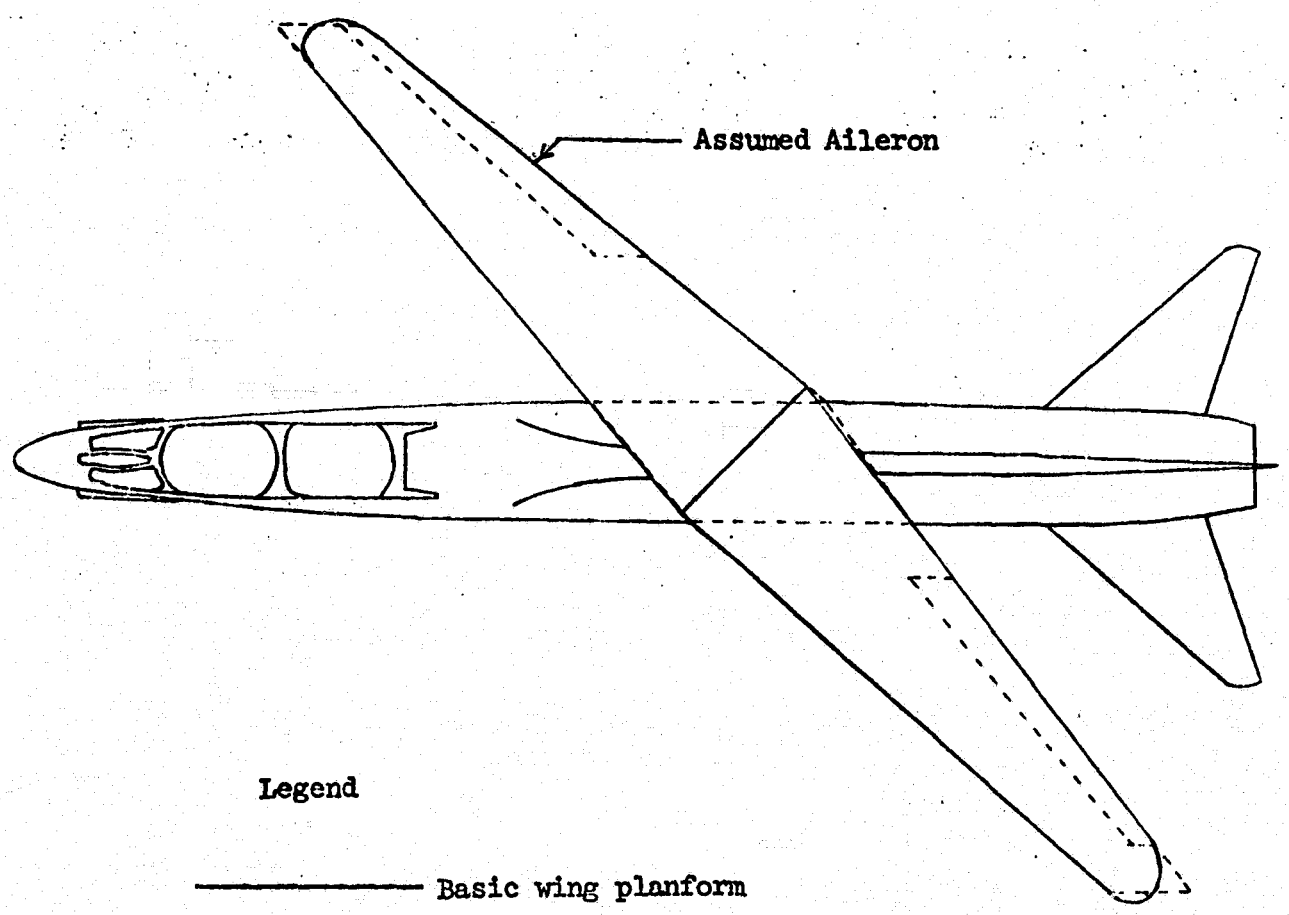

FIGURE 4.1-1 - Oblique Wing Planform Geometry used in Theoretical Calculations. Wing in 45° Skew Position on 2-Place F-8 Airplane.

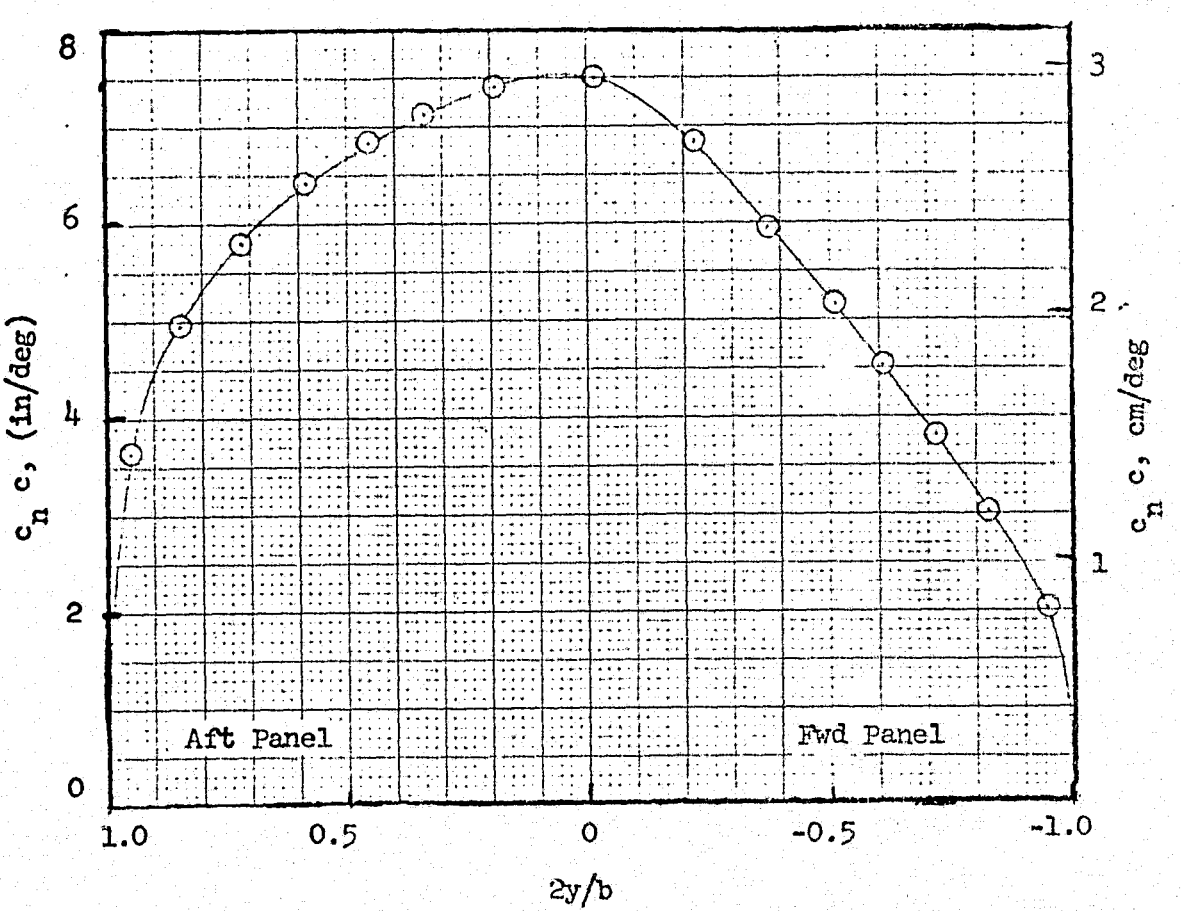

FIGURE 4.1-2 - Spanwise Distribution of Additional Lift for Wing Pivot at 50% of Root Chord. M = 0.90

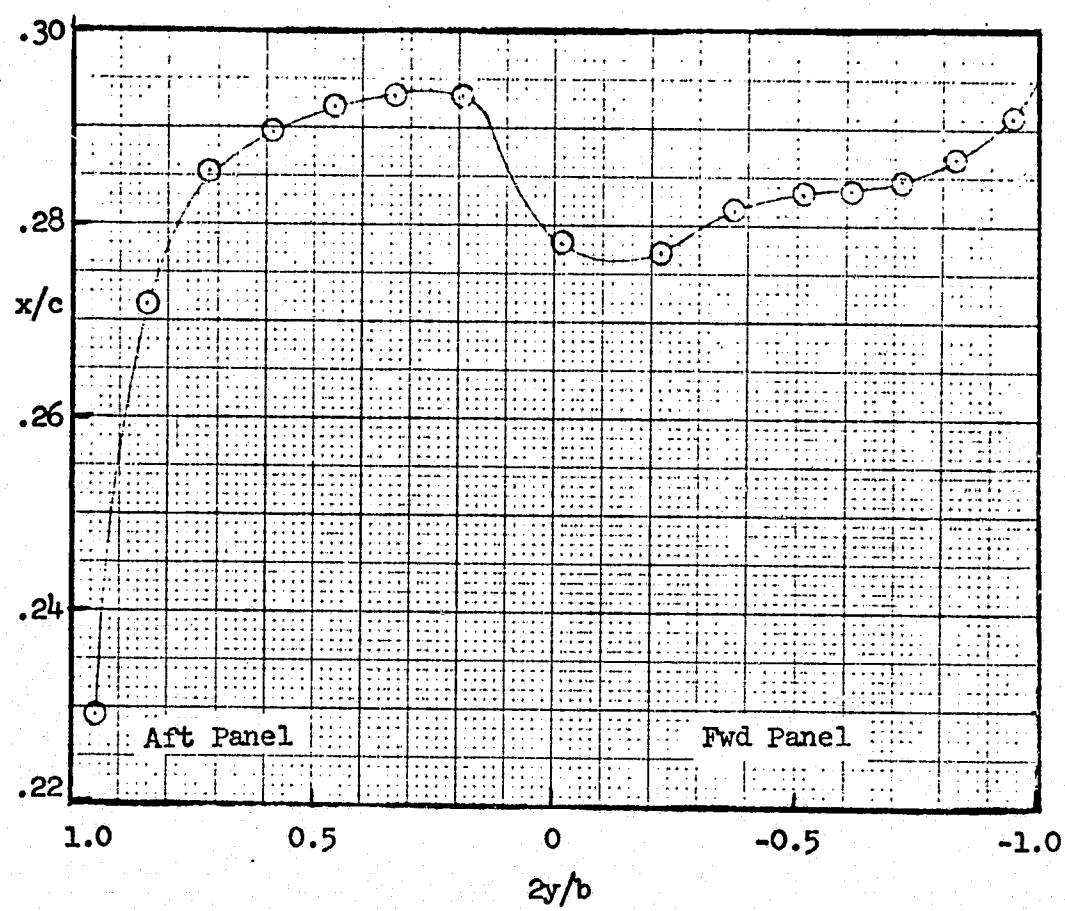

FIGURE 4.1-3 - Spanwise Variation of Section Center of Pressure for Additional Lift. Wing Pivot at 50% of Root Chord. M = 0.90

aerodynamic analysis. Subsequent design requirements dictated a movement of the pivot to the 0.40 chord location. This does not materially affect the aerodynamic loadings, so this correction was accomplished by a transfer of the forces in the stress analysis.

The slope of the theoretical value of normal force coefficient with angle of attack is compared to Wind Tunnel data for a similar configuration in Figure 4.1-4. Displacement of the Wind Tunnel data at an α of zero degrees is due to the camer of the airfoil section. This changes the value of α for a given normal force coefficient C_N, but not the variation with α. It is shown that the variation of C_N with α does not change significantly with Mach number and the theoretical variation of loading provides a good representation of the experimental results.

The variation of lift coefficient with pitching moment coefficient shown in Figure 4.1-5 is used to establish the variation of the wing-body center of pressure for three values of Mach number. The break in the data near a C_L of 0.20 is the result of flow breakdown on the configuration and indicates the presence of viscous effects which were not duplicated theoretically. The displacement of the pitching moment at zero lift coefficient is due to airfoil section camber and body effects. This shift is important in determining the static balance of the airplane but does not alter the additional lift center of pressure which is represented by the slope of the curve. The slope of the theoretical data is shown as a line drawn through zero C_L. This slope represents the structural loading simulation of the theoretically derived lift distribution. Below a C_L of 0.20 for Mach 0.98, the theoretical distribution may have less loading on the trailing wing than experimental data indicate, based on the differences in slope of the experimental and theoretical data. For larger C_L values however, theory maintains the loading on the trailing wing. The net result, considering both slope, camber and fuselage effects on the experimental data, is a more aft c.p. of wing loading.

4.1.3 Aileron Deflection

Spanwise loading due to deflection of the assumed aileron is required to balance the assymetric lateral forces associated with the oblique wing span load distribution. The distribution of section normal force coefficient for one degree of aileron deflection was calculated using the same theoretical methods as used in calculating additional lift. The distributions of section normal force and c.p. with span are presented in Figures 4.1-6 and 4.1-7.

Validation of the theoretical method was obtained by comparing the calculated rigid rolling moment with ailerson deflected to wind tunnel data. Wind tunnel data at a Mach of 0.95 with the left wing forward, gave $C_{\ell_{\delta_a}}$ values of -.00368 and -.00372 at angles of attack of 0° and 2° respectively.

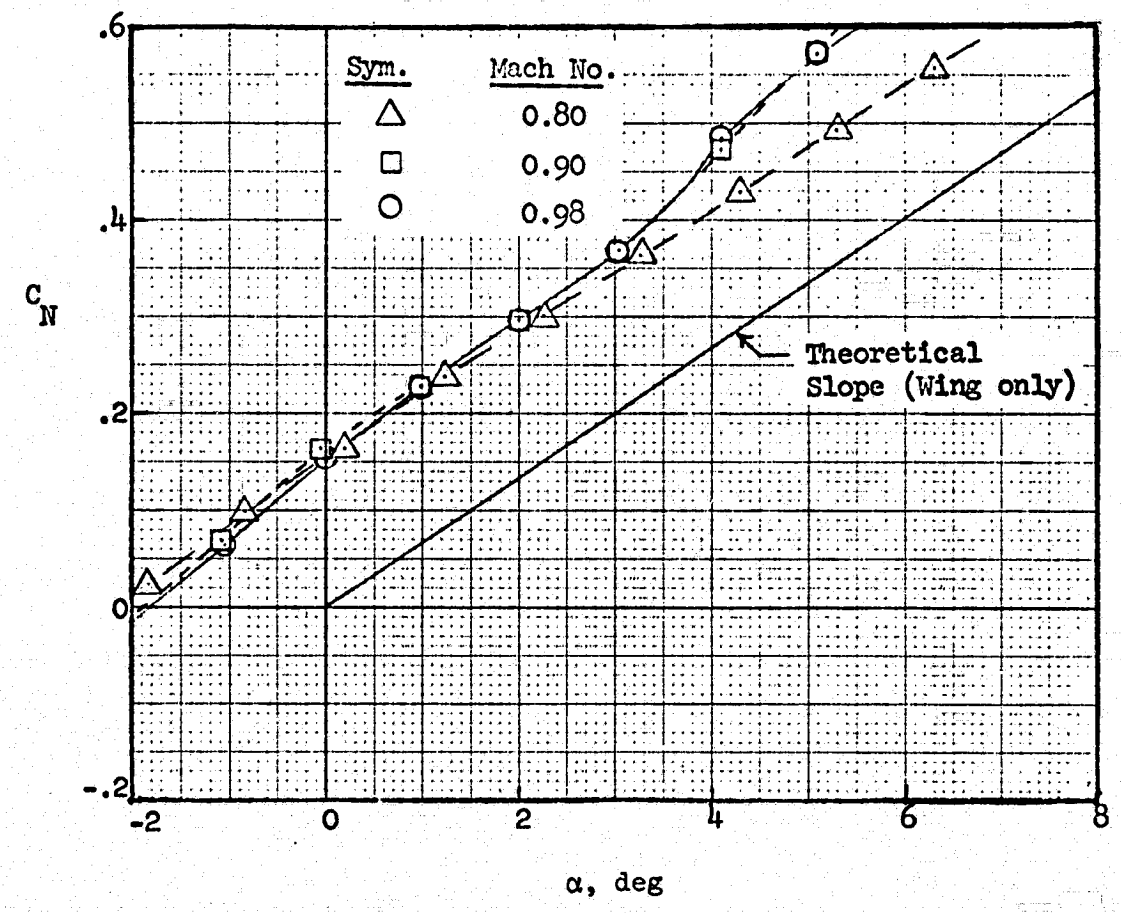

FIGURE 4.1-4 - Comparison of Theoretical Normal Force With Wind Tunnel Test Results for a Wing-Body Combination. M = 0.90

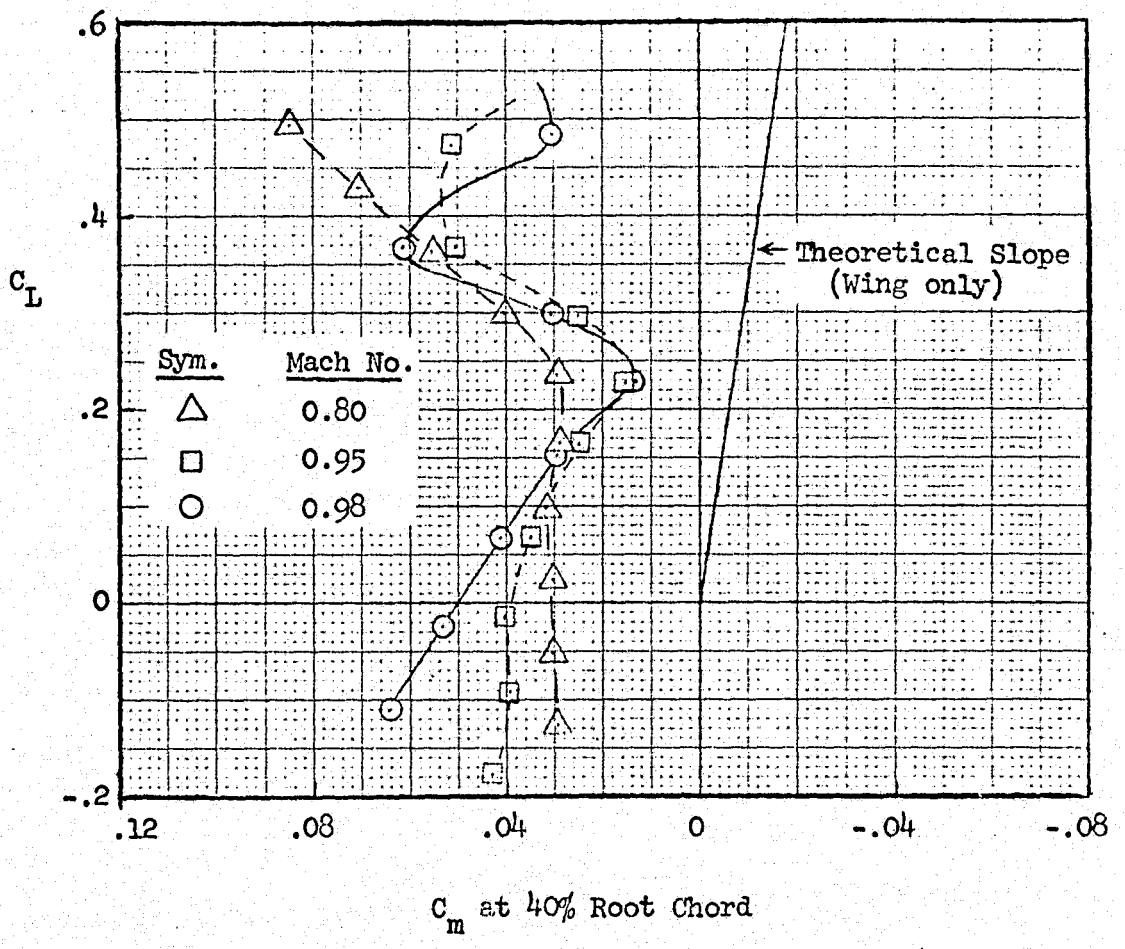

FIGURE 4.1-5 - Comparison of Theoretical Value of Pitching Moment with Wind Tunnel Test Results for a Wing-Body Combination, M = 0.90

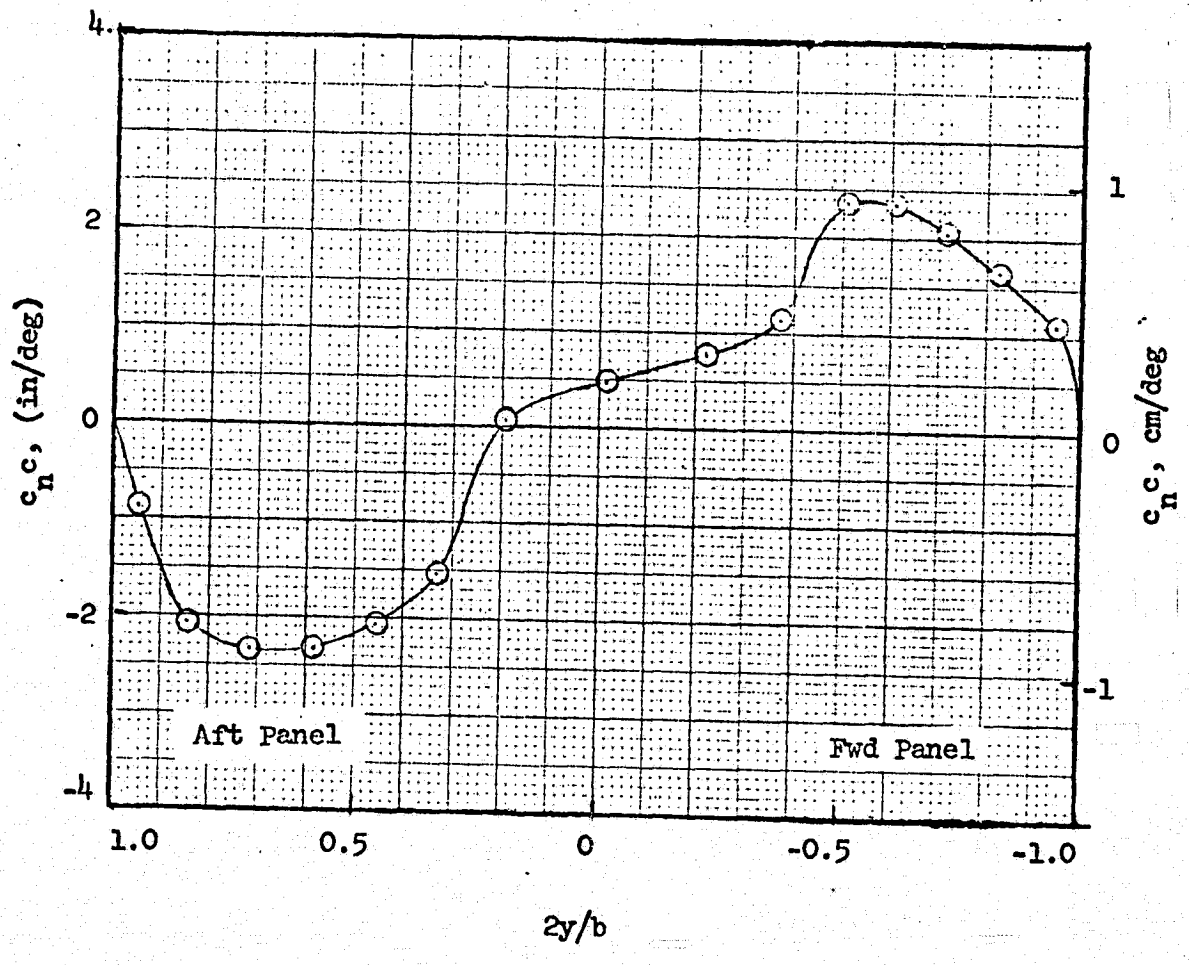

FIGURE 4.1-6 - Spanwise Distribution of Lift Due to Aileron Deflection. Wing Pivot at 50% of Root Chord. M = 0.90

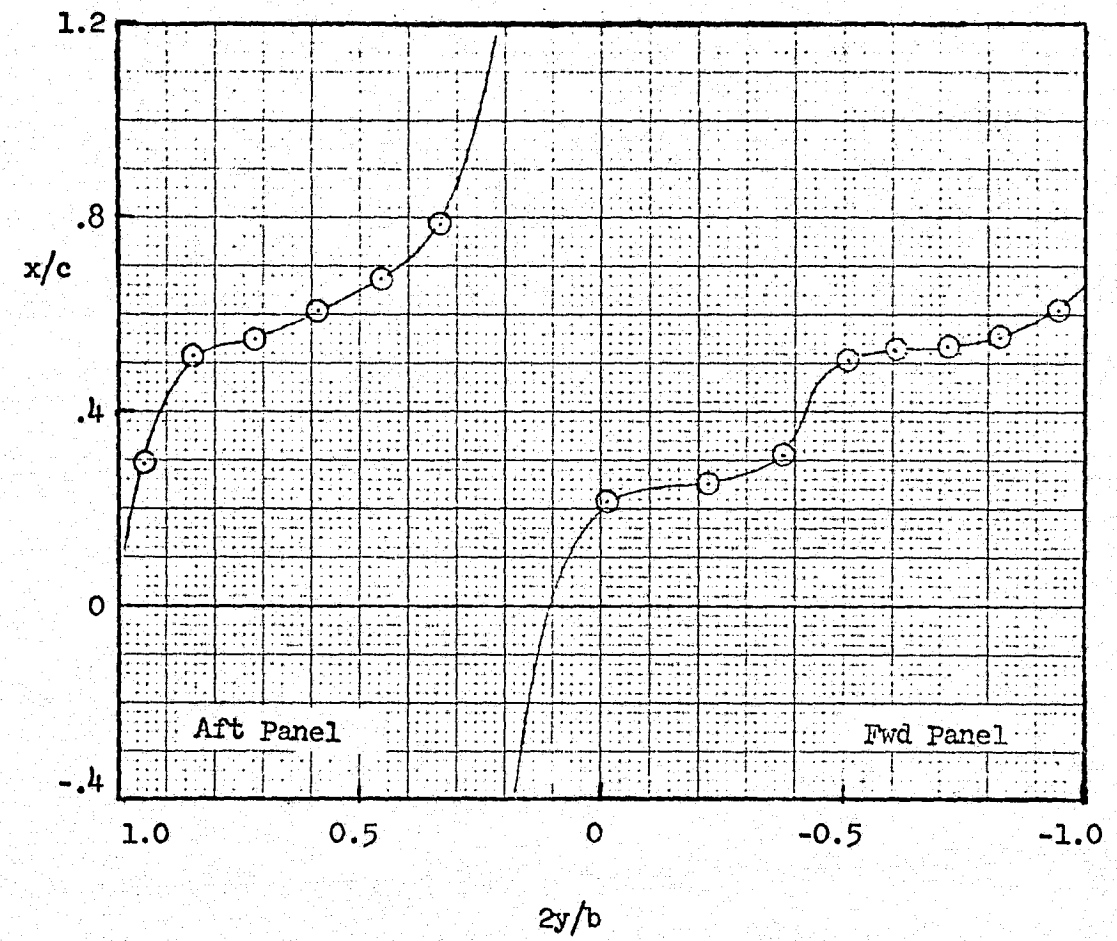

FIGURE 4.1-7 - Spanwise Variation of Section Center of Pressure for Aileron Deflection. Wing Pivot at 50% of Root Chord. M = 0.90

4.2 Structural Dynamics

4.2.1 General

The swept-forward portion of the F-8 Oblique Wing configuration presented unique aeroelastic problems. The unsteady aerodynamic formulation required forward/aft wing sweep and asymmetric fuselage interference considerations. Intensive investigation of wing bending stiffness was required to ascertain a design which would preclude divergence and flutter of the swept-forward half of the wing. To this end, a complete, asymmetric, dynamic aeroelastic analysis of the oblique wing, as attached to the F-8 fuselage, was conducted. The basic assumptions which affect the dynamic analysis are included in the general assumptions of section 3.1.

4.2.2 Analytical Methods

The inertial, damping, and stiffness terms in the linear equations of motion of the F-8 oblique wing airplane were derived in terms of 18 generalized coordinates. These differential equations have the general form

$$[m]\ddot{\underset{\sim}{q}}(t) + [c]\dot{\underset{\sim}{q}}(t) + [k]\underset{\sim}{q}(t) = \underset{\sim}{F}(t) \qquad (4.2.2\text{-}1)$$

where $\underset{\sim}{q}(t)$, $\dot{\underset{\sim}{q}}(t)$, $\ddot{\underset{\sim}{q}}(t)$ are the generalized displacements, velocities, and accelerations, repsectively.

[m] is the inertial matrix

[c] is the damping matrix from aerodynamic/viscous/structural origin

[k] is the stiffness matrix from elastic/aerodynamic origin

$\underset{\sim}{F}(t)$ is the system external forcing function vector

t is time

The generalized coordinates used in the analysis are described in section 4.2.3. These equations were transferred to the frequency domain to pose a complex eigenvalue problem for the purpose of studying the static and dynamic aeroelastic stability characteristics of the airplane. The static equilibrium solution for the airplane deflected shape at design velocity was obtained from the forced equations of motion as a special case of the transient response problem.

The wing inertial and elastic characteristics were determined using finite element methods which used discrete beam elements for the elastic properties and discrete panels for the inertial properties. Collocation points to describe these inertial/elastic wing properties were located on the wing leading and trailing edges at equal 1/20 span intervals. These points formed the boundaries of the 20 wing panels

with each pair of forward/aft points located on lines which were perpendicular to the wing elastic axis (40% wing chord line). The wing coordinates of the 42 collocation points are shown in Figure 4.2-1. The wing coordinate system is oriented along the wing 40% chord line with the origin at the wing pivot point. The collocation points are ordered as shown in Figure 4.2-1.

Unsteady aerodynamic forces for the wing were obtained using the doublet-lattice subsonic aerodynamic formulation for the entire wing. Sixty-three aerodynamic control points were used on the wing (3 chordwise (streamwise) points at 21 spanwise stations) to obtain the Mach 0.98 complex aerodynamic influence coefficient matrix for the wing at 45° sweep angle. Wing camber effects were included, but viscous (local shock) effects were not considered. Successive transformations were derived which represented the aerodynamic forces at the 42 wing collocation points and finally to the 18 airplane generalized coordinates.

Aerodynamic forces were not included on the airplane fuselage or empennage, although the aerodynamic stiffness effect on the empennage was included as an elastic spring in the various rigid airplane coordinates. Later in the analysis, an aerodynamic damping term was included in the airplane pitch coordinate. These stiffness and damping parameters were selected on the basis of typical F-8 airplane measured data. Wing control surface aerodynamics were not included.

The wing inertial distribution is given in Section 4.5. These properties were distributed to the wing collocation points on the basis of the kinetic energy of the wing due to the coordinate velocities normal to the plane of the wing. The resultant wing inertial matrix was transformed to airplane generalized coordinates and used in the flutter analyses.

The wing stiffness distribution is shown in Figures 4.4-1, 2. This bending/torsional stiffness distribution was determined from flutter requirements. Extensive stiffness variations were considered in the analyses from which these requirements developed, as described in Section 4.2.4. The wing/fuselage pivot bearing stiffness used in the dynamic analysis was 1.15×10^6 kg m/rad (1.00×10^6 in lb/rad) about both wing roll and pitch axes. (the kilogram is used here as a measure of force; the weight of a kilogram mass in a standard gravitational field). Variations of this stiffness were studied for their effect on flutter and divergence as detailed in Section 4.2.4.

Only the wing and wing pivot bearing were considered flexible in these analyses. The airplane fuselage and empennage were assumed rigid.

~~LOCATION OF~~ WING COLLOCATION POINTS FOR DYNAMIC ANALYSES

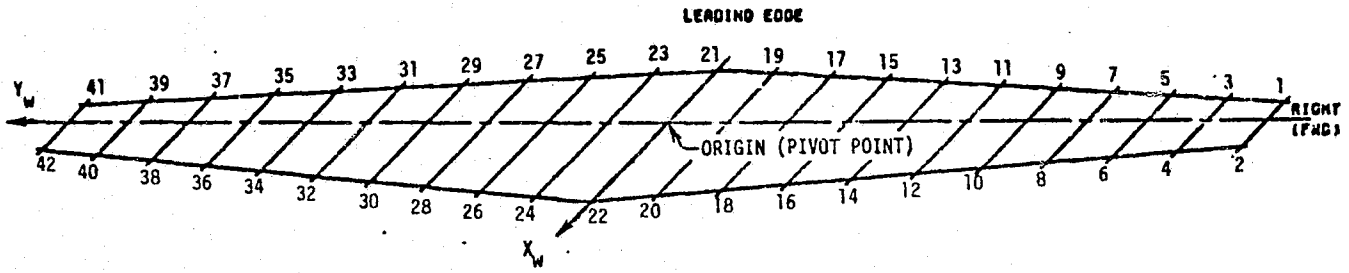

POINT NO.	XW-M	XW-(IN)	YW-M	YW-(IN)	POINT NO.	XW-M	XW-(IN)	YW-M	YW-(IN)
1	-.30809	-12.12960	-7.62000	-300.00000	22	1.36666	53.80560	0.00000	0.00000
2	.46214	18.19440	-7.62000	-300.00000	23	-.85081	-33.49632	.76200	30.00000
3	-.36839	-14.50368	-6.85800	-270.00000	24	1.27621	50.24448	.76200	30.00000
4	.55259	21.75552	-6.85800	-270.00000	25	-.79050	-31.12224	1.52400	60.00000
5	-.42870	-16.87776	-6.09600	-240.00000	26	1.18576	46.67336	1.52400	60.00000
6	.64304	25.31664	-6.09600	-240.00000	27	-.73020	-28.74816	2.28600	90.00000
7	-.48900	-19.25184	-5.33400	-210.00000	28	1.09530	43.12224	2.28600	90.00000
8	.73350	28.87776	-5.33400	-210.00000	29	-.66990	-26.37408	3.04800	120.00000
9	-.54930	-21.62592	-4.57200	-180.00000	30	1.00485	39.56112	3.04800	120.00000
10	.82395	32.43888	-4.57200	-180.00000	31	-.60960	-24.00000	3.81000	150.00000
11	-.61960	-24.00000	-3.81000	-150.00000	32	.91440	36.00000	3.81000	150.00000
12	.91440	36.00000	-3.81000	-150.00000	33	-.54930	-21.62592	4.57200	180.00000
13	-.66990	-26.37408	-3.04800	-120.00000	34	.82395	32.43888	4.57200	180.00000
14	1.00485	39.56112	-3.04800	-120.00000	35	-.48900	-19.25184	5.33400	210.00000
15	-.73020	-28.74816	-2.28600	-90.00000	36	.73350	28.87776	5.33400	210.00000
16	1.09530	43.12224	-2.28600	-90.00000	37	-.42870	-16.87776	6.09600	240.00000
17	-.79050	-31.12224	-1.52400	-60.00000	38	.64304	25.31664	6.09600	240.00000
18	1.18576	46.67336	-1.52400	-60.00000	39	-.36839	-14.50368	6.85800	270.00000
19	-.85081	-33.49632	-.76200	-30.00000	40	.55259	21.75552	6.85800	270.00000
20	1.27621	50.24448	-.76200	-30.00000	41	-.30809	-12.12960	7.62000	300.00000
21	-.91111	-35.87040	0.00000	0.00000	42	.46214	18.19440	7.62000	300.00000

FIGURE 4.2-1 - Wing Collocation Points for Dynamic Analisis

4.2.3 Modal Description

The 18 generalized coordinates used in the dynamic analyses are listed in Table 4.2-1. These degrees-of-freedom may be classified as 10 uncoupled, elastic wing coordinates; 3 elastic wing/fuselage pivot bearing coordinates; and 5 airplane rigid-body coordinates.

Since the original wing concept required consideration of asymmetric structure, the 10 wing coordinates selected consisted of uncoupled bending and torsional modes for the left (aft) and right (forward) portions of the wing, taken separately. This choice of wing elastic coordinates facilitated rapid flutter and divergence analyses for numerous independent variations of torsional/bending - forward/aft wing stiffness distributions. Additionally, any symmetric, anti-symmetric, or asymmetric wing deformations are permitted with this choice of modal coordinates. The wing elastic modes are shown in Figures 4.2-2 through 4.2-6.

The 3 elastic wing/fuselage pivot bearing coordinates are wing roll (left wing down positive), wing pitch (nose up positive), and wing vertical translation (down positive). These coordinates were taken at the wing pivot point (W.S. = 35.87, W.B.L. = 0 and F.S. = 463.53, W.L. = 143.0). The generalized stiffness for both wing roll and pitch were assumed to be 1.15×10^6 kg-m/rad (1.00×10^8 in-lb/rad). For the vertical translation coordinate the generalized stiffness was assumed to be 2.15×10^3 kg/m (1.20×10^6 lb/in). The 5 airplane rigid-body coordinates selected were fuselage roll (left wing down positive), pitch (nose up positive), yaw (nose right positive), lateral translation (left positive), and vertical translation (down positive). These coordinates were defined at FUS STA = 454.4, WL = 96.4, BL = 0, the approximate fuselage center of mass. Generalized stiffnesses associated with these coordinates were based on estimated, airplane-without-wing-aerodynamics, rigid-body frequencies of .01, .7, .7, .01, .01 Hz, respectively.

It should be noted that in the initial portion of the study, only wing elastic and pivot bearing coordinates were used for dynamic analyses. It quickly became evident that the flutter results from these analyses were not realistic. This was particularly evident in the case of wing divergence, since without control surfaces on the wing, the clamped fuselage condition produced an artificial wing divergence which could not occur with the inclusion of fuselage degrees-of-freedom. Thus, the 5 fuselage coordinates were used in subsequent dynamic analyses. The effect of selected degrees-of-freedom on airplane flutter is described in Section 4.2.4. References 2 and 3 detail similar results on other oblique wing configurations.

4.2.4 Aeroelastic Results

4.2.4.1 Wing Deflected Shape at Design Velocity

The aeroelastic wing deflected shape at design velocity was obtained from Equation 4.2.2-1 with only the static terms retained.

$$[k]\, \underset{\sim}{q} = \underset{\sim}{F} \qquad (4.2.4.1\text{-}1)$$

TABLE 4.2-1

AIRPLANE MODAL COORDINATE DESCRIPTION

COORD NO.	DESCRIPTION	FREQ (Hz)
1	WING BENDING, FWD (RT), TIP UP	6.24
2	WING BENDING, AFT (LFT), TIP UP	6.24
3	WING BENDING, AFT (LFT), TIP UP	20.4
4	WING BENDING, FWD (RT), TIP DWN	20.4
5	WING BENDING, FWD (RT), TIP UP	47.2
6	WING BENDING, AFT (LFT), TIP DWN	47.2
7	WING TORSION, AFT (LFT), TIP NOSE UP	67.7
8	WING TORSION, FWD (RT), TIP NOSE DWN	67.7
9	WING TORSION, AFT (LFT), TIP NOSE UP	115.
10	WING TORSION, FWD (RT), TIP NOSE DWN	115.
11	PIVOT BEARING, ROLL (XW), LFT WNG DWN	3.80
12	PIVOT BEARING, PITCH (YW), NOSE UP	40.1
13	PIVOT BEARING, VERT TRANSL, DWN	50.0
14	FUSELAGE, ROLL, LFT WNG DWN	0.01
15	FUSELAGE, PITCH, NOSE UP	0.70
16	FUSELAGE, YAW, NOSE RT	0.70
17	FUSELAGE, LAT TRANSL, LFT	0.01
18	FUSELAGE, VERT TRANSL, DWN	0.01

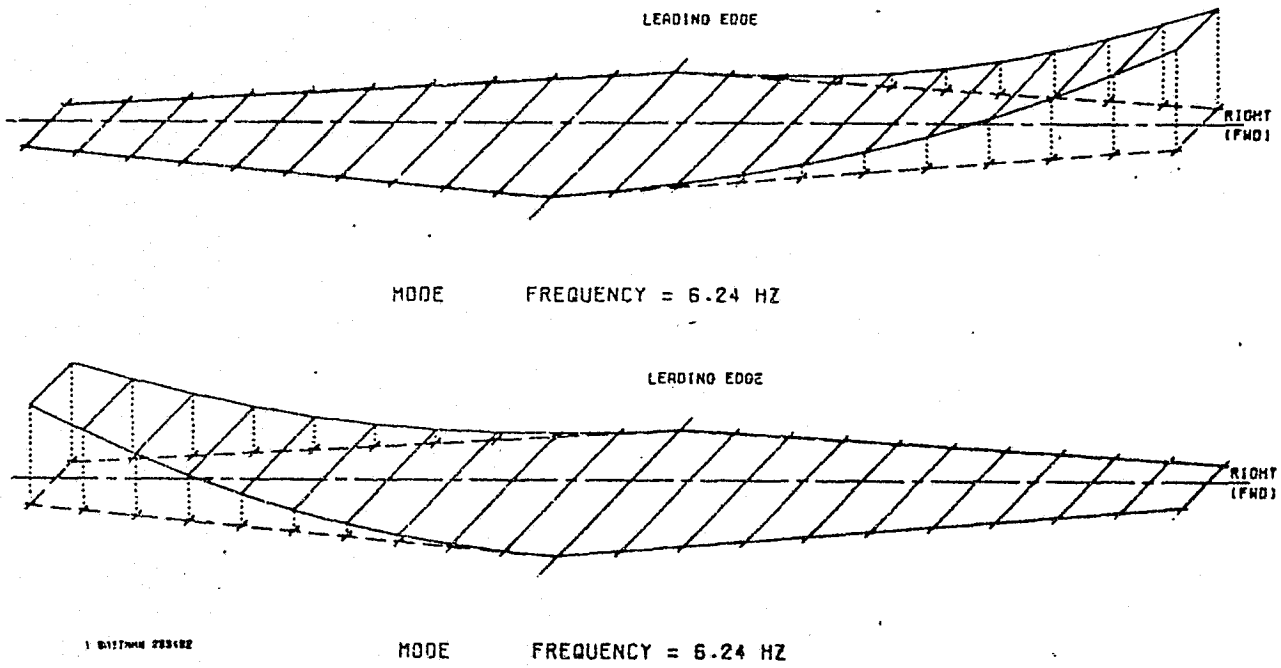

FIGURE 4.2-2 - Uncoupled Elastic Modes. First Wing Bending (Cantilevered at Center).

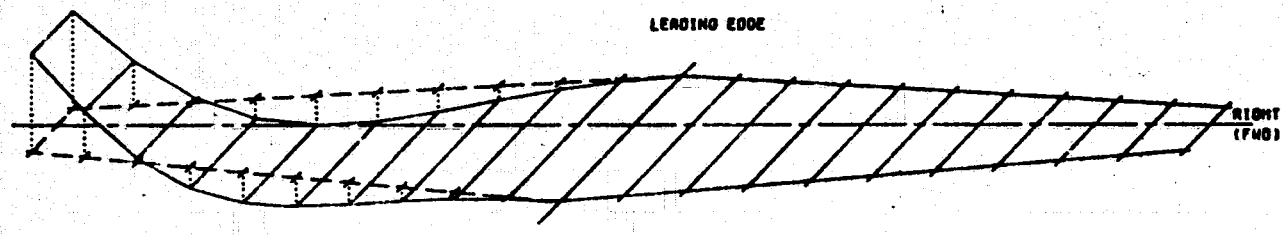

MODE FREQUENCY = 20.44 HZ

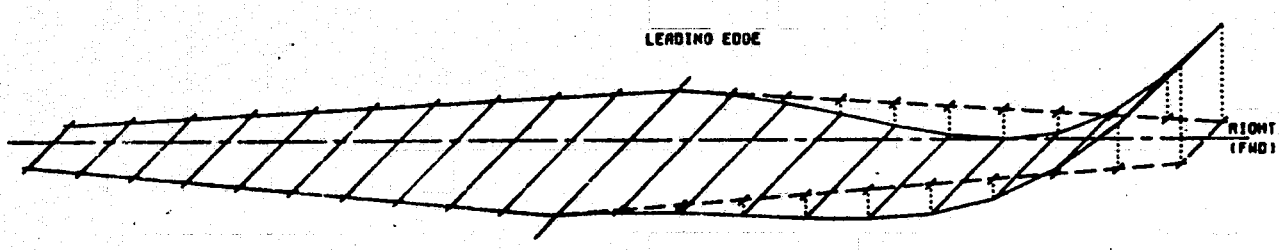

MODE FREQUENCY = 20.44 HZ

FIGURE 4.2-3 - Uncoupled Elastic Modes. Second Wing Bending (Cantilevered at Center).

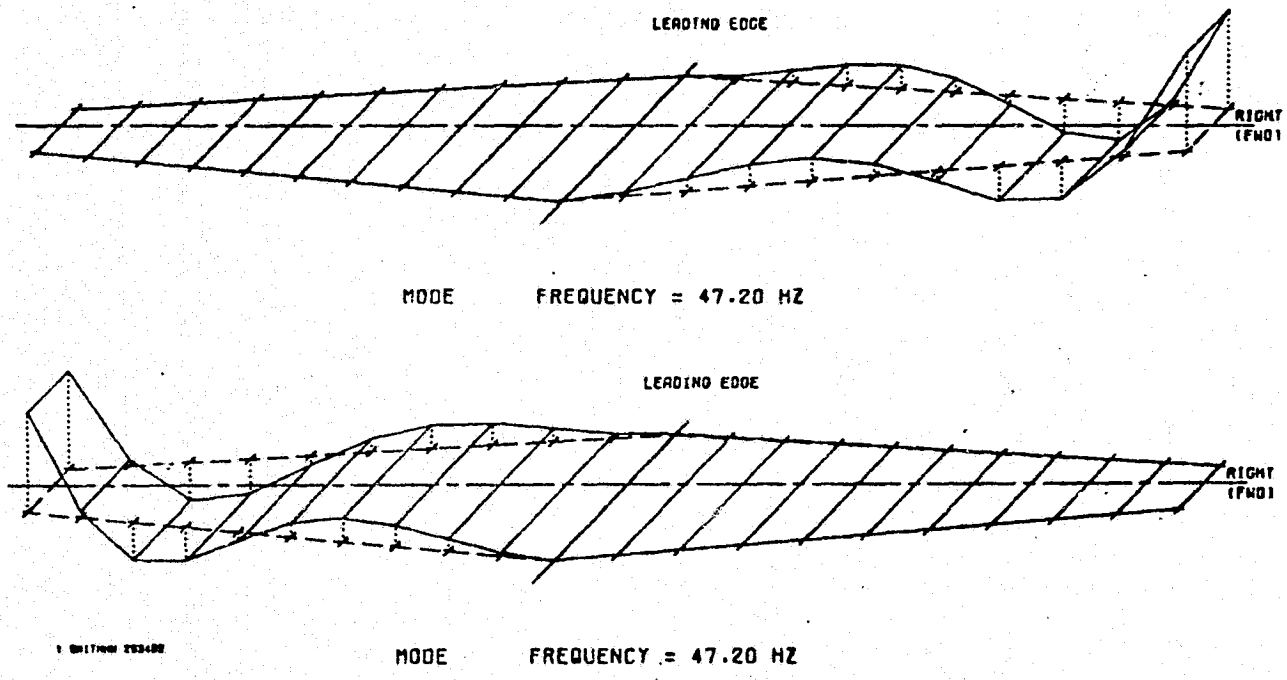

FIGURE 4.2-4 - Uncoupled Elastic Modes. Third Wing Bending (Cantilevered at Center).

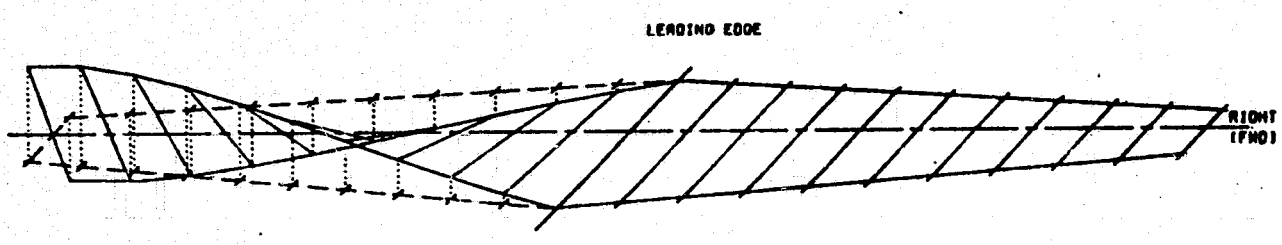

MODE FREQUENCY = 67.66 HZ

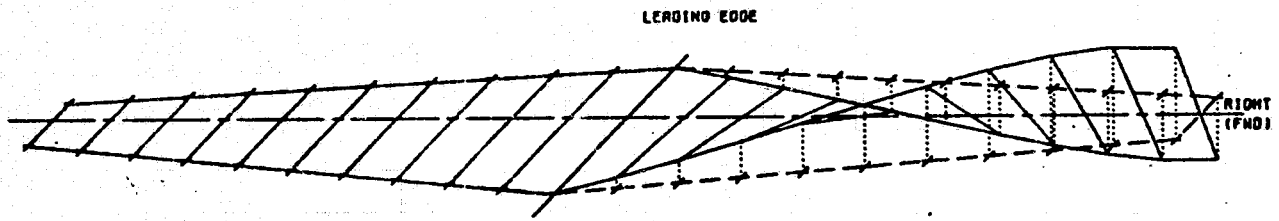

MODE FREQUENCY = 67.66 HZ

FIGURE 4.2-5 - Uncoupled Elastic Modes. First-Wing Torsion (Cantilevered at Center).

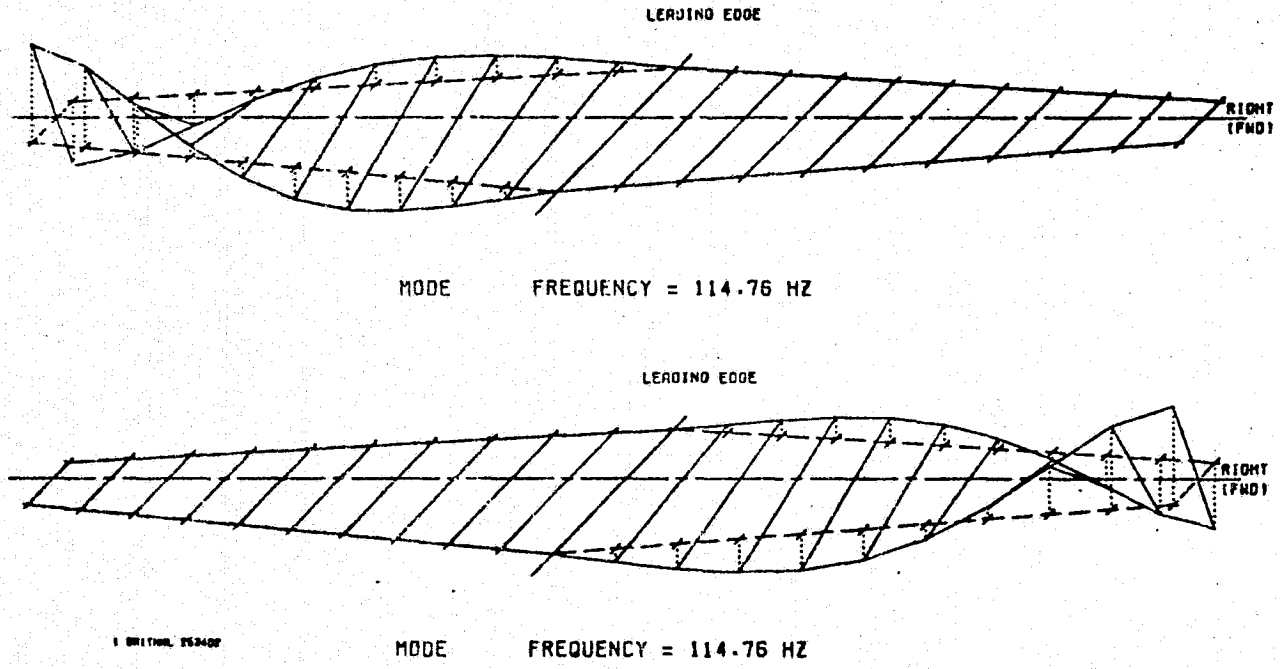

FIGURE 4.2-6 - Uncoupled Elastic Modes. Second Wing Torsion (Cantilevered at Center).

Here the total stiffness matrix, $[k]$, is composed of elastic and aerodynamic stiffness terms. The forcing function, $\underset{\sim}{F}$, is the vector of generalized weights. Since control surfaces were not included in the analyses, the straightforward solution of this problem for the generalized displacements, $\underset{\sim}{q}$, in the form

$$\underset{\sim}{q} = [k]^{-1} \underset{\sim}{F} \qquad (4.2.4.1\text{-}2)$$

would produce extremely large airplane roll and vertical translation displacements. Therefore, these 2 coordinates were constrained. Further equilibrium conditions in airplane roll and pitch were neglected to obtain a 16th order system of equations with a non-singular coefficient matrix. This matrix equation was solved for the generalized displacements, $\underset{\sim}{q}$.

The resultant wing displacements are shown in Figure 4.2-7. The design point is Mach 0.98 at 6.1 km (20,000 ft.), 226.4 m/s (440 knots) equivalent air speed. The upper plot shows the total wing deformation including the elastic wing/fuselage pivot bearing. The lower plot shows only the elastic wing deformation without the contribution of the flexible bearing. Note that the forward (right) wing deforms considerably more than the aft wing. The slope of the elastic wing only deformation along the wing elastic axis is 5.84×10^{-2} rad (3.33°) up (above the undeformed wing plane) on the forward (right) wing tip and 2.67×10^{-2} rad (1.53°) up on the aft wing tip.

4.2.4.2 Airplane Divergence

Aeroelastic divergence of swept-forward wings has long been recognized as a limiting factor on wing design. For symmetric airplanes, the tranditional cantilever wing analysis for divergence has some merit. For the oblique wing configuration, however, a cantilever wing or clamped fuselage analysis for divergence is not realistic since for the free airplane there is no static mechanism to sustain the high airplane rolling moments which occur prior to wing divergence. Hence, for the wing without control surfaces, the cantilevered wing and clamped fuselage stability analyses were performed only for reference purposes and were not used as stiffness design criteria. As a matter of record, the clamped fuselage and cantilevered wing divergence analyses for the design wing showed divergence velocity margins of 23% and 45%, respectively, above the design velocity.

The complete airplane divergence analyses were included as special cases for all the flutter analyses performed on the various stiffness designs. The divergence results for the selected design stiffness are shown in Figure 4.2-8 as a wing displaced shape for the lowest airplane divergence speed. The associated divergence velocity is 221 m/s (430 knots) EAS, or 2% below the design velocity. Note that the figure shows very little wing elastic deformation in the divergence mode. In fact, this mode of divergence is quite distinct from the clamped or cantilevered divergence results. Nevertheless, the flexibility of the wing remains essential to the existence of this mode of instability, as subsequent analyses showed that divergence did not exist for a completely rigid airplane. The "almost rigid" airplane

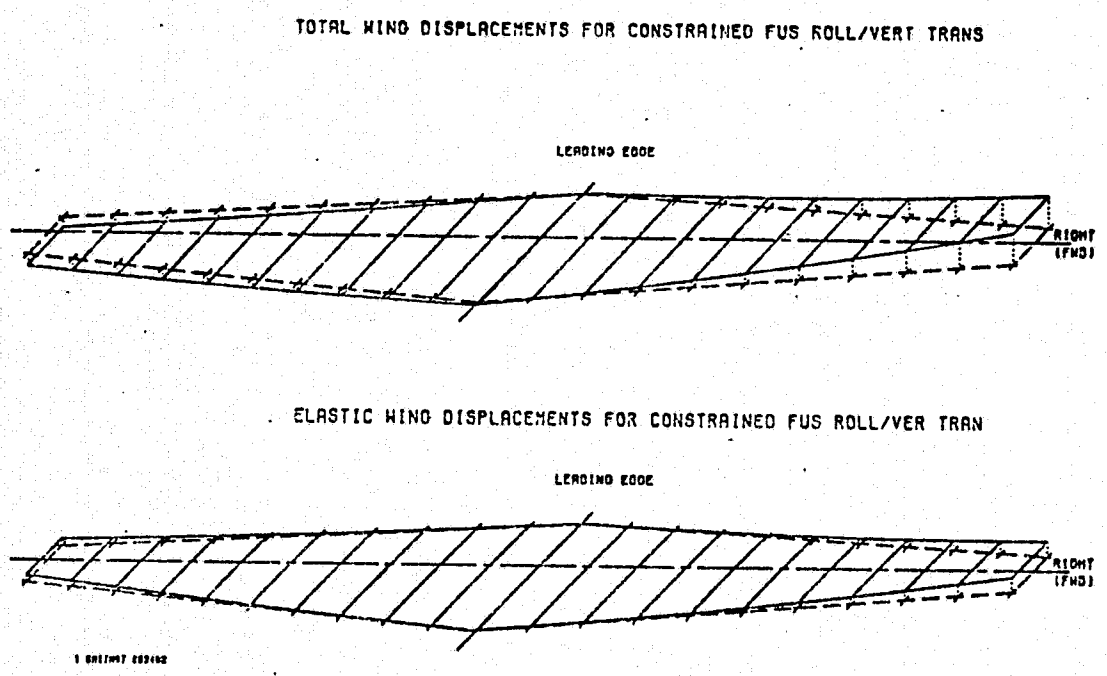

FIGURE 4.2-7 - Design Velocity Displaced Shape of the Wing.

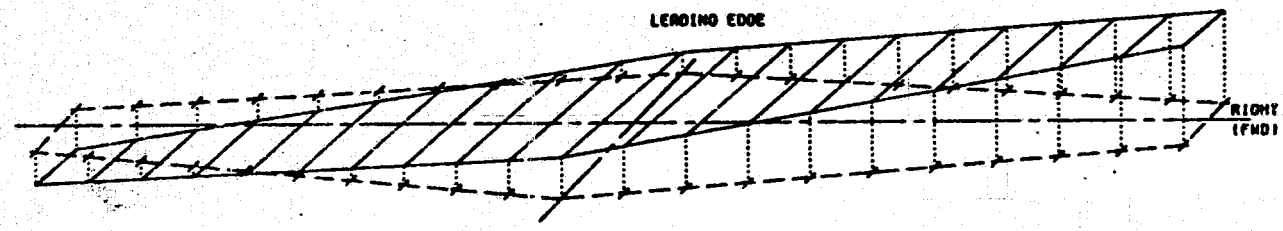

FIGURE 4.2-8 - Wing Displaced Shape at Lowest Airplane Divergence Speed.

divergence implied by these results would be resolved by the inclusion of control surfaces in the analyses. Hence, the low divergence velocity obtained for this mode was not considered a detriment to the wing design and was not critical to the wing stiffness selection.

4.2.4.3 Airplane Flutter

Flutter was the primary phenomenon which set the wing stiffness shown in Section 4.4. The basic airplane flutter plot ("v-g" plot) is shown in Figure 4.2-9. Note here that positive damping corresponds to unstable points on the plot. The two lowest velocity flutter branches are shown by broken lines in the figure. All other flutter points are in excess of twice the design velocity.

The basic airplane flutter branch shows flutter occurring at 309 m/s (600 knots) EAS at 2.5 Hz. This represents a flutter margin of 36% in excess of the design velocity. The key modes involved in this flutter are forward (right) wing bending and airplane roll. Figure 4.2-10 shows the wing displacement in the complex flutter mode at 1/8th period time intervals of the flutter cycle. Instead of classical bending-torsion type of flutter, this flutter has a local streamwise angle-of-attack variation resulting from spanwise wing bending as its primary characteristic and energy source mechanism.

The lowest velocity flutter branch shown in Figure 4.2-9 has airplane flutter occurring at 252 m/s (490 knots) EAS at .56 Hz, or a flutter margin of only 11% on the design velocity. Figure 4.2-11 shows the wing displacements in the complex flutter mode during one flutter cycle. Note the wing motion involves primarily airplane pitch, roll, and vertical translation - or only rigid airplane modes. Actually, the small wing bending involvement in this instability is essential to its existence. This low frequency flutter was evident in the study from the first time airplane pitch and roll degrees-of-freedom were added to the wing elastic modes. It usually occurred at a low velocity (60-70% of design velocity) at a frequency of .7 Hz (near the airplane short-period mode frequency). It was determined that the essential damping in the pitch mode was inadequately represented by only wing aerodynamics (empennage aerodynamics are not considered) and artificial airplane aerodynamic damping of 20% critical damping in the pitch mode was added to the flutter formulation. Thus, in the flutter plot, it is seen that this flutter branch exhibits near 40% structural damping characteristics at low velocities before becoming unstable at a much greater velocity than the unaltered case. This low frequency flutter result is not considered a major detriment to the wing design because:

(a) The actual instability mode characteristics cannot accurately be determined until unsteady empennage aerodynamics are included in the analyses

(b) If a more complete analysis confirms the existence of this mode at relatively low velocity, the very low frequency of the motion (.56 Hz) would ideally be included in the control system design to permit automatic stabilization of this mode.

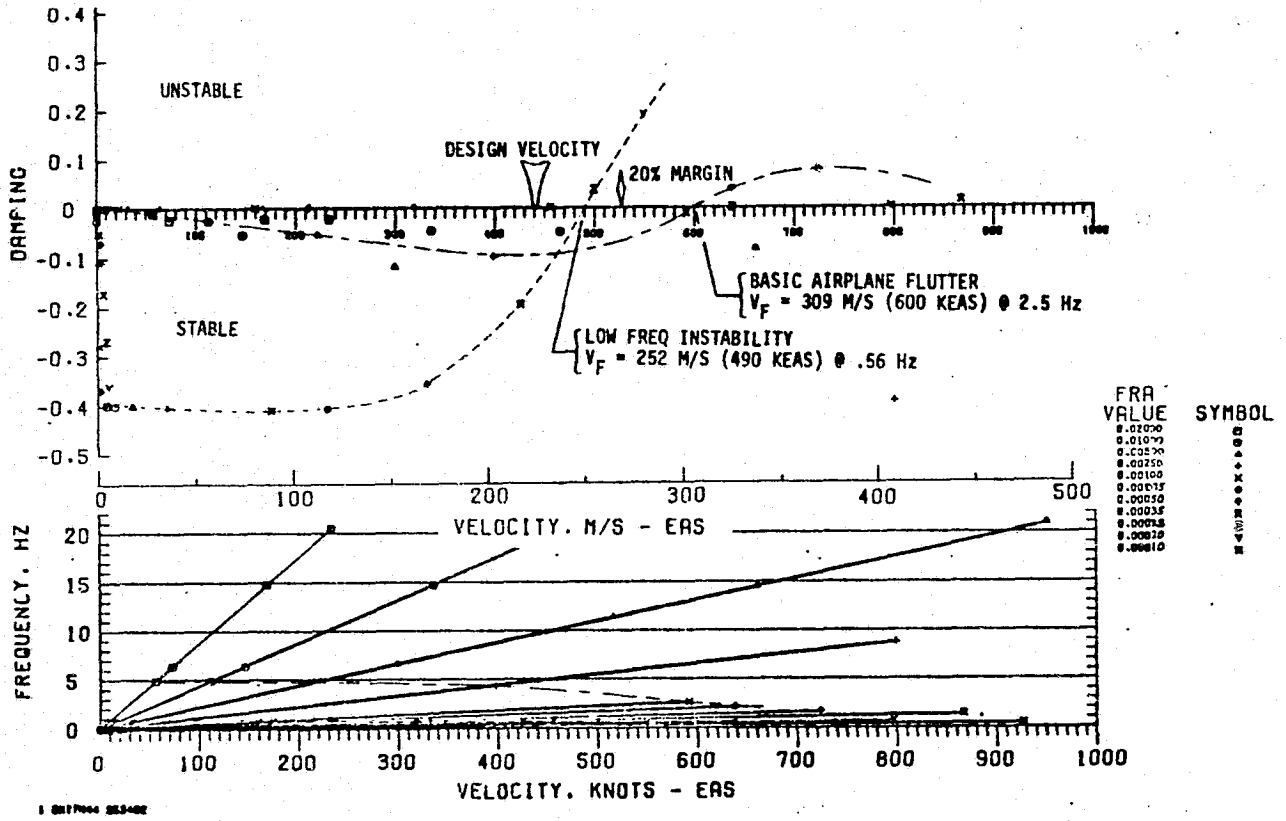

FIGURE 4.2-9 - Basic Airplane Flutter

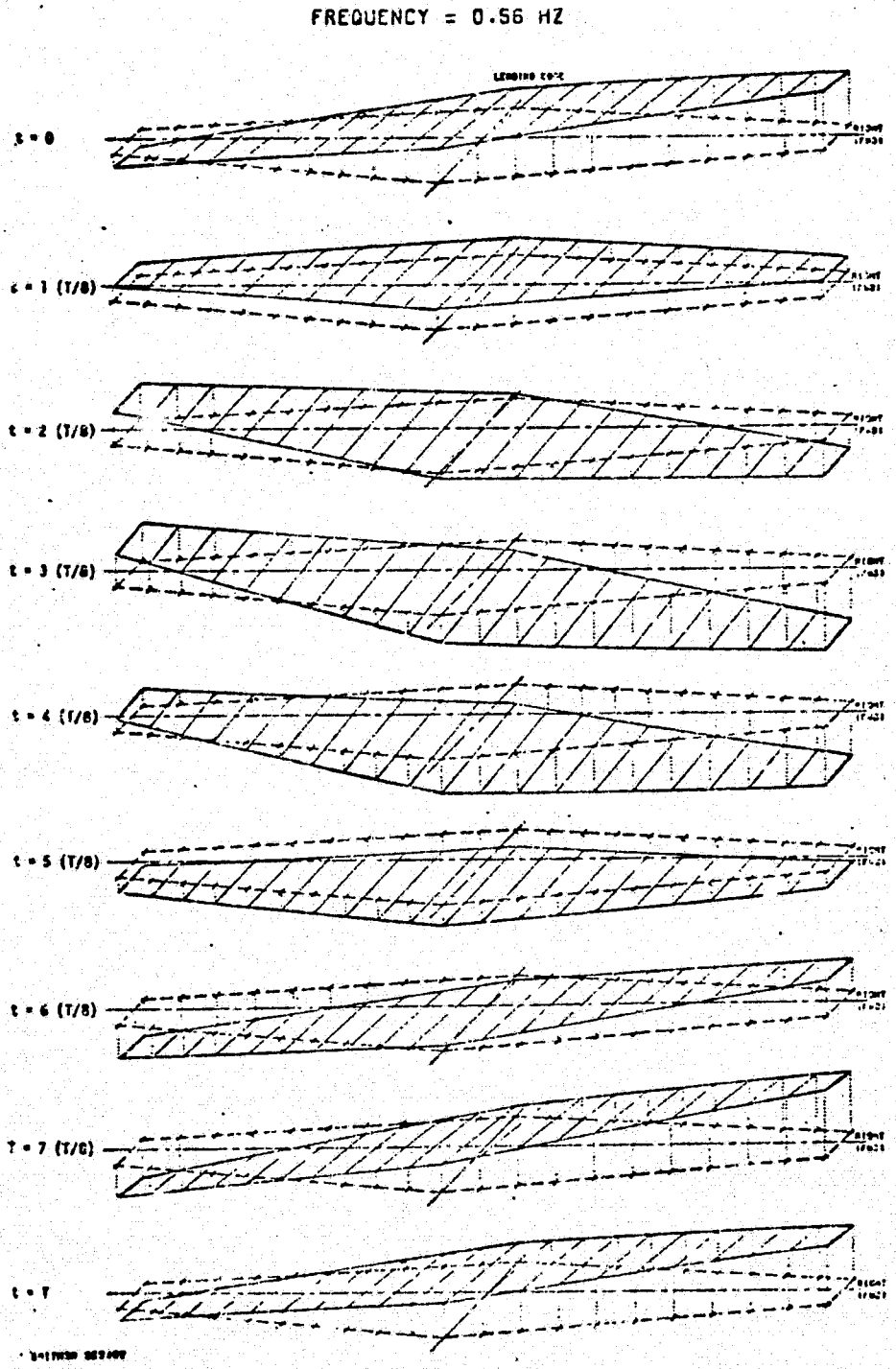

FIGURE 4.2-10 - Low Frequency Flutter Mode. Wing Shape at 1/8 period Intervals

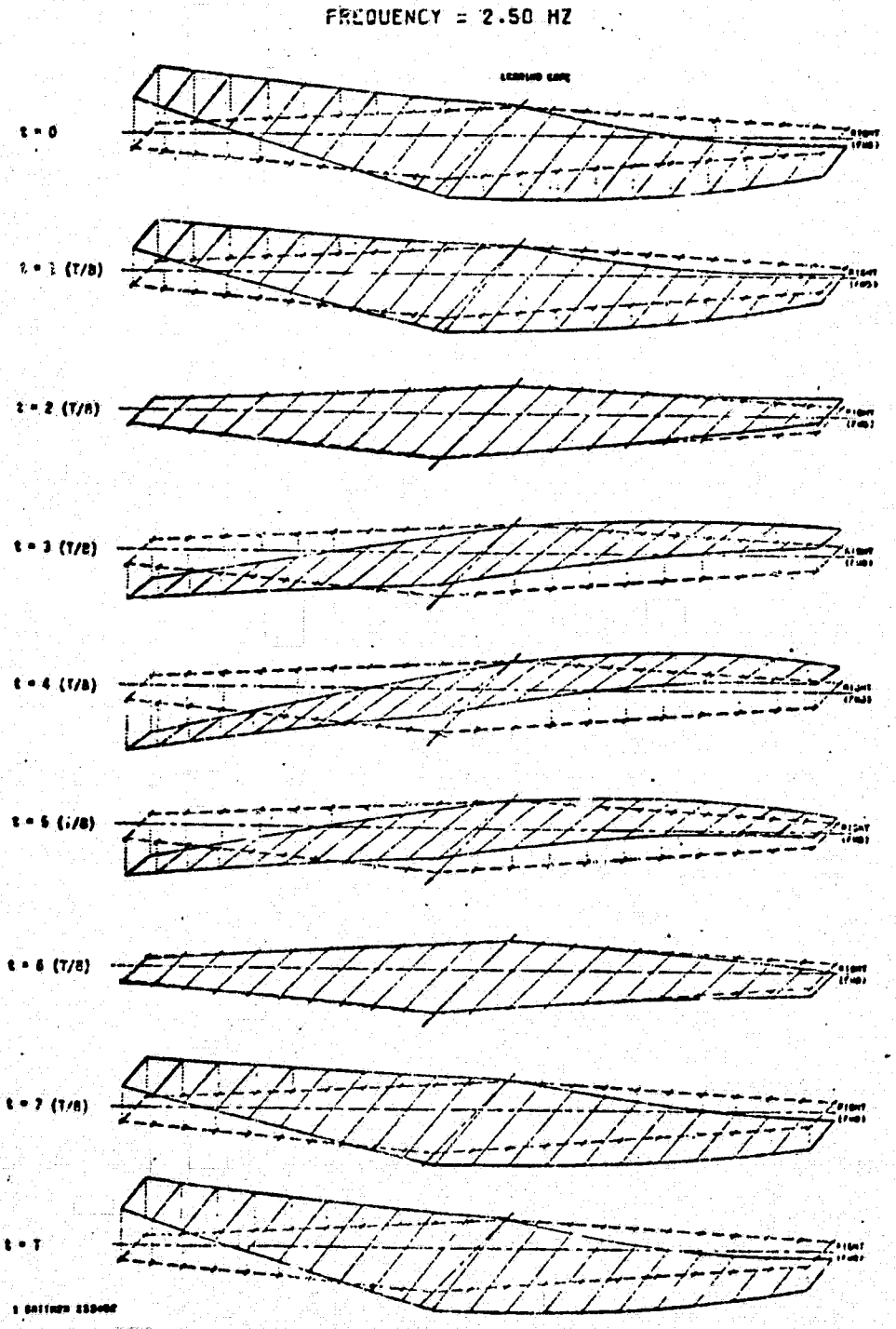

FIGURE 4.2-11 - Basic Airplane Flutter Mode. Wing Shape at 1/8 period Intervals.

Most of the computational effort in the flutter analyses was devoted to wing stiffness variations. The objective of these variations was a simple, structurally efficient wing which would show the required 20% flutter margin. The trend of these analyses pointed toward a wing with greater bending than torsional stiffness and with the forward (right) portion of the wing 2-3 times as stiff as the aft. As the study progressed, the requirement of simplicity gradually took precedence over the requirement of structural efficiency, and as a consequence, a stiff, symmetric wing design was chosen.

The flutter margin of 36% on the basic airplane flutter branch implies that the oblique wing is stiffer than required for a 20% margin. The implication is correct - this is a consequence of the wing elastic stiffness being fixed before the complete set of other design parameters were determined. Administrative constraints required that the iterative design process stop at this point. As refined data (particularly inertial data) were included in the flutter analyses, the basic flutter speed increased. In fact, preliminary analyses indicated that a reduction in wing elastic stiffness of up to 30% would still permit the attainment of the required 20% margin on basic airplane flutter and divergence. Recommendations for continued analyses are offered below.

Sensitivity of flutter to wing bending, torsion, and pivot bearing stiffness variations was determined about the design point. The basic airplane flutter gradients or sensitivities for small changes of these parameters are:

(a) Wing bending - 40%

(b) Wing torsion - 10%

(c) Pivot bearing roll/pitch - 20%

E.g., if the pivot bearing roll stiffness were increased 10%, the basic airplane flutter speed would increase about 2%, etc. Similarly, the low frequency flutter showed sensitivities of:

(a) Wing bending - 10-20%

(b) Wing torsion - 0%

(c) Airplane pitch -4%

(d) Pivot bearing roll/pitch - 0%

It should be emphasized that these were approximate sensitivities for small changes; large changes could produce drastically different flutter results, including a change of sign of the sensitivity.

The effect of various degrees-of-freedom on the flutter and divergence results was studied at length. Analyses ranged from 2-coordinate to 18-coordinate complex eigenvalue problems. The degrees-of-freedom necessary for the existence of the following instabilities were determined to be:

(a) Low frequency flutter - wing elastic + fuselage roll + fuselage pitch

(b) Basic airplane flutter - wing elastic + fuselage roll

(c) Basic airplane divergence - wing elastic + fuselage pitch

Of course, flutter instabilities for only wing coordinates did exist, but the associated velocities were above the range of interest.

For a completely rigid airplane, no instabilities were evident within the velocity range of interest. The effect of adding these rigid fuselage coordinates to the wing coordinates is illustrated in Figure 4.2-12. This figure was constructed for comparison with a similar figure of Reference 2. Note here that positive damping corresponds to a stable condition. The significant difference in this figure and the corresponding figure of Reference 2 is the existence of the low frequency flutter branch which became unstable at a velocity lower than the clamped fuselage wing divergence velocity. The dynamic pressure used for normalization of the abscissa in this figure is the wing-with-flexible-pivot-bearing divergence speed (i.e. the clamped fuselage wing divergence speed).

Although the F-8 oblique wing design is free of primary aeroelastic instabilities within the required 20% margin on the design velocity, the need for additional dynamic analyses is indicated. These studies are included in Phase I and should be pointed toward:

(a) Improving the mathematical model of the airplane by including empennage unsteady aerodynamics and by including a flexible fuselage

(b) Structural optimization of the wing with the effects of the improved model considered.

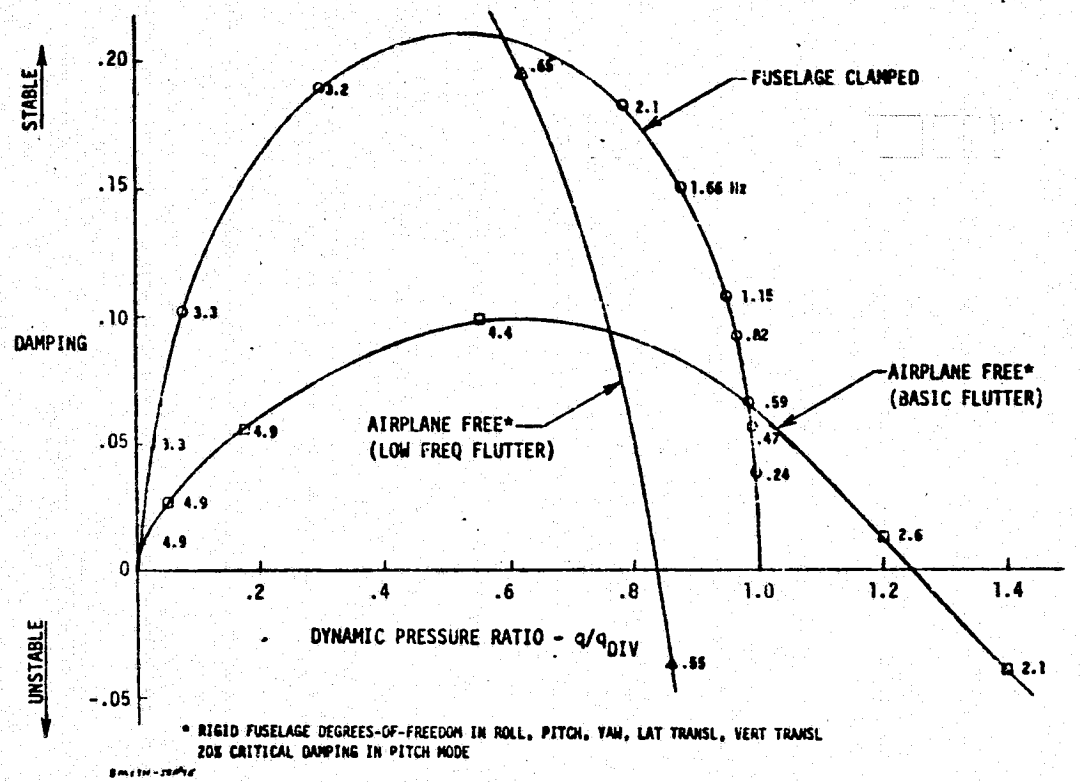

FIGURE 4.2-12 - Aeroelastic Stability. Effect of Fuselage Freedom on Flutter.

4.3 Loads

Wing loads are calculated using the NASA-Ames supplied computer routine AIRLOD (reference 4). This routine will analyze the subsonic aeroelastic characteristics of an oblique swept wing. AIRLOD was modified to include the effects of compressibility, to calculate distributed airload and moment due to aileron deflection, and to calculate the combined center of pressure distribution for additional lift plus aileron deflection. The $c_{m_{\delta_A}}$ distribution was ratioed to match the aileron center of pressure distribution generated by the Carmichael-Woodward aerodynamic routine (see Section 4.1).

The aeroelastic running load distributions include the effects of angle-of-attack, aileron deflection, structural twist due to airload, and twist due to mass distribution. The oblique wing does not have built-in-tist. Wing camber effects are not included in the study since the computer routine AIRLOD does not have this capability. Roll trim is achieved using only aileron control. Only steady state symmetrical pull-up and push-over maneuvers are considered. For a symmetric pull-up manuever with a flexible wing the aileron, deflection produces a right-wing-down rolling moment to maintain roll equilibrium.

The loads work was completed prior to the decision to move the pivot location from the 50% chord to the 40% chord. Consequently the airload distributions are based on wing geometry associated with the 50% chord pivot. These loads are still adequate for the purpose of the present feasibility study.

The oblique wing running load and center of pressure distributions were determined for the symmetric steel wing and asymmetric steel/aluminum wing where the right wing (fwd) is steel and the left wing (aft) is aluminum. The n_z due to a maximum equivalent gust velocity of 15.24 m/s (50 ft/s) of a single gust at Mach = 0.90 and altitude = 4816 m (15 800 ft) need not be considered since $n_{z_{gust}}$ = 1.0 ± 1.5 = +2.5, -0.5, which is less than symmetric maneuver load factor. The following conditions were investigated:

a. Mach = 0.90 (see Section 4.1)

b. Altitude = 4816 m(15 000 ft)

c. Dynamic pressure = 3198 kg/m^2 (655 psf)

d. n_z = 3.0, -1.0

e. Airplane gross weight = 12,118 kg (26 720 pounds)

f. Wing is skewed $\frac{\pi}{4}$ (45°) with the right semi-span forward.

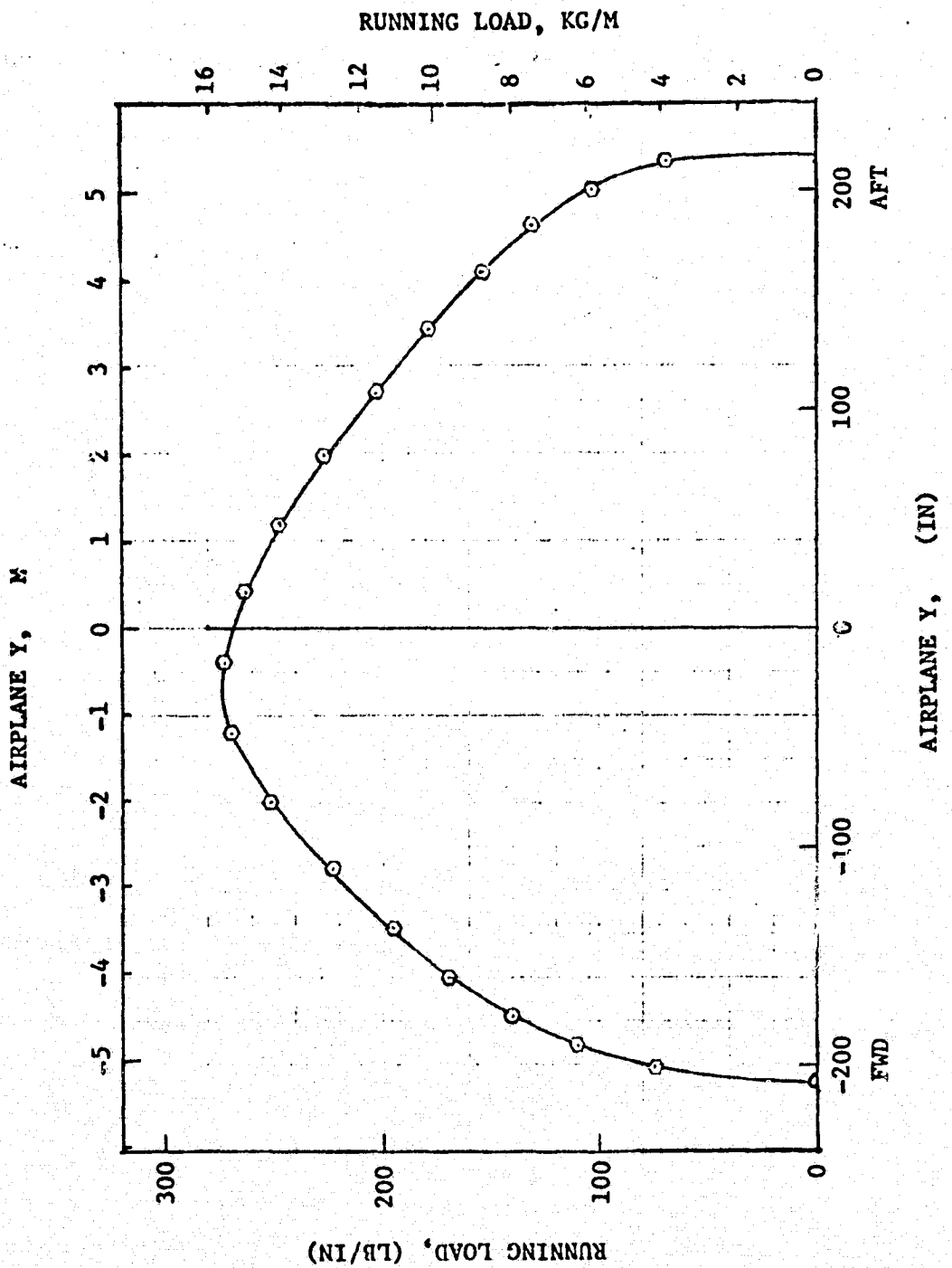

FIGURE 4.3-1 - RUNNING LOAD, n_z = 3.0

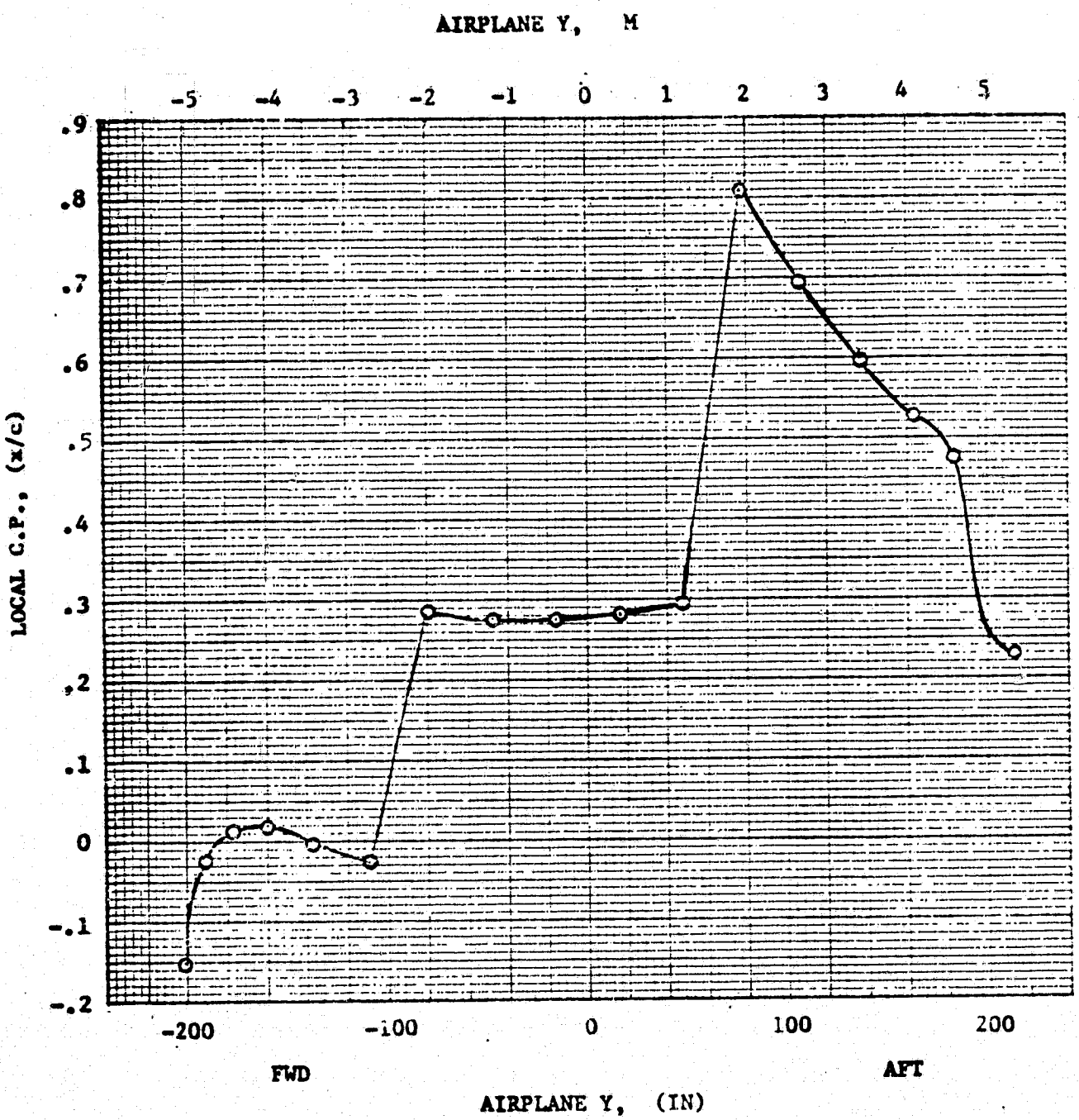

FIGURE 4.3-2 - LOCAL CENTER OF PRESSURE

Results for the symmetric steel wing at $n_z = 3.0$ are presented in Figures 4.3-1 and 4.3-2, where running load distribution is presented in Figure 4.3-1 and center of pressure (C.P.) distribution is shown in Figure 4.3-2. Due to the lack of wing camber influence the running load distribution for $n_z = -1$ has the same shape as $n_z = 3.0$ and its magnitude is lower by a factor of three. The airplane coordinate system (Section 2.1) is used. Wing net shear, moment, and torsion plots are provided in Section 4.4.1.2.

4.4 Structures Design

4.4.1 Wing

4.4.1.1 Wing Stiffness and Stiffness Design Policies

Stiffness Requirements

The wing planform is straight tapered,

$$C(y) = C(0) - Ay,$$

where C is the chord and y the spanwise position (wing system). $C(0) = 2.27$ m (89.676"), $A = .19784$. The wing thickness is given by

$$T(y) = T(0) - Qy$$

where $T(0) = .273$ m (10.671 in.), and $Q = 0.02980$.

The skin thickness was assumed to taper in proportion to the chord. The resulting distribution of EI and GJ is given by:

$$EI(y) = EI(0) \left(\frac{C(y)}{C(P)}\right)^2 \left(\frac{T(y)}{T(0)}\right)^2$$

$$GJ(y) = GJ(0) \left(\frac{C(y)}{C(0)}\right)^2 \left(\frac{T(y)}{T(0)}\right)^2,$$

Further, based on F-8 data, it was assumed that $GJ(0) = 1.15\ EI(0)$.

The stiffness requirements for wing originate in the dynamic study (Section 4.2). The value used in this study is $EI(0) = 5.27 \times 10^6$ kg m^2 (1.8×10^{10} lb in^2). This value reflects the dynamic analysis at the time the design iteration stopped. Further analysis has since shown this value to be conservative (see Section 4.2.4.3). The resulting distributions of EI and GJ are shown in Figures 4.4-1 and 4.4.2.

Choice of Material and Skin Thickness

Table 4.4-1 compares the stiffness and densities of several materials considered for the main structural box of the wing.

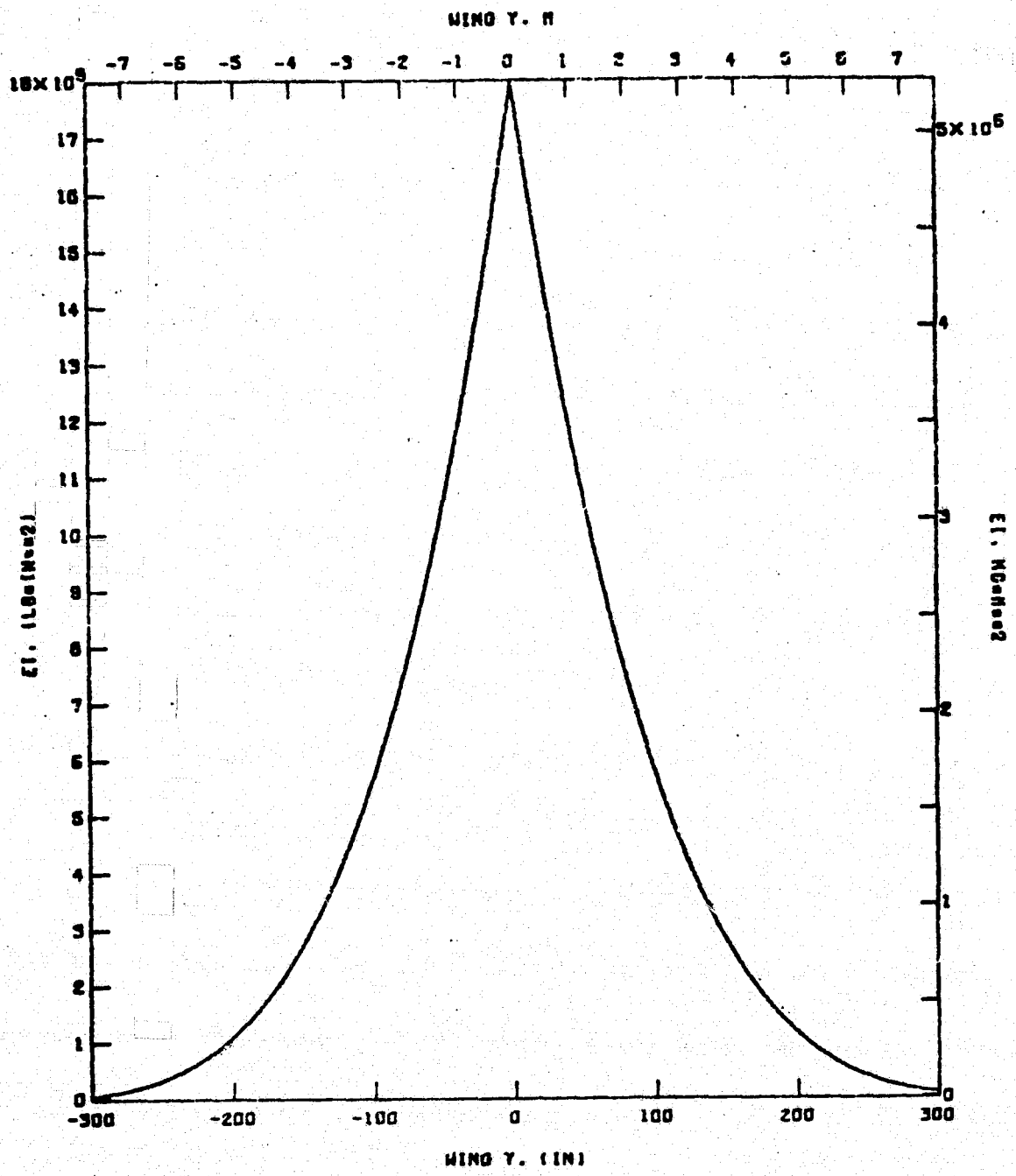

FIGURE 4.4-1 - EI Distribution

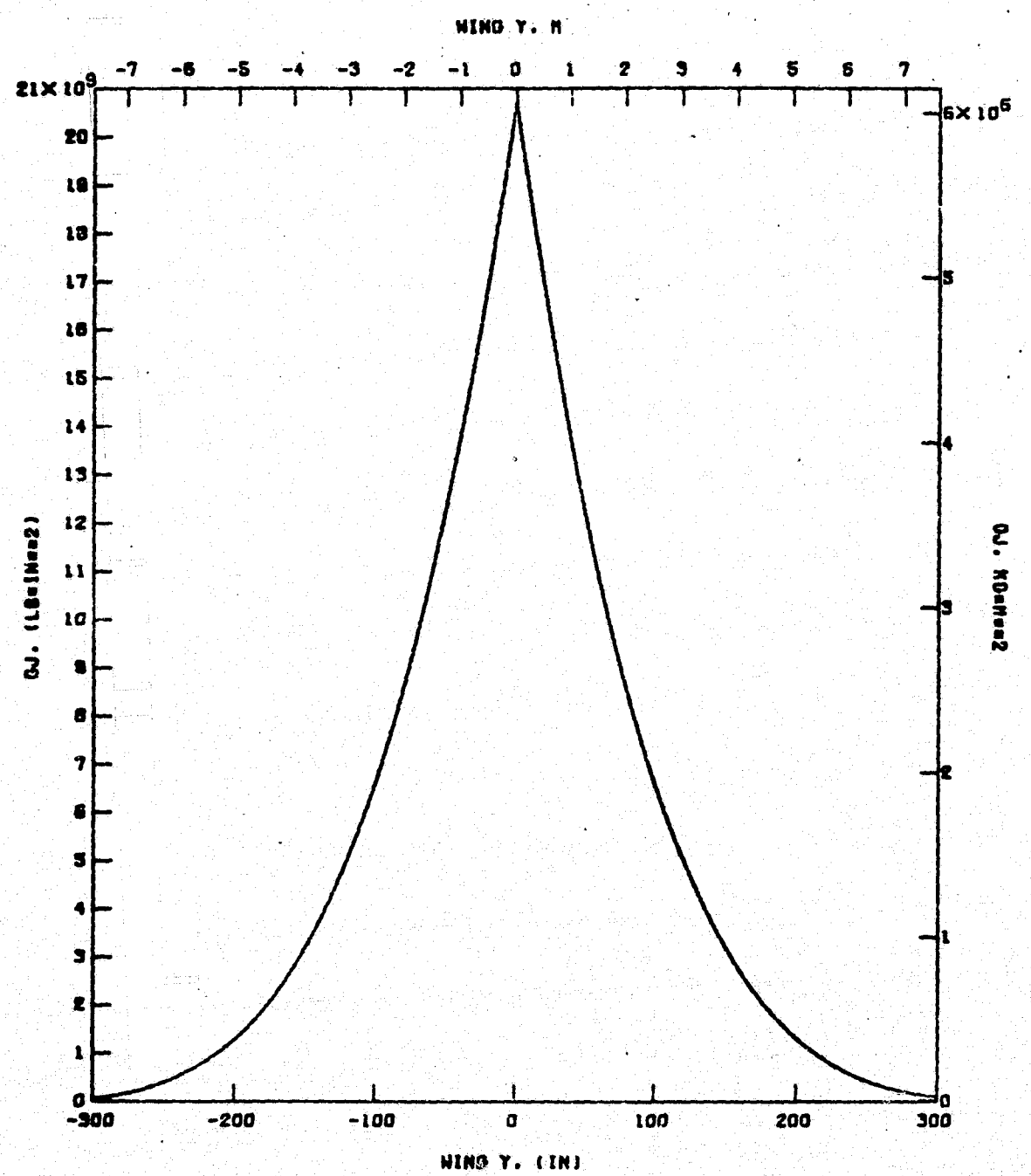

FIGURE 4.4-2 - GJ Distribution

Table 4.4-1- Weight and Stiffness Properties of Aircraft Structural Metals

MATERIAL	YOUNG'S MODULUS E 10^9kg/m^2 (10^6 psi)	DENSITY ρ 10^3kg/m^3 (lb/in^3)	E/ρ 10^6m (10^6 in)
MAGNESIUM	4.6 (6.5)	1.74 (.063)	2.6 (103)
ALUMINUM	7.24 (10.3)	2.8 (.10)	2.6 (103)
TITANIUM	11.2 (16)	4.4 (.16)	2.5 (100)
STEEL	20.4 (29)	7.94 (.287)	2.6 (103)

It is seen that conventional aircraft metals are all comparable in their ratio of stiffness to weight. However, use of the softer and lighter materials would result in thicker skins which in turn would place skin centroids well inside the wing contour and reduce the effectivity of the skin in producing wing section moment of inertia. The end result is that the lighter materials would lead to a higher structural weight of the wing. This effect is illustrated in Figure 4.4-3. The figure shows skin thickness at root versus required EI at root for steel (40% chord main box) and for aluminum(40% and 60% chord main box). Various EI requirements are marked. Requirement A (free fuselage flutter) is the governing stiffness requirement. The weights of the resulting wing (half wing) are called out. It is seen that the steel wing is the lightest - 950 kg (2100 lb) per side - and this is the construction chosen.

Strictly speaking, the stiffness requirement C applies only to the forward wing. The aft wing could be less stiff and lighter. The possibility of an asymmetric wing was not pursued because of the increase in complexity and cost.

4.4.1.2 Distributions of Load and Stress

The wing design loads for n_z = 3 and -1 conditions have been established in Section 4.3. These are flexible wing loads and include aileron loads necessary for balance in roll and effects of the aileron on wing twist. The loads work was performed before the decision was made to move the pivot location from 50% chord to 40% chord. Consequently the wing load balance and the aileron deflection effects are not quite correct. The loads are still adequate for the purpose of the concept study. Additional aileron moment is assumed in Section 4.4.3.1 where applicable.

The loads are summarized in terms of running load and center of pressure (C.P.) location in Table 4.4-2. The table entries are in terms of airplane coordinates. For the purpose of analyzing the wing it is desirable to transform the loads into wing coordinates.

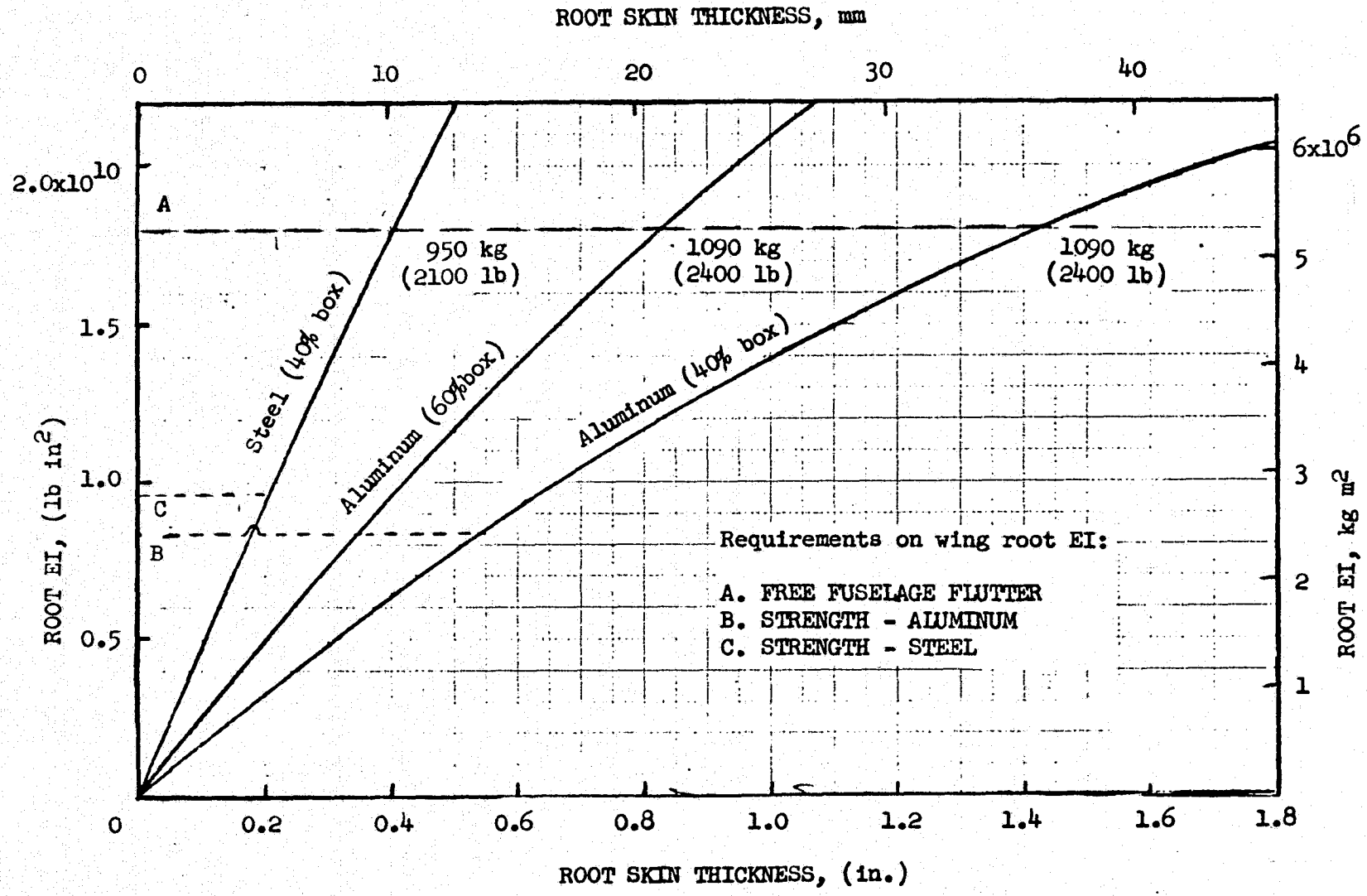

FIGURE 4.4-3 - Skin Thickness

TABLE 4.4-2

AERODYNAMIC RUNNING LOADS - STREAMWISE SYSTEM

Y		CP	RUNNING LOAD	
M	(IN.)		KG/M	(LB/IN)
5.55	(218.47)	.230	0.0	(0.00)
5.41	(213.00)	.230	1245.9	(69.77)
5.11	(201.00)	.250	1860.6	(104.19)
4.67	(184.00)	.478	2358.5	(132.07)
4.14	(163.00)	.527	2766.2	(154.90)
3.48	(137.00)	.600	3220.3	(180.33)
2.72	(107.00)	.695	3659.8	(204.94)
1.96	(77.00)	.820	4087.2	(228.87)
1.19	(47.00)	.294	4414.9	(247.22)
.41	(16.00)	.282	4700.2	(263.20)
-.41	(-16.00)	.274	4875.2	(273.00)
-1.22	(-48.00)	.278	4825.9	(270.24)
-2.02	(-79.50)	.284	4509.5	(252.52)
-2.79	(-110.00)	-.025	4004.5	(224.24)
-3.49	(-137.50)	-.001	3501.8	(196.09)
-4.06	(-160.00)	.020	3020.9	(169.16)
-4.52	(-178.00)	.012	2512.4	(140.69)
-4.85	(-191.00)	-.024	1971.7	(110.41)
-5.11	(-201.00)	-.151	1334.4	(74.72)
-5.23	(-205.79)	.300	0.0	(0.00)

NOTES:

* Spanwise location y is the airplane y coordinate with the 50% chord at y=0.
* CP location is presented as fraction of streamwise chord.
* Running load is design limit load per unit of airplane y.

TABLE 4.4-3

AERODYNAMIC RUNNING LOADS - WING SYSTEM

Y		CP	RUNNING LOAD	
M	(IN.)		KG/M	(LB/IN)
7.62	(300.00)	.198	0.0	(0.00)
7.25	(285.55)	.198	881.0	(49.33)
6.82	(268.56)	.216	1315.7	(73.67)
6.41	(252.43)	.430	1667.7	(93.39)
5.72	(225.13)	.479	1956.0	(109.53)
4.89	(192.68)	.553	2277.1	(127.51)
3.99	(157.18)	.653	2587.9	(144.91)
3.18	(125.21)	.790	2891.1	(161.84)
1.17	(45.87)	.256	3121.8	(174.81)
-.01	(-.27)	.245	3323.6	(186.11)
-.98	(-38.53)	.316	3447.3	(193.04)
-2.10	(-82.72)	.320	3412.5	(191.09)
-3.20	(-126.16)	.326	3188.7	(178.56)
-4.76	(-187.24)	-.031	2831.6	(158.56)
-5.63	(-221.84)	-.002	2476.1	(138.66)
-6.36	(-250.37)	.023	2136.1	(119.61)
-6.97	(-274.37)	.014	1776.6	(99.48)
-7.44	(-292.75)	-.030	1394.2	(78.07)
-7.87	(-309.99)	-.192	943.6	(52.84)
-7.62	(-300.00)	.344	0.0	(0.00)

NOTES:

* Spanwise location y is the wing y coordinate.
* CP location is presented as fraction of wing chord.
* Running load is design limit load per unit of wing y.

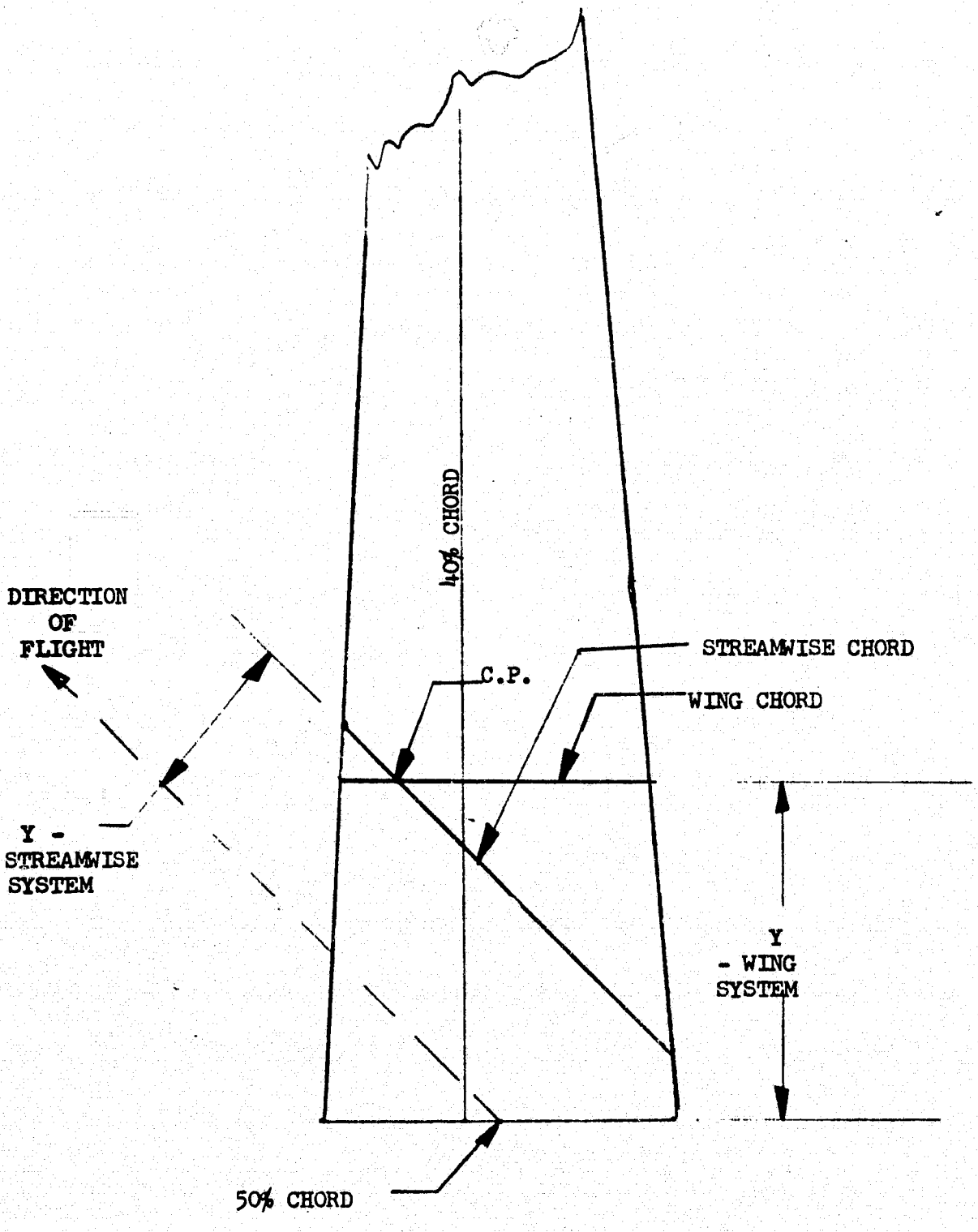

FIGURE 4.4-4 - Relationship between Streamwise and Wing System Load Data.

This is done in Table 4.3. See Figure 4.4-4 for the relationship between the entries in Tables 4.4-2 and Table 4.4-3.

The airloads of Table 4.4-3 are combined with inertial loads and integrated to yield shear and bending moment distributions along the span (Figures 4.4-5 through 4.4-8). Loads are based on a distribution of the wing structural weight of 1900 kg (4200 lb). The final weight distribution (Section 4.5) which includes also systems weight was not available at the time of these calculations, however, the distribution used is adequate for the purpose of the present feasibility study.

The bending moment distribution yields the spanwise distribution of maximum skin stress (Mc/I) in Figure 4.4-9. The 40% chord line, which is the center of the wing main box, is assumed to be the flexural axis. Running torque (twisting moment) around this axis is obtained from the running load and CP position (Figure 4.4-10) and integrated to yield a torsion distribution in Figure 4.4-11. The related shear stress in the skin is shown in Figure 4.4-12. Numerical tabulations of the information in Figures 4.4-5 through 4.4-12 is provided in Appendix A. No data is presented for the -1g condition. With the omission of camber effect by the AIRLOD routine (Section 4.3) the -1g data may be obtained from the 3g data by scaling in the ratio of -1 to 3.

Discontinuities at the origin appear in many of the loads distributions. These indicate loads fed into the pivot. In symmetric flight, roll balance is achieved by the wing ailerons and no rolling moment (airplane system) is fed into the pivot. In the wing system and at a skew angle of $\frac{\pi}{4}$ (45°) this translates into the pitching moment (up, wing system) being equal to the rolling moment (toward aft wing, wing system), Figure 4.4-13. The rolling and pitching moments through the pivot are the discontinuities in the distributions of bending and torsion respectively. The condition for balance is not met, because, as explained above, the wing was balanced about the 50% chord rather than the 40% point. Further discussion of this point and of the additional aileron moment required is provided in Section 4.4.2.1. The loads as provided in Figures 4.4-5 through 4.4-12. (Tables A-1 through A-12) are considered adequate for sizing the wing structure in the feasibility study.

4.4.1.3 Skins

Static Safety

The maximum stresses in the distributions of Figure 4.4-9 and 4.4-12 occur at the root. They are:

Tension, compression 33.8×10^6 kg/m^2 (48.1×10^3 psi)

Shear 9.1×10^6 kg/m^2 (13.0×10^3 psi).

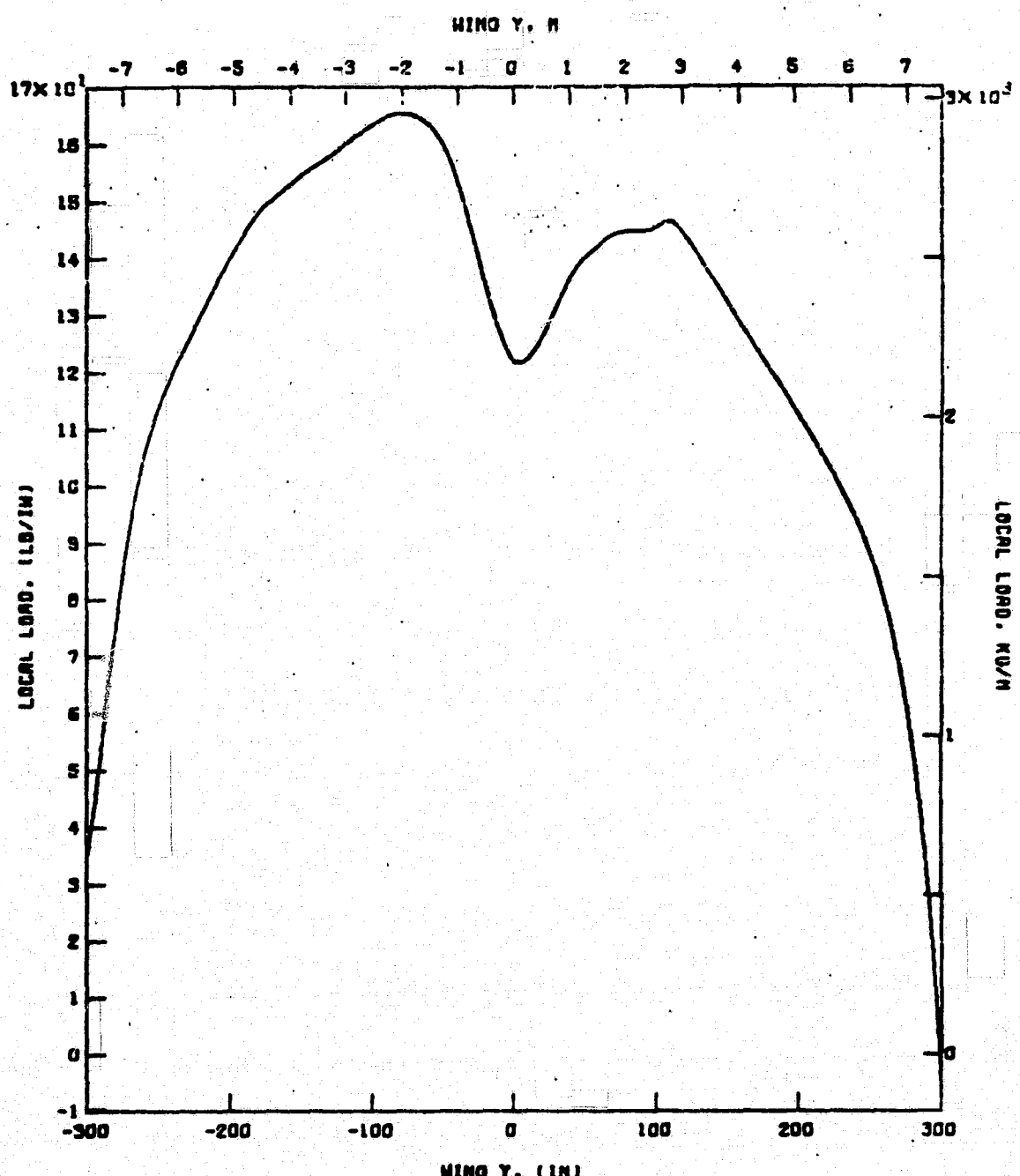

FIGURE 4.4-5 - Distribution of Net Running Load.

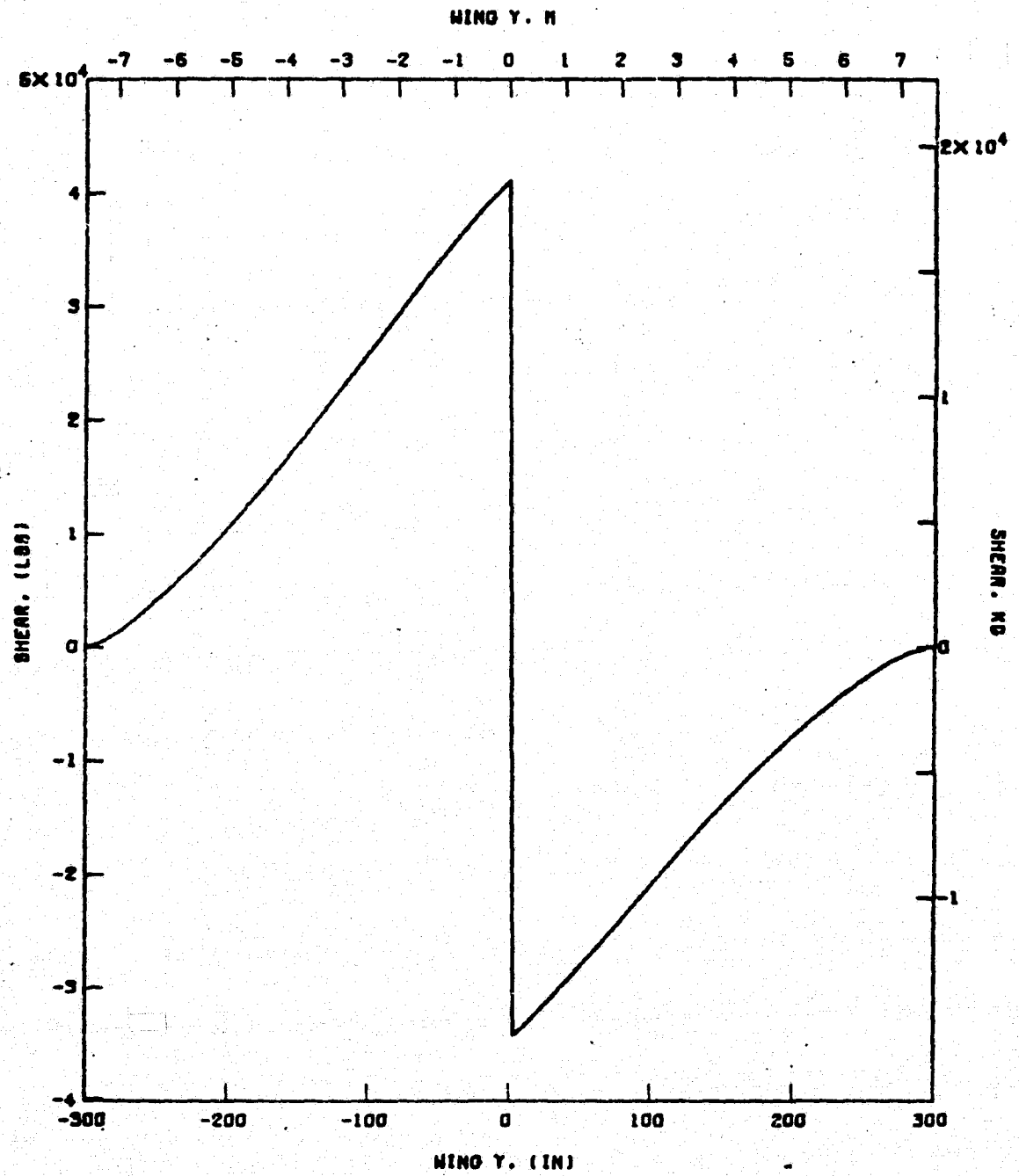

FIGURE 4.4-6 - Shear Distribution

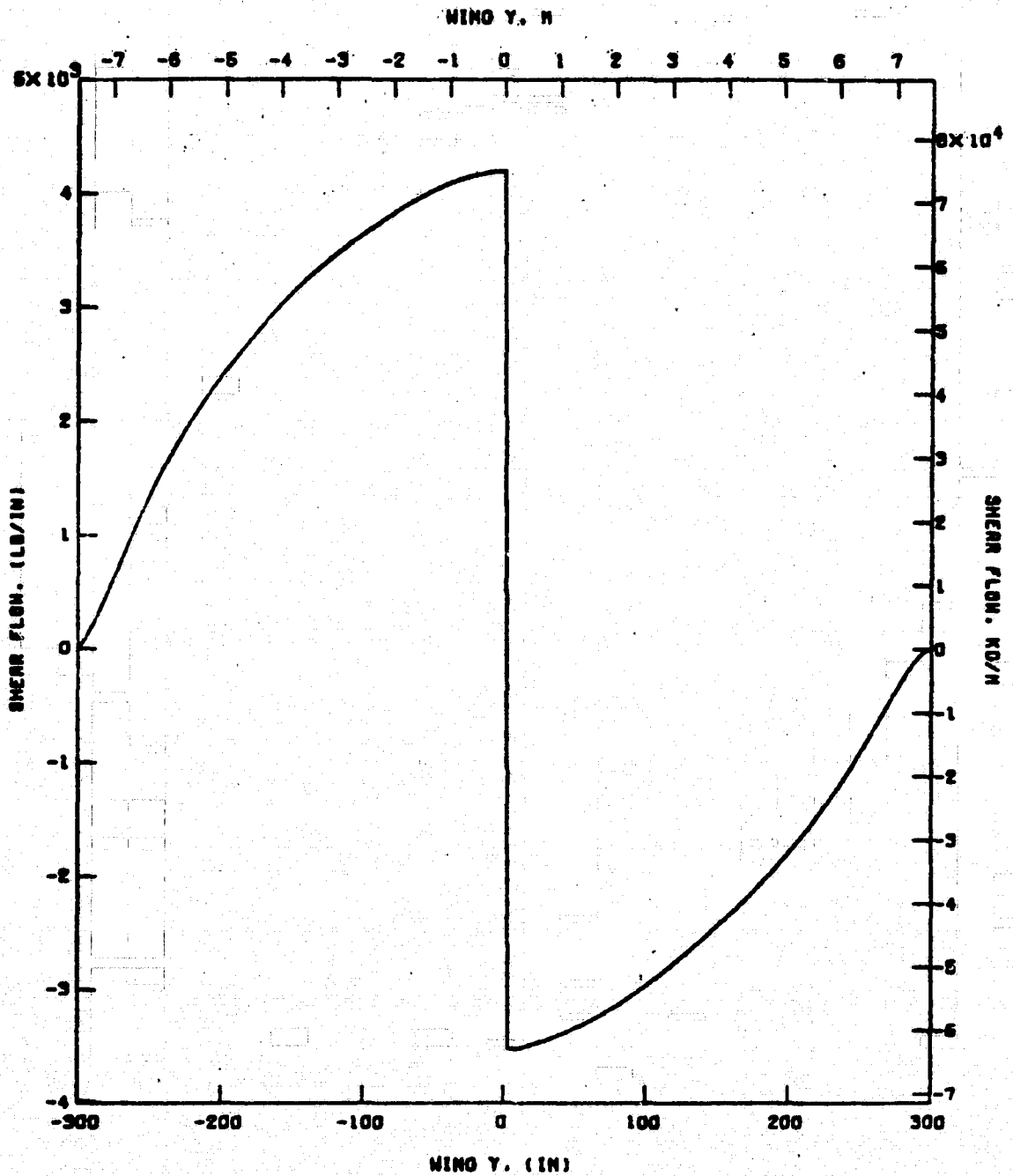

FIGURE 4.4-7 - Shear Flow

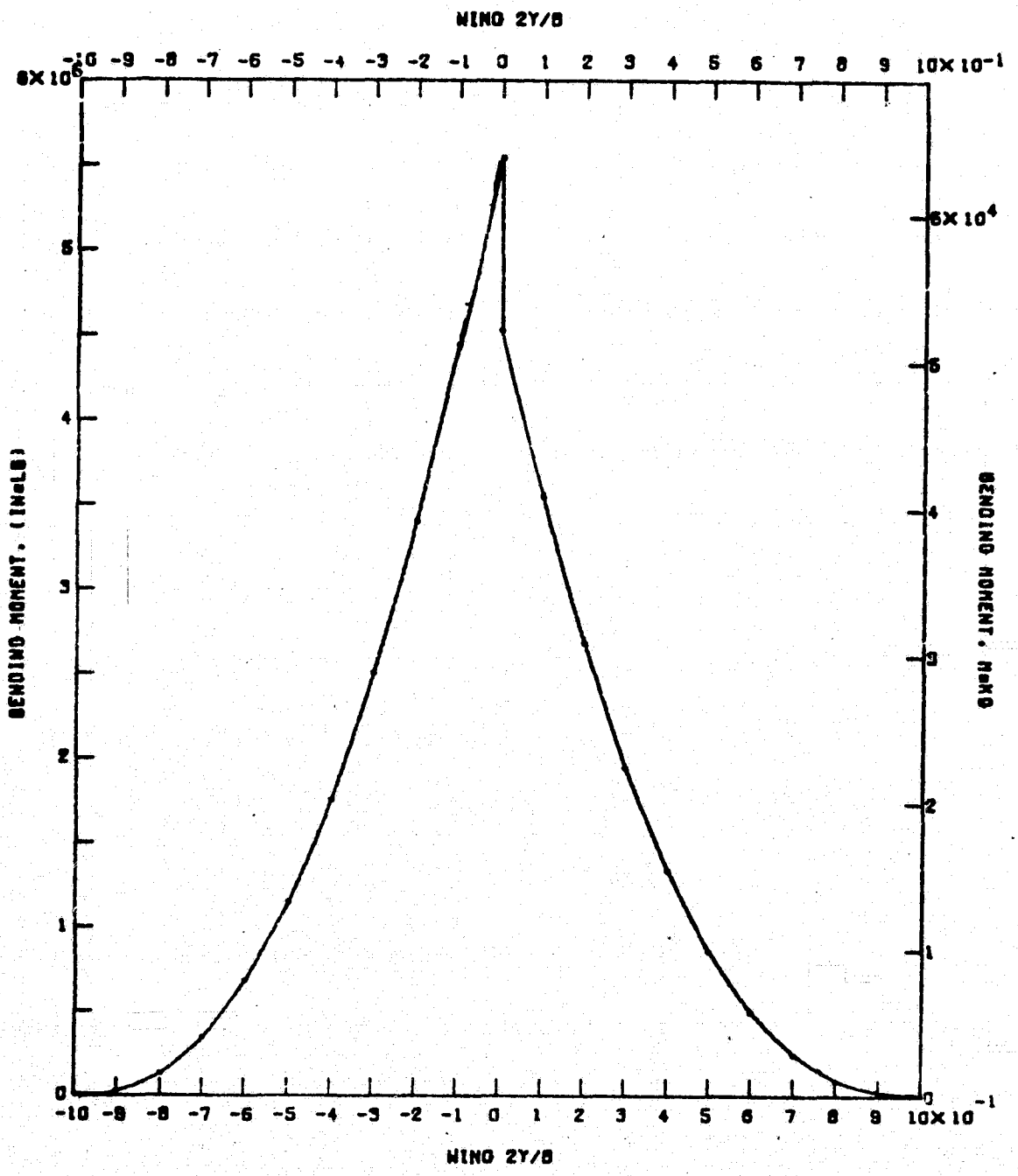

FIGURE 4.4-8 - Bending Distribution

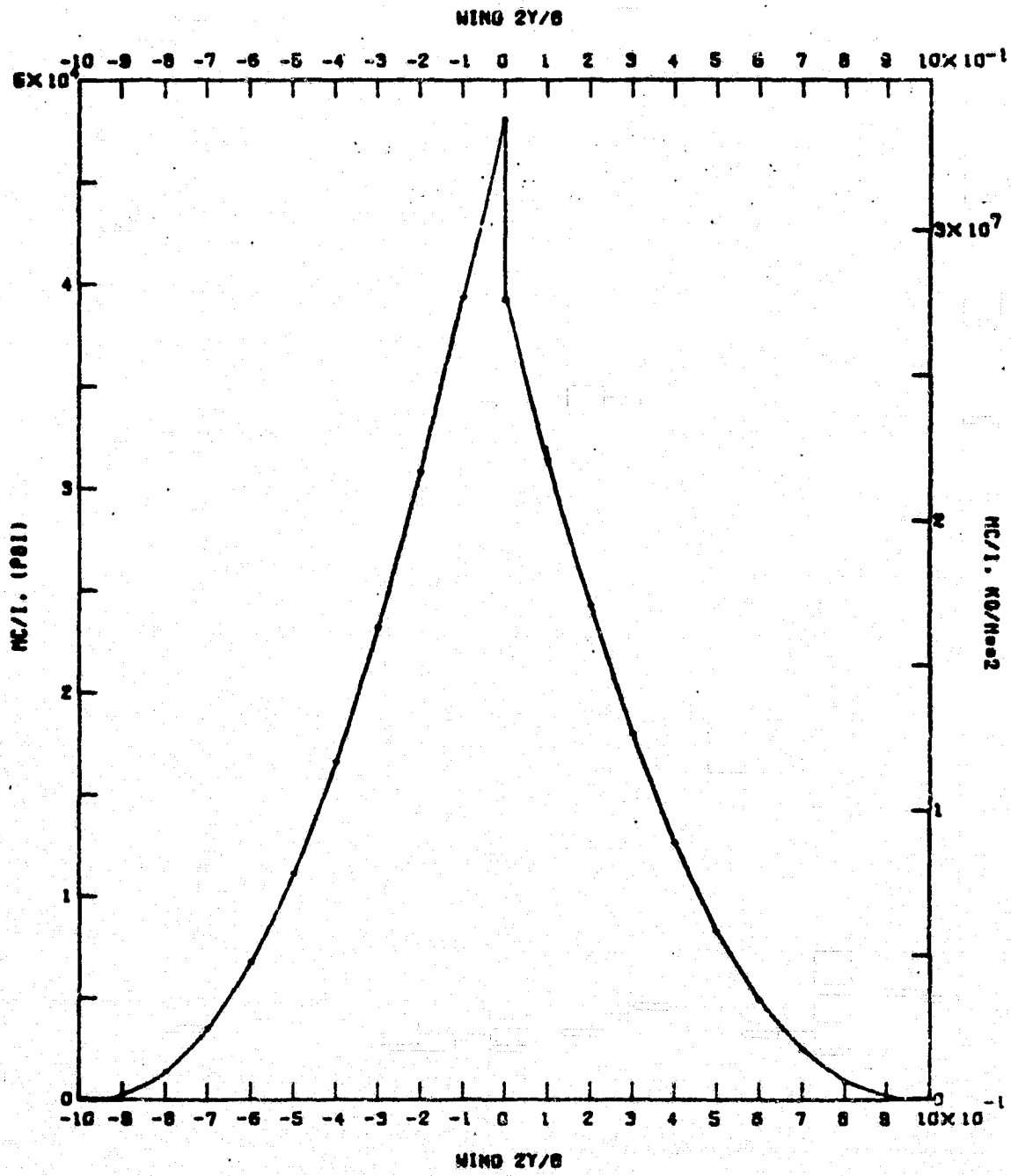

FIGURE 4.4-9 - Spanwise Distribution of Mc/I

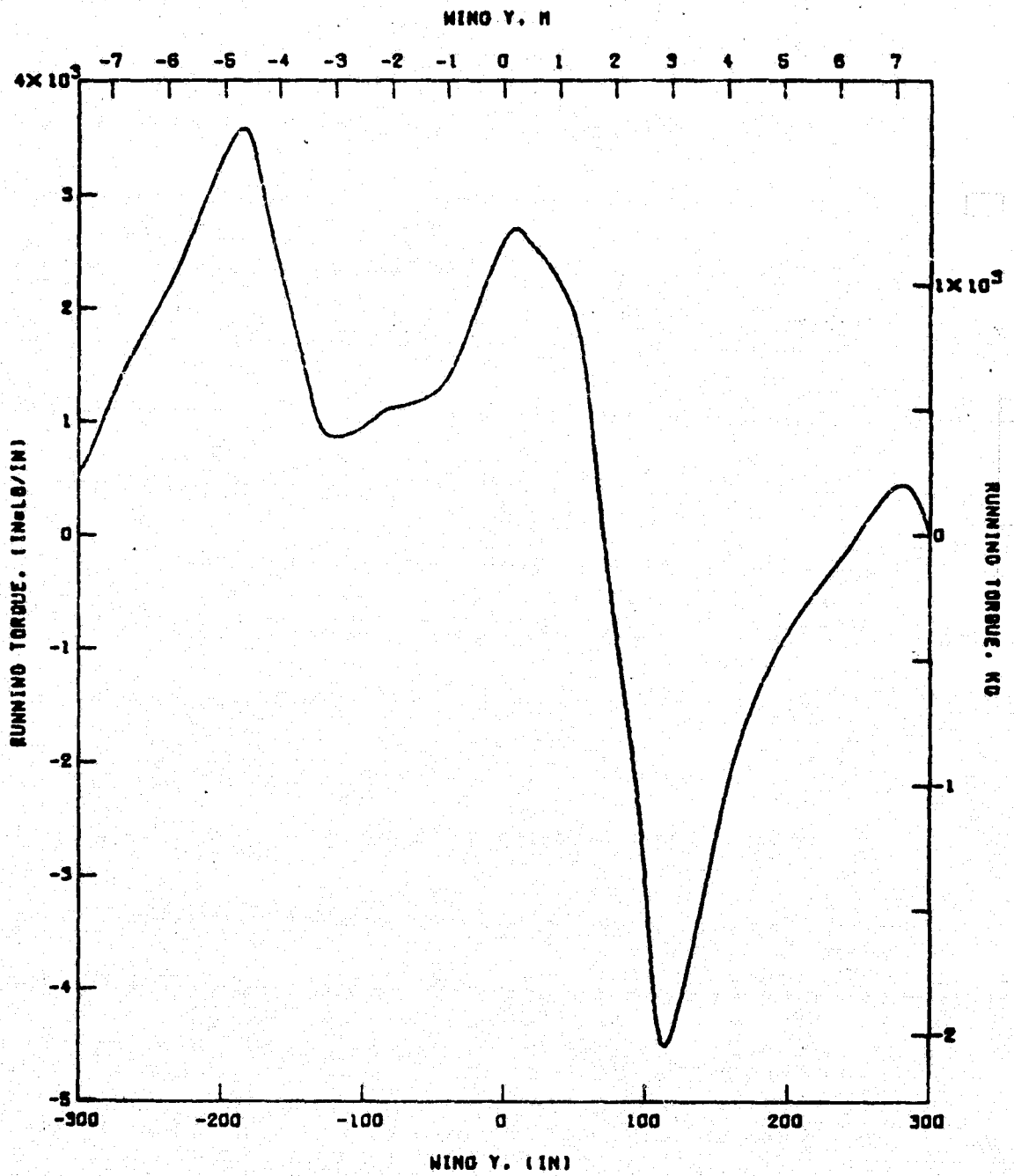

FIGURE 4.4-10 - Running Torque

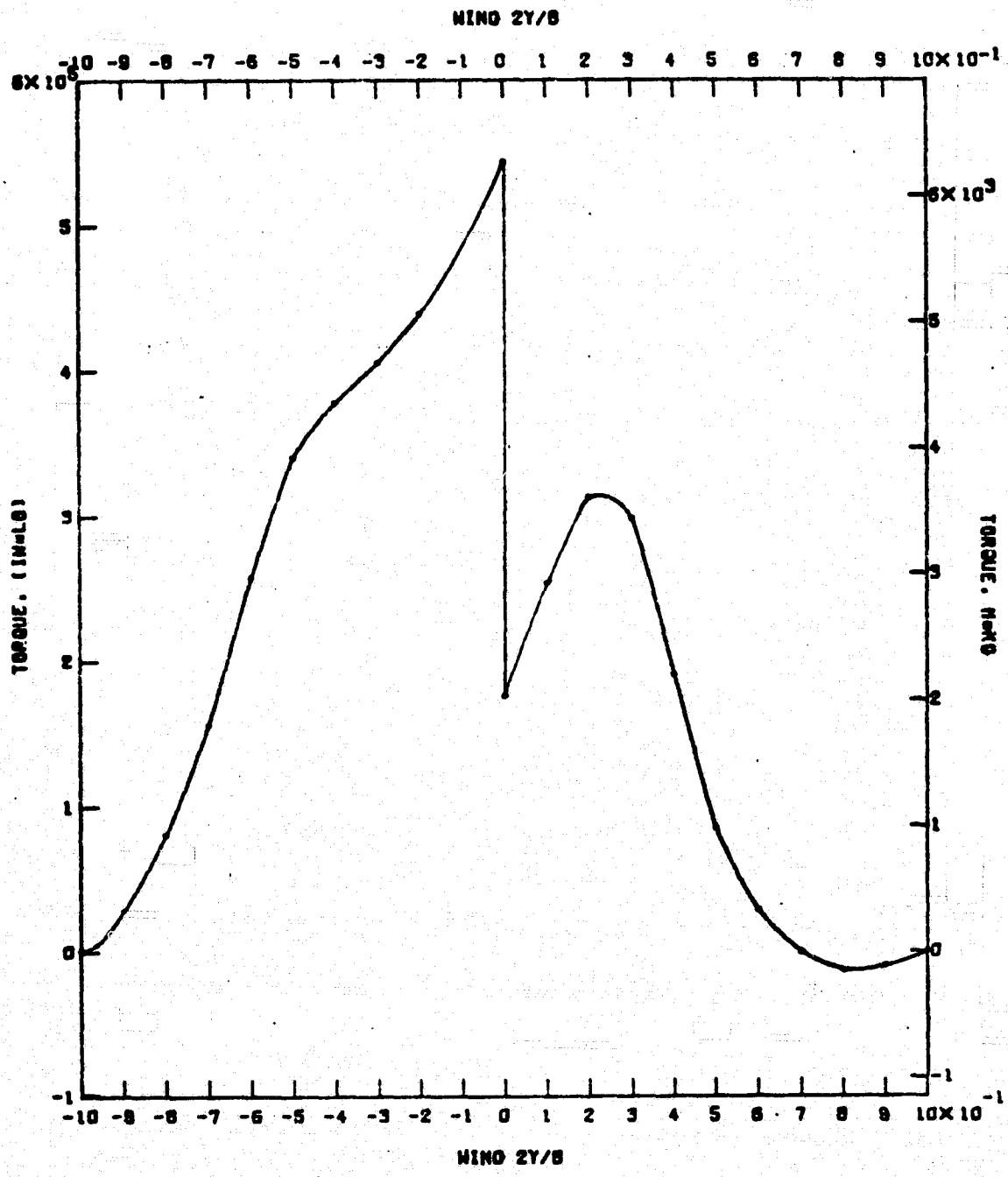

FIGURE 4.4-11 - Torsion

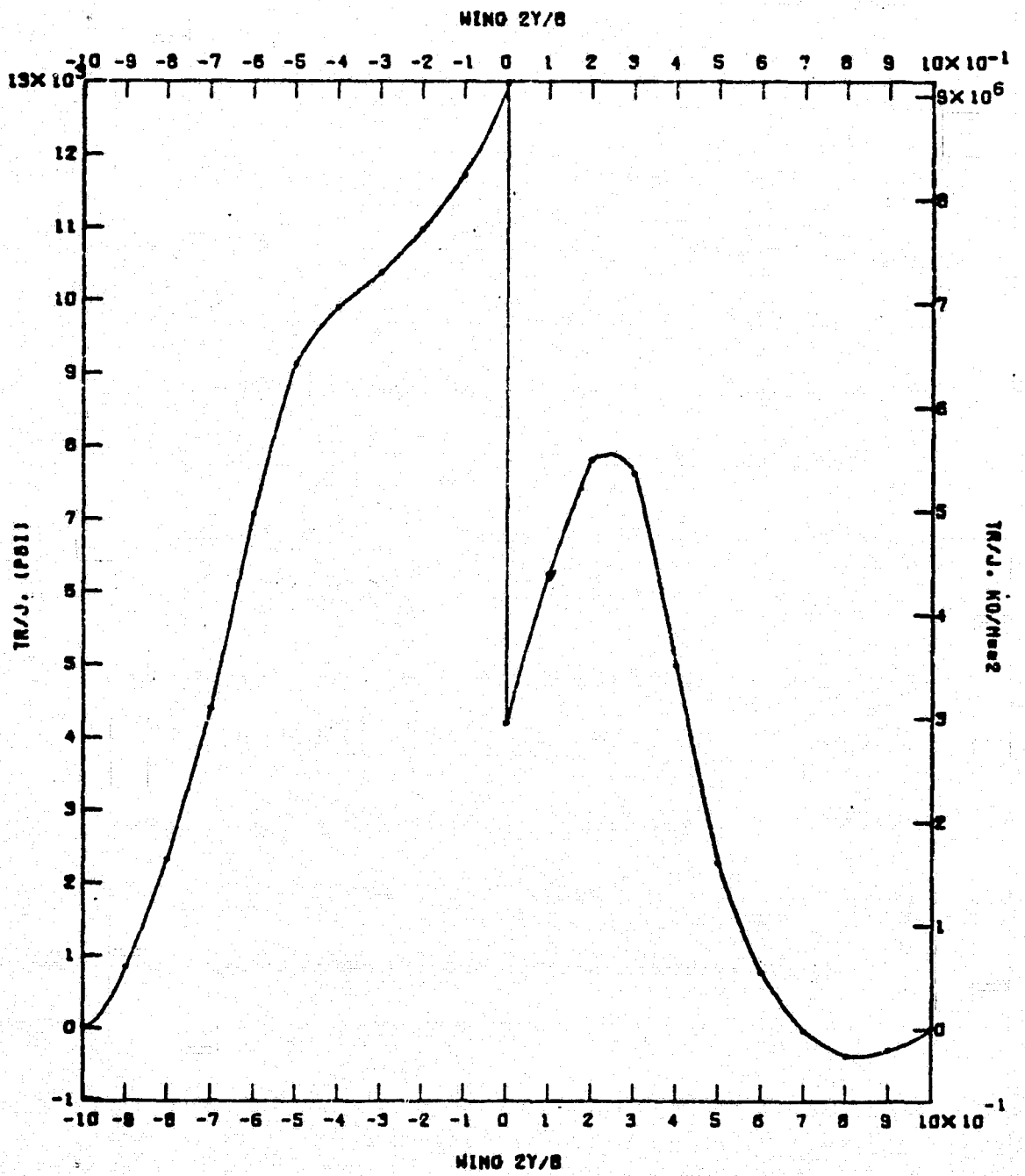

FIGURE 4.4-12 - Spanwise Distribution of Tr/J

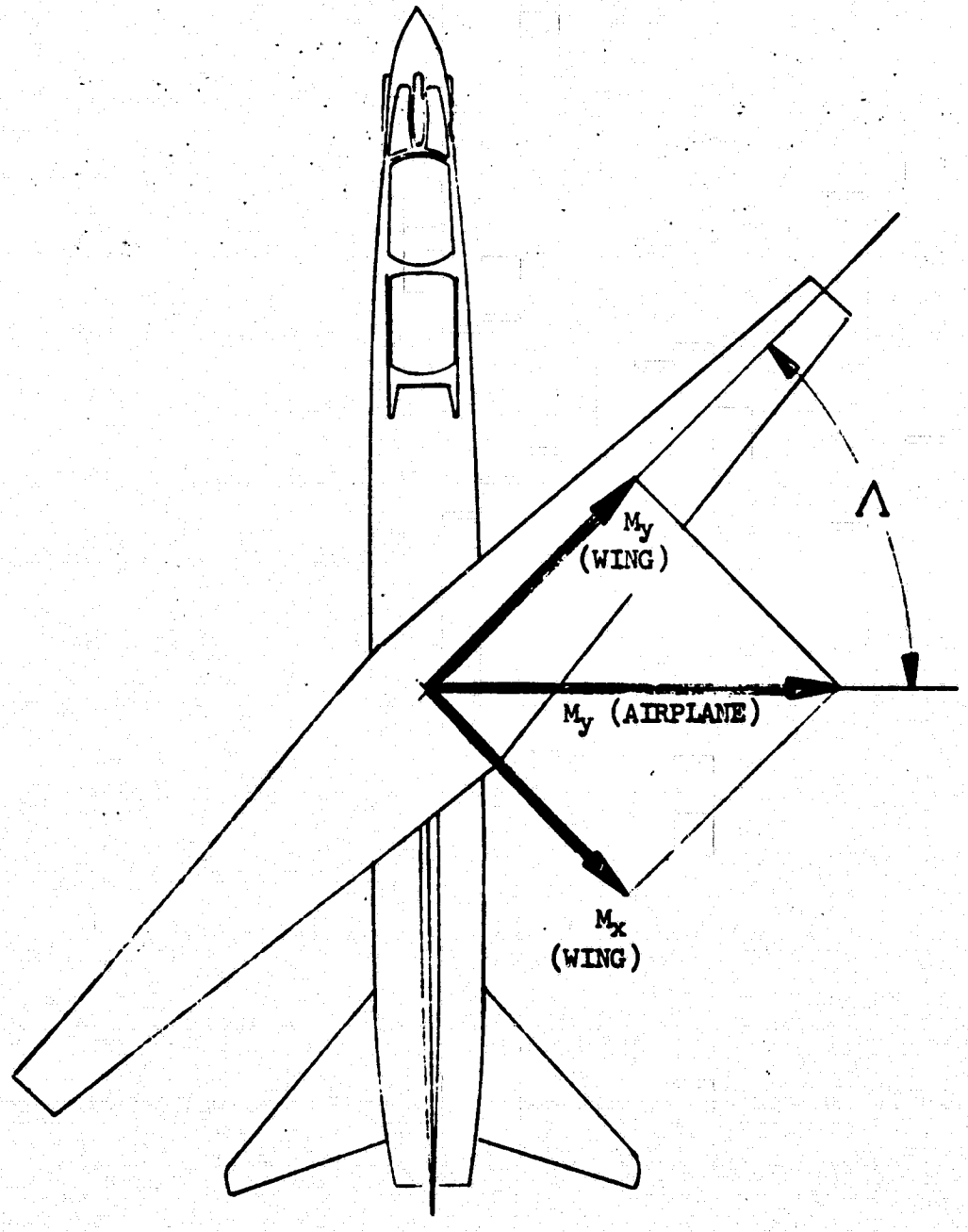

FIGURE 4.4-13 - Moments Through Pivot in Symmetric Flight in Wing System and Airplane System.

These are design limit stresses. Ultimate design stresses are twice these values. They are well short of the allowables of the steel to be used (17-4 heat treated to 180 ksi):

Tension 127×10^6 kg/m^2 (180×10^3 psi)

Shear 76×10^6 kg/m^2 (108×10^3 psi) (reference 5).

The margin of safety for the skin is

$$\left\{\left(\frac{2 \times 33.8}{127}\right)^2 + \left(\frac{2 \times 9.1}{76}\right)^2\right\}^{1/2} - 1 = 0.71$$

Buckling of upper skin.

The critical panel dimensions are:

length $a = 1.02$ m (40")

width $b = .29$ m (11.5")

thickness $t = 1$ cm (0.4")

The compression buckling coefficient is $K_c = 3.6$. The buckling stress is $Fcc = K_c E (\frac{t}{b})^2 = 3.6 \times 20.4 \times 10^9 (1/29)^2 = .87 \times 10^6$ kg/m^2 (124×10^3 psi). The compression stress in the 3g condition (last subsection) is only 33.8×10^6 kg/m^2 (48.1×10^3 psi). No buckling occurs either at design limit or design ultimate load, and no stiffening of panel is required.

Attachments in the skin

The main box skins attach to the bearing fitting. The attachments pass the carry through loads. The design limit tension and compression at the root is $F_t = 33.8 \times 10^6$ kg/m^2 (48.1×10^3 psi). With skin thickness of 1cm (0.4 in) this amounts to 6.76×10^3 kg/cm (38.4×10^3 lb/in).

Shear in Attachments

The shear requirements for the attachments may be estimated by

$$n\frac{\pi}{4}D^2 F_{su\ fast.} \geq p\,DtSF_{t\ skin},$$

where D is the fastener diameter, pD the fastener spacing, and n the number of rows of fasteners. S is the factor of safety, S = 2. Using high strength fasteners with $F_{su} = 110 \times 10^6$ kg/m^2 (156×10^3 psi), the condition becomes:

$$\frac{n}{p} D \frac{4}{\pi} t \frac{F_{t\ skin}}{F_{su\ fast.}} = 0.80 \text{ cm } (0.21 \text{ in}) \qquad (a)$$

The fastener spacing parameter p is limited by the net section requirement.

$$\frac{p}{p-1} \leq \frac{F_{tu}}{SF_t}$$

or

$$p \geq \left(1 - \frac{SF_t}{F_{tu}}\right)^{-1} = \left(1 - \frac{2 \times 33.8}{127}\right)^{-1} = 2.1.$$

Condition (a) may be satisfied with:

$p = 3$

$n = 2$

$D = 1.27$ cm (1/2 in)

The particular choice of attachments and placement should be determined at the time of detail design. It is clear that two rows of attachments would be required to keep the fastener diameter within reasonable limits.

Bearing of Attachments

The requirement for adequate bearing allowable is $nF_{bru} \geq pSF_t$. The bearing allowable is $F_{bru} = 229 \times 10^6$ kg/m^2 (326×10^3 psi) (reference 5). The requirement is easily satisfied by the choices of p and n of the last paragraph. It could also be satisfied for $p = 3$, $n = 1$ or for $p = 4$, $n = 2$.

Fatigue Life.

Using the fastener spacing of the last subsection, the stress concentration factor at the fastener holes based on gross section is estimated as 3.9. With $F_t/F_{tu} = .27$, the fatigue life is about 10^5 cycles. No data is available on the proposed usage of this airplane. However, it seems reasonable that the number of occurrences of 3g in 200 flight hours will be well short of 10^5.

4.4.1.4 Spars

The maximum vertical shear flow in the wing (design limit load) is 74.9×10^3 kg/m (4.19×10^3 lb/in). This load is distributed among the

four spars in the wing main box. The shear flow in each spar is $q = 18.7 \times 10^3$ kg/m (1.05×10^3 lb/in).

For a bay of depth b the buckling stress is $KE(\frac{t}{b})^2$, where t is the web thickness. Setting this equal to the ultimate stress Sq/t, we find

$$t = \left(\frac{Sqb^2}{KE}\right)^{1/3}.$$

At the wing root b = .25 m (10 in). For a long bay with simply supported edges K = 4.84. The thickness required for a non buckling web is

$$t = \left(\frac{2 \times 18.7 \times 10^3 \times .25^2}{4.84 \times 20.4 \times 10^9}\right)^{1/3} = 0.0029 \text{ m } (0.113 \text{ in}).$$

Non buckling webs will be used in end bays. Thinner buckling webs are considered for the rest of the spars.

4.4.1.5 Bearing Fitting

The bearing fitting connects the wing to the pivot bearing. It also serves as a center rib for the wing main box (Figure 3.3-3). The skins of the right and left wing sections bolt to the bearing fitting. The tension and compression load path continuity for the skins is through the bottom web of the fitting and the structural door in the top. The main box spars attach to tabs on the fitting. The shear load path is from the spar webs to the fitting tabs which in turn distributes through the fitting web to the bearing.

Carry Through Loads

The attachments of the skins to the bearing are discussed in Section 4.4.1.3. The lower web of the fitting is integral. The attachment problems of the structural door on the top of the fitting are similar to those of the skin. The door is stiffened against buckling by stiffeners that divide it into bays smaller than skin bays.

The structural door at the top of the fitting is a cylindrical surface which matches the conical surfaces of the skins at the joint. Turing loads across the joint are reacted by the fitting web.

The bottom web of the fitting is plane. The contoured wing bottom skin is displaced from this plane by amounts that vary around the fitting. The step is minimized for the 40% chord position. The load component perpendicular to the circumference of the fitting causes a bending of the fitting flange. The bending moment per unit of circumference is $M = ps\cos^2\theta$, where p is the load (tension or compression) per unit chord, s is the step and θ is the angular position on the fitting measured from the 40% chord (see Figure 4.4-14). A plot of s and $s\cos^2\theta$ vs. θ is provided in Figure 4.4-15. The highest value of $s\cos^2\theta$ occurs at $\theta = \frac{\pi}{6}$ (30°) and amounts to .99 cm (.39 in). The design

limit load in the skin is p = 3.38 x 10^3 kg/cm (19.2 x 10^3 lb/in (see section 4.4.1.3). The highest bending per unit circumference is thus

$$M = 3.38 \times 10^3 \text{ kg/cm} \times 0.99 \text{ cm} = 3.35 \times 10^3 \text{ kg } (7.4 \times 10^3 \text{ in lb/in}).$$

Eccentricity also exists in the joint of the 1.0 cm (0.40 in) skin to the 1.27 cm (.050 in) flange (Figure 4.4-16). The eccentricity here is 1/2 (1.0 + 1.27) = 1.14 cm (0.45 in), and the bending moment

$$M = 3.38 \times 10^3 \text{ kg/cm} \times 1.14 \text{ cm} = 3.86 \times 10^3 \text{ kg } (8.5 \times 10^3 \text{ in lb/in}).$$

The flanges are stabilized against these moments by gussets from the top flange to the bottom flange being approximately b = 9 cm (3.5 in) wide on each side of the web.

The gussets are plates about 25 cm x 9 cm (10 in.x 3.5 in) fixes at the flanges, simply supported at the web, and free at the other edge. Their buckling stress is

$$F_{buckling} = KE \left(\frac{t}{b}\right)^2,$$

with K = 0.75. The bending stress in the gusset is

$$F_{bending} = \frac{6Ma}{4b^2t},$$

where a is the gusset spacing. Assume a = 7.62 cm (3 in). Putting the buckling stress equal to the ultimate bending stress we find

$$t = \left(S\frac{3Ma}{2KE}\right)^{1/3} = 0.39 \text{ cm } (0.15 \text{ in}).$$

This is the minimum thickness for buckling safety. The stress level involved (limit) is obtained by substituting this thickness in either one of the stress expressions. The result is F = 24.4 x 10^6 kg/m^2 (20.5 x 10^3 psi). The margin of safety is high.

Pivot Loads

Bolt Loads

The wing bearing fitting transfers loads to the pivot bearing as follows

(a) vertical load Z,

(b) pitching moment,

(c) rolling moment.

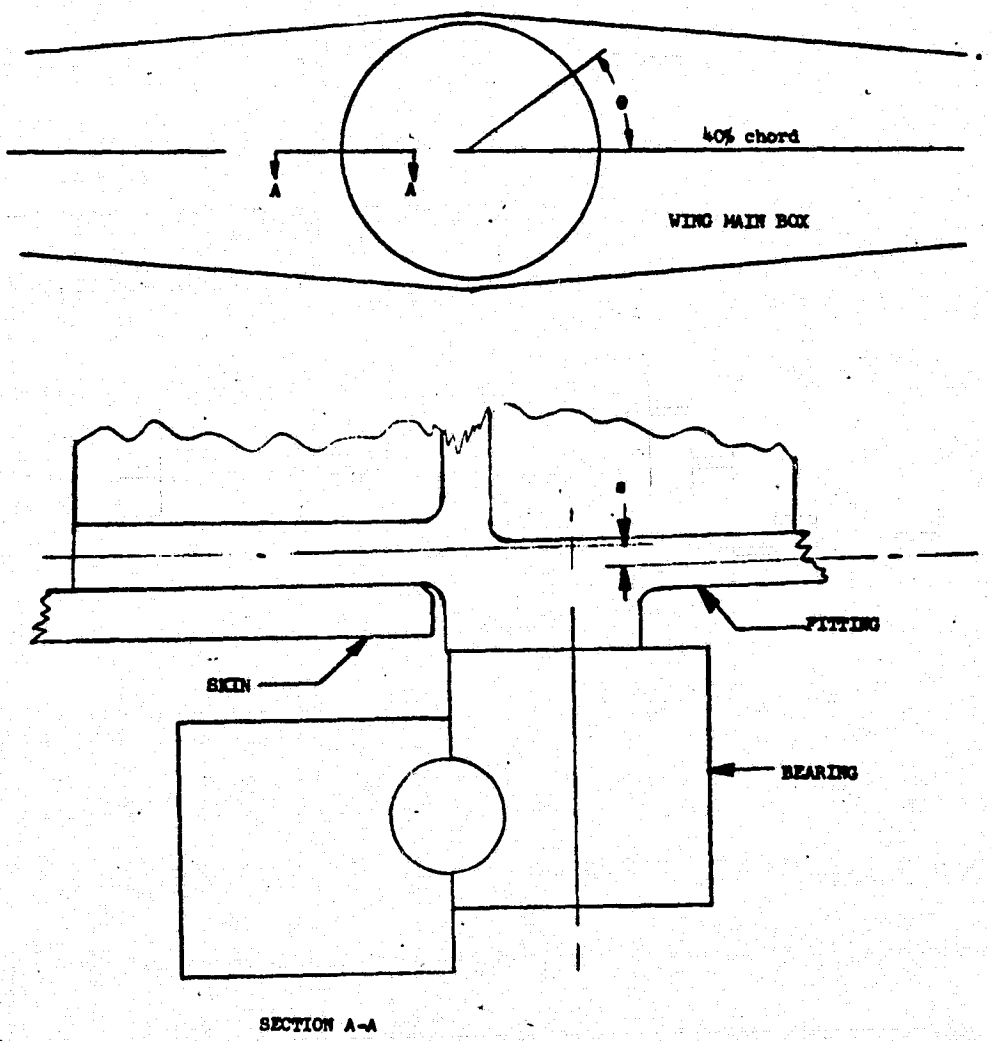

FIGURE 4.4-14 - Eccentricities in Lower Flange of Wing Bearing Fitting.

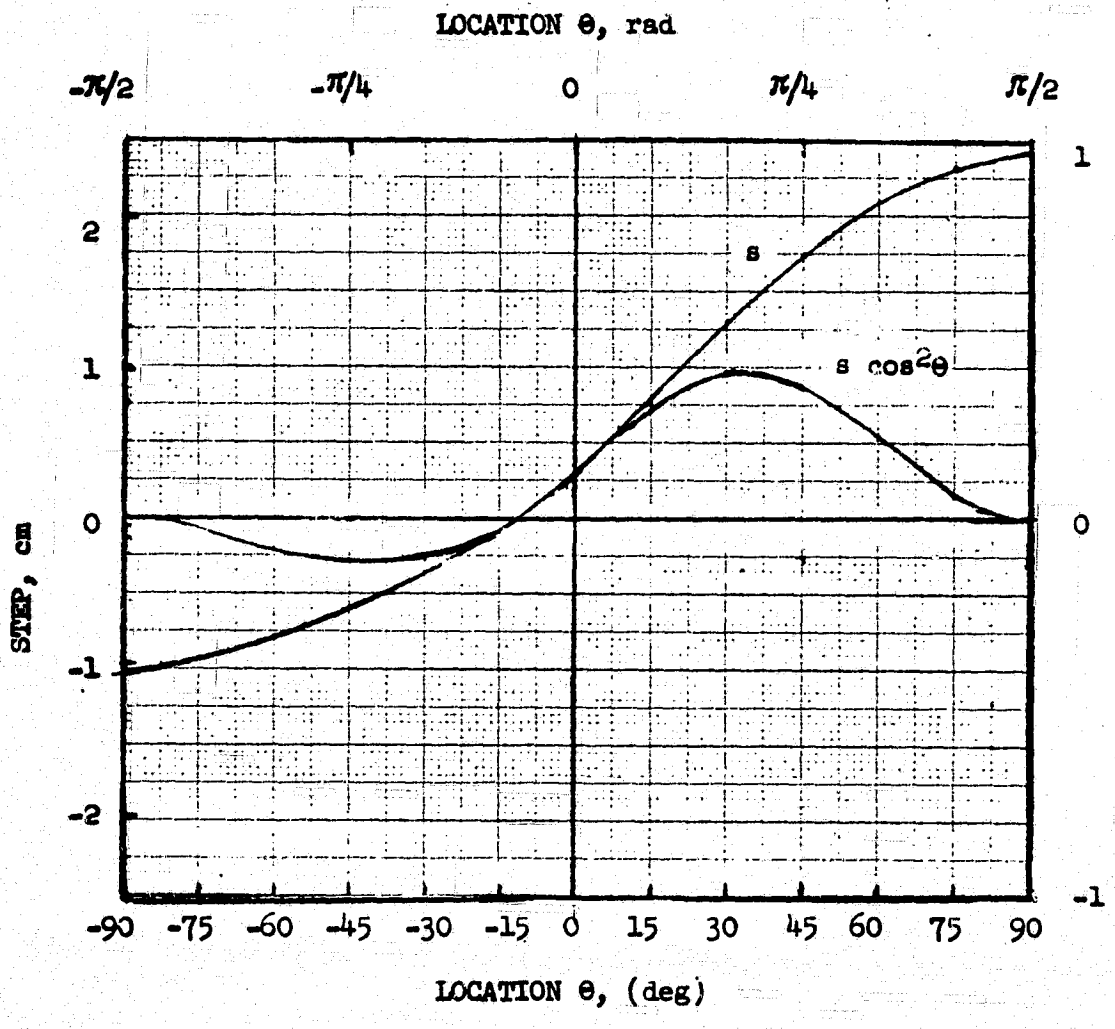

FIGURE 4.4-15 - Eccentricity in lower flange of wing bearing fitting (curve).

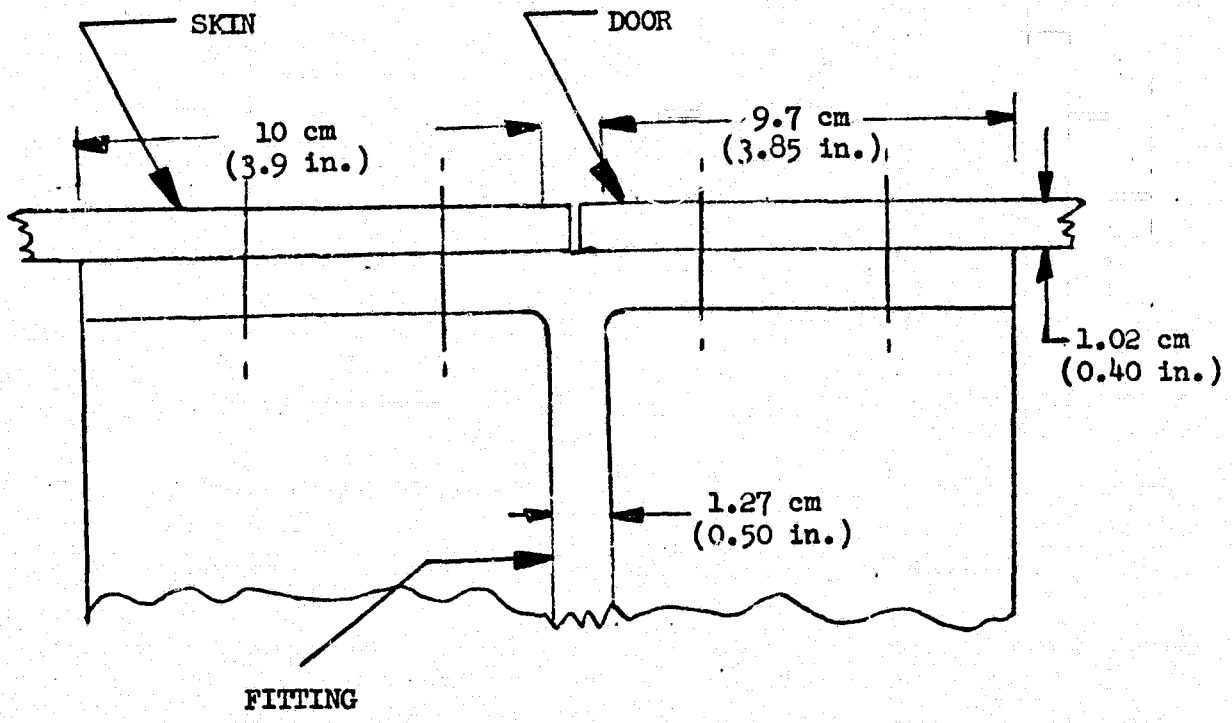

FIGURE 4.4-16 - Joint of Upper Flange of Wing Bearing Fitting to Skin and Structural Door.

These loads are distributed as vertical load along the circumference of the bearing. Denoting the angle from the 40% chord line by θ, the distribution of load per unit circumference is

$$w \quad \frac{Z}{2\pi R} + \frac{M_y}{\pi R^2} \sin\theta + \frac{M_x}{R^2} \cos\theta,$$

where R is the radius of the bearing, R = 39.37 cm (15.25 in). The maximum running load is

$$w_{max} = \frac{Z}{2\pi R} + \frac{1}{\pi R^2} (M_y^2 + M_x^2)^{1/2}.$$

The maximum occurs at $\theta = \arctan (M_y/M_x)$. The bearing is attached to the wing by N = 32 1.43 cm (9/16 in) bolts. The maximum load per bolt is

$$P_{max} = w_{max} \frac{2R}{N} = \frac{Z}{N} + \frac{2}{NR} (M_y^2 + M_x^2)^{1/2}.$$

The loads through the pivot are given in Section 4.4.3.1. Using these loads, Table 4.4-4 presents the maximum running load, maximum bolt load and their location.

TABLE 4.4-4: PIVOT LOADS ON WING BEARING FITTING

(WING SYSTEM DESIGN LIMIT LOADS)

CONDITION skew angle = $\frac{\pi}{4}$ (45°)	w_{max} kg/cm (lb/in)	P_{max} kg (lb)	θ location of max load rad (deg)
3g symmetric	260 (1456)	2010 (4431)	$\frac{\pi}{4}$ (45)
2.4g max roll acceleration toward aft wing	452 (2530)	3994 (8805)	.27 (15)

The ultimate tensile strength of the fastener is (reference 5 p8-64) 15.67 x 10^3 kg (34.54 x 10^3 lb). The margin of safety is

$$\frac{15.67}{2 \times 3.99} - 1 = 0.96.$$

The large number of bolts provides fail safe capability.

Twisting of Fitting Flange

The bolts which carry the vertical load into the bearing are displaced by 2.0 cm (0.79 in) from the centerline of the fitting web. This leads to a moment per unit circumference of 452 kg/cm x 2 cm =

904 kg (1893 in lb/in). This moment is small compared to the one treated in Section 4.4.1.5 and for which the margin of safety is high.

4.4.2 Pivot

4.4.2.1 Loads Through Pivot

The loads through the pivot are as follows:

Vertical Load

The highest vertical load occurs in the 3g symmetric flight condition. This load which appears as the shear discontinuity in Figure 4.4-6 is 34.3×10^3 kg (75.7×10^3 lbs).

Pitching Moment (wing coordinate system)

The pitching moment transmitted through the pivot appears as the torsion discontinuity in Figure 4.4-11. Its value (for the 3g condition) is 4.24×10^3 m x kg ($.368 \times 10^6$ in x lb).

Rolling Moment (wing coordinate system)

During symmetric flight the airplane is balanced in roll by use of ailerons and no rolling moment (airplane system) is transmitted through the pivot. In wing coordinates this condition translates in (see Figure 4.4-13).

$$M_x \cos\Lambda - M_y \sin\Lambda = 0,$$

where Λ is the skew angle. For $\Lambda = \frac{\pi}{4}$ (45°) the relationship reduces to $M_x = M_y$, or roll moment (toward aft wing) equals pitch (up). Total moment through bearing is

$$\sqrt{2} \times 4.24 \times 10^3 \text{ m kg} = 6.00 \times 10^3 \text{ m kg } (0.520 \times 10^6 \text{ in lb}).$$

The roll moment which appears as the moment discontinuity in Figures 4.4-8 is 11.75×10^3 m kg (1.02×10^6 in lb) which is not equal to the pitching moment in 4.4.2.1. The discrepancy is there because in the loads work the airplane was balanced in roll for the pivot at 50% chord instead of 40% chord and because of slight differences in handling geometry. 0.83 degrees of aileron were applied in the loads work to create a rolling moment (wing system) of 4.97×10^3 m kg (0.431×10^6 in lb) toward forward wing. An additional moment of 7.51×10^3 m kg ($.0652 \times 10^6$ in lb) toward forward wing is required to reduce the unbalanced rolling moment toward the aft wing to 4.24×10^3 m kg (0.368×10^6 in lb) - to match the pitching moment. The total roll moment (wing system) generated by ailerons in the symmetric 3g condition is 12.48×10^3 m kg (1.083×10^6 in lb) toward the forward wing. We assume that aileron authority is twice this value.

The highest roll acceleration occurs when full aileron is applied towards the aft wing. We consider this at 80% of the highest load factor, i.e., at $n_z = 2.4$. In the following it is assumed that all loads for this condition are 80% of their values for 3g symmetric. When full aileron is applied toward the aft wing at 2.4g the unbalanced moments on the airplane are (wing system)

aileron contribution: $2 \times 12.48 \times 10^3$ m kg

flex. wing $.8 \times 12.48 \times 10^3$ m kg

TOTAL 34.94×10^3 m kg (3.03×10^6 in lb)

The instantaneous application of this moment causes an angular acceleration of the airplane and is reacted by inertia. The part of the moment reacted by fuselage inertia is transmitted through the pivot.

Application of the inverse inertia matrix of the airplane to the moment yields the angular acceleration. Application of the fuselage and tail inertia matrix to the angular acceleration yields the moment reacted by fuselage inertia through the pivot. The matrices of inertia are presented in Table 4.4-5 (4.4-6). The angular acceleration comes out as (wing system):

TABLE 4.4-5- Inertial Properties of Wing and Airplane

Wing Inertia (Wing System)		kg m^2
1.95×10^4	0	0
0	1.74×10^2	0
0	0	1.96×10^4

Fuselage Inertia (A/P System)		kg m^2
5.16×10^3	0	3.65×10^3
0	1.333×10^5	0
3.65×10^3	0	1.320×10^5

Airplane Inertia (Wing System)		kg m^2
8.87×10^4	6.41×10^4	2.58×10^3
6.41×10^4	6.94×10^4	-2.58×10^3
2.58×10^3	-2.58×10^3	1.516×10^5

Airplane Inverse Matrix of Inertia (Wing System) kg m^2		
3.40×10^{-5}	-3.14×10^{-5}	-1.12×10^{-6}
-3.14×10^{-5}	4.35×10^{-5}	1.28×10^{-6}
-1.12×10^{-6}	1.28×10^{-6}	6.64×10^{-6}

Apply this matrix to A/P moment to find fuselage reaction (dimensionless)		
.337	.613	.022
.005	.992	-.000
.022	-.025	.870

TABLE 4.4-6- Inertial Properties of Wing and Airplane (English Units)

Wing Inertia (Wing System)		(lb in^2)
.6660 x 10^8	0.	0.
0.	.5940 x 10^6	0.
0.	0.	.6700 x 10^8

Fuselage Inertia (A/P System)		(lb in^2)
.1763 x 10^8	0.	.1248 x 10^8
0.	.4555 x 10^9	0.
.1248 x 10^8	0.	.4511 x 10^9

Airplane Inertia (Wing System)		(lb in^2)
.3032 x 10^9	.2189 x 10^9	.8827 x 10^7
.2189 x 10^9	.2372 x 10^9	-.8827 x 10^7
.8827 x 10^7	-.8827 x 10^7	.5181 x 10^9

Airplane Inverse Tensor of Inertia (Wing System) 1/(lb in^2)		
.9951 x 10^{-8}	-.9199 x 10^{-8}	-.3263 x 10^{-9}
-.9199 x 10^{-8}	.1272 x 10^{-7}	.3735 x 10^{-9}
-.3263 x 10^{-9}	.3735 x 10^{-9}	.1942 x 10^{-8}

Apply this Matrix to A/P Moment to Find Fuselage Reaction (dimensionless)		
.337	.613	.022
.005	.992	-.000
.022	-.025	.870

roll ω_x = -11.7 rad/s^2

pitch ω_y = -10.8 rad/s^2

yaw ω_z = -0.38 rad/s^2

The moment reacted through the pivot is (wing system).

roll M_x = 11.7 x 10^3 m x kg (1.022 x 10^6 in x lb)

pitch M_y = 0.16 x 10^3 m x kg (0.014 x 10^6 in x lb)

yaw M_z = 0.76 x 10^3 m x kg (0.066 x 10^6 in x lb)

The yaw moment is resisted by the wing pivot mechanism. The roll and pitch components are transmitted through the pivot along with the roll and pitch moments of the static balanced condition of 4.24 x 10^3 m kg (0.368 x 10^6 in lb) each. The total overturn moment through the bearing is:

$$M = \{(11.7 + 4.24)^2 + (0.16 + 4.24)2\}^{1/2} \times 10^3 \text{ m kg} =$$

16.60 x 10^3 m kg (1.44 x 10^6 in lb).

This moment is to be applied in combination with a vertical load of

$$V = 0.80 \times 34.3 \times 10^3 \text{ kg} = 27.4 \times 10^3 \text{ kg } (60.4 \times 10^3 \text{ lb}).$$

Summary of Conditions and Loads

TABLE 4.4-7- Pivot Loads

(Design Limit Load)

Condition	Load Through Pivot			
	Vertical Load		Overturn moment	
Skew angle = $\frac{\pi}{4}(45°)$	10^3 kg	(10^3 lb)	10^3 m kg	(10^6 in lb)
3g Symmetrical	34.3	(75.7)	6.00	(0.520)
2.4g maximum roll acceleration	27.4	(60.4)	16.6	(1.44)

4.4.2.2 Sizing of Bearing

The bearing selected is the Kaydon Bearing Division part No. S325. Figure 4.4-17 shows the combined load envelope for this bearing reduced by a factor of safety of two as supplied by Kaydon and the points representing the two limit load conditions of the last subsection. It is seen that the design points are well within the envelope.

4.4.2.3 Stiffness of Bearing.

Data on stiffness of bearing is not available.

4.4.3 Wing Support Structure.

4.4.3.1 Fuselage Loads

The loads through the pivot as obtained in 4.4.2 are presented in the following table.

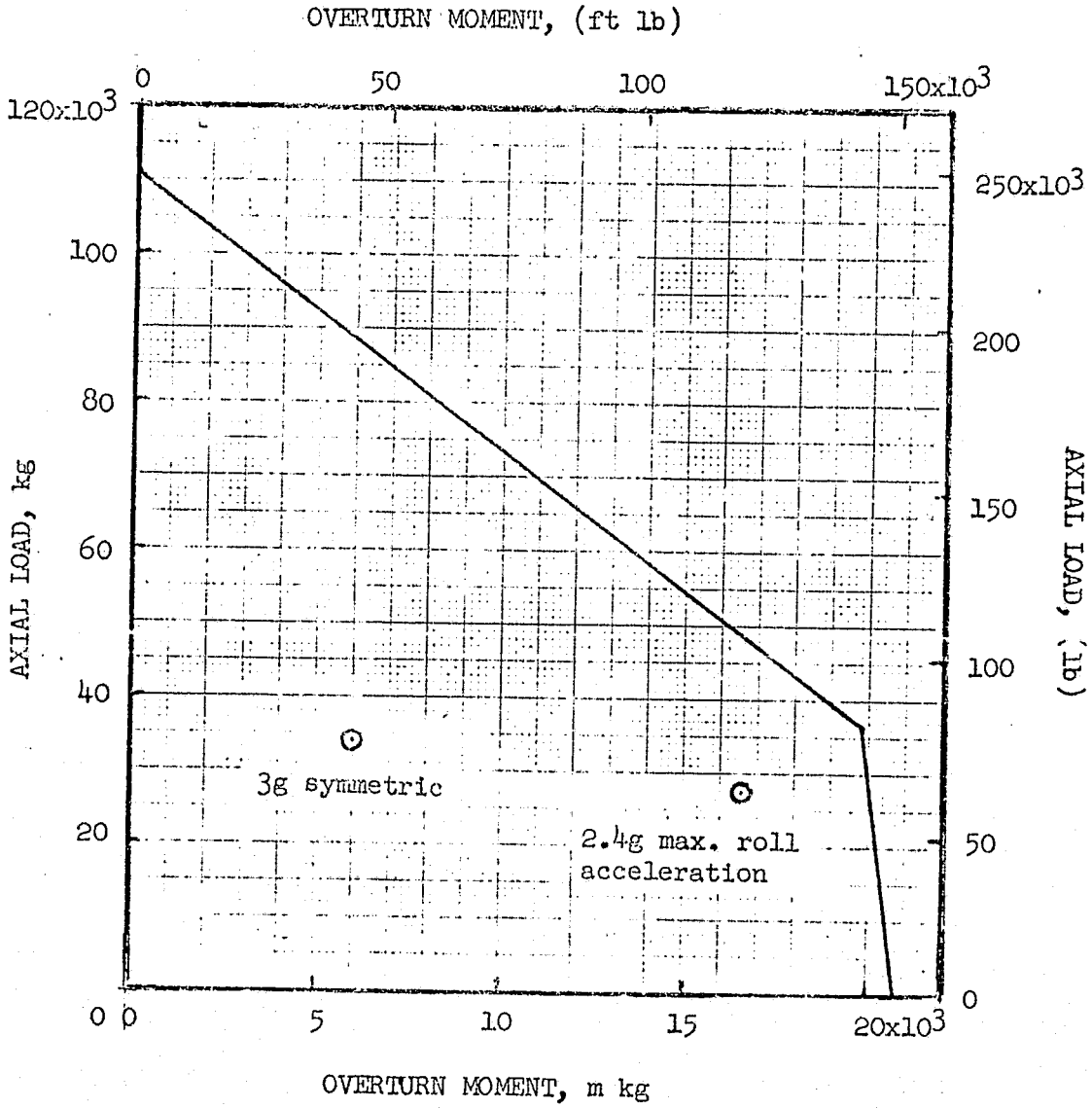

FIGURE 4.4-17 - Structural Envelope of Bearing and Pivot Load

TABLE 4.4-8- Pivot Loads. Wing System

(Design Limit Load)

Condition	Vertical Loads		Moments			
			Pitch		Roll	
Skew angle = $\frac{\pi}{4}$ (45°)	10^3 kg	(10^3 lb)	10^3 m kg		(10^6 in lb)	
3g Symmetric	34.3	(75.7)	4.24	(0.368)	4.24	(0.368)
2.4g max roll accel. toward aft wing	27.4	(60.4)	4.40	(0.382)	16.01	(1.390)

When translated to airplane system the loads of the last table become:

TABLE 4.4-9- Pivot Loads Airplane System
(Design Limit Load)

Condition	Vertical Loads		Moments			
			Pitch		Roll	
Skew angle = $\frac{\pi}{4}$ (45°)	10^3 kg	(10^3 lb)	10^3 m kg		(10^6 in lb)	
3g symmetric	34.3	(75.7)	6.00	(0.520)	0	
2.4g max roll accel. toward aft wing	27.4	(60.4)	14.44	(1.253)	8.21	(0.713)

These loads are reacted at the two F-8 wing attach lugs and the two forward F-8 down load points (wing incidence fittings) which the present design adapts for uploads as well as down loads. The wing support structure connects to the A-frame (truss assembly) leading to these points through a ball joint which passes no moment. The load at this joint is always distributed equally to both points. Rolling moment is reacted as a couple in the wing attach lugs. The reactions to the fuselage points are:

TABLE 4.4-10- Fuselage Attach Loads

(Design Limit Load)

Condition	Reaction 10^3 kg (10^3 lbs)					
	Wing attach lugs				forward	
Skew angle = $\frac{\pi}{4}$ (45°)	Fwd. Wing		Aft Wing			
3g Symmetric	13.6	(29.9)	13.6	(29.9)	3.62	(7.98)
2.4g Max roll accel. toward aft wing	16.0	(35.3)	0.61	(1.34)	5.42	(11.96)

4.4.3.2 Bearing Fitting

Bolt Loads.

The outside race of the bearing is attached to the fuselage by 28 1.43 cm (9/16 in) bolts. The radius of this bolt pattern is 43.82 cm (17.25 in). The maximum bolt loads obtained as in Section 4.4.1.5 are shown in the following table.

TABLE 4.4-11- Load Transfer from Bearing

(Airplane System, Design Limit Loads)

Condition	Flange Load w_{max} kg/cm	(lb/in)	Bolt Load p_{max} kg	(lb)	θ Location of max load rad	(deg)	Margin of safety of Bolt
3 g Symmetric	224	(1255)	2203	(4856)	$\frac{\pi}{2}$	(90)	high
2.4 g max roll Accel.	375	(2099)	3688	(8730)	1.05	(60)	1.12

Lateral Bending

The lateral distribution of load on the bearing fitting is sketched in Figure 4.4-18. The distributed load on the bearing is obtained by the methods of Section 4.4.1.5 using the loads data above. The load per unit of y (fuselage system is)

$$w = \frac{P_F + P_A + P_C - 2M_x y/R^2}{\pi\sqrt{R^2 - y^2}}, \qquad -R \leq y \leq R.$$

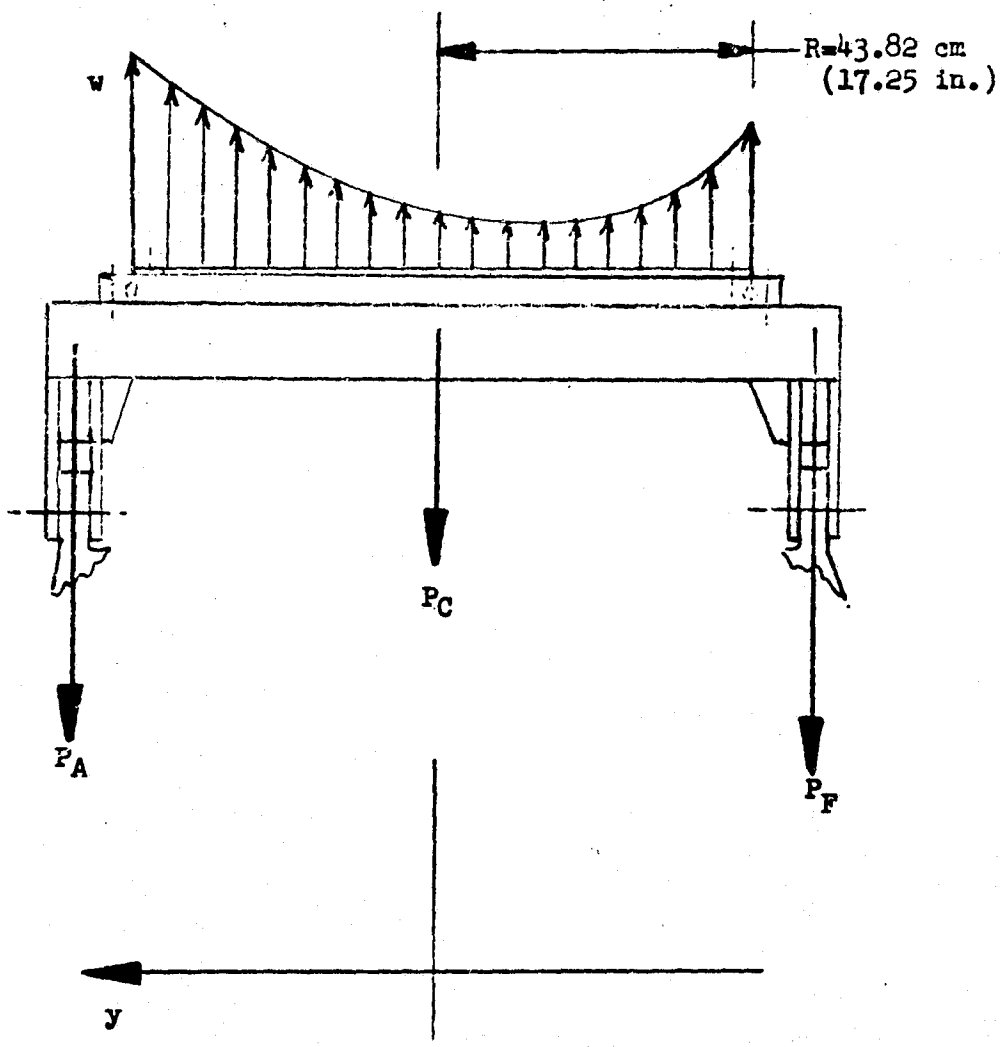

FIGURE 4.4-18 - Lateral Distribution of Load on Wing Support Structure (sketch)

R is 43.82 cm (17.25 in). The other parameters are given by Table 4.4-12.

TABLE 4.4-12- Load Data for Wing Support Structure
(Airplane System, Design Limit Load)

Condition	P_F	P_A	P_C	M_x
	10^3 kg		(10^3 lb)	10^3 m kg (10^6 in lb)
3g Symmetric	13.6 (29.9)	13.6 (29.9)	7.24 (15.96)	0
2.4g max roll accel.	16.0 (35.3)	0.61(1.34)	10.84 (23.92)	8.21 (0.713)

The shear distribution that results is

$$S = \begin{cases} -P_F, & y \leq -R \\ \dfrac{-P_F + P_A + P_C}{2} + \dfrac{P_F + P_A + P_C}{\pi} \arcsin \dfrac{y}{R} + \dfrac{2M_x}{\pi R^2}\sqrt{R^2 - y^2}, & -R \leq y \leq 0 \\ \dfrac{-P_F + P_A - P_C}{2} + \dfrac{P_F + P_A + P_C}{\pi} \arcsin \dfrac{y}{R} + \dfrac{2M_x}{\pi R^2}\sqrt{R^2 - y^2}, & 0 \leq y \leq R \\ P_A, & R \leq y \end{cases}$$

This distribution is shown in Figures 4.4-19 and 4.4-20. The resulting bending moment distributions are given in Figures 4.4-21 an4.4-22 and in Tables 4.4-13, and 4.4-14. The highest bending moment is 2.70×10^3 m kg (0.243×10^6 in lb). The minimum section through the fitting bearing is shown in Figure 4.4-22. The section properties (Figure 4.4-23) are $I = 3587$ cm^4 (86.2 in^4), $c = 10.19$ cm (4.01 in).

Using the highest moment with the weakest section results in a stress level of 7.7×10^6 kg/m^2 (10.9×10^3 psi). The actual stress levels are lower.

The purpose of the overstrength design of the support structure is to maintain high stiffness in the bearing support. The stiffness may be estimated as $8EI/\ell$ (reference 6 p113 #37), where $\ell = 106.7$ cm (42 in) is the distance between fuselage lugs. This estimate results in a stiffness of 5.5×10^6 m kg/rad (4.8×10^8 in lb/rad). Since the minimum section was used, the actual value will be higher and well in excess of the requirement set forth in Section 4.2. This value does not include the flexibility of the bearing itself.

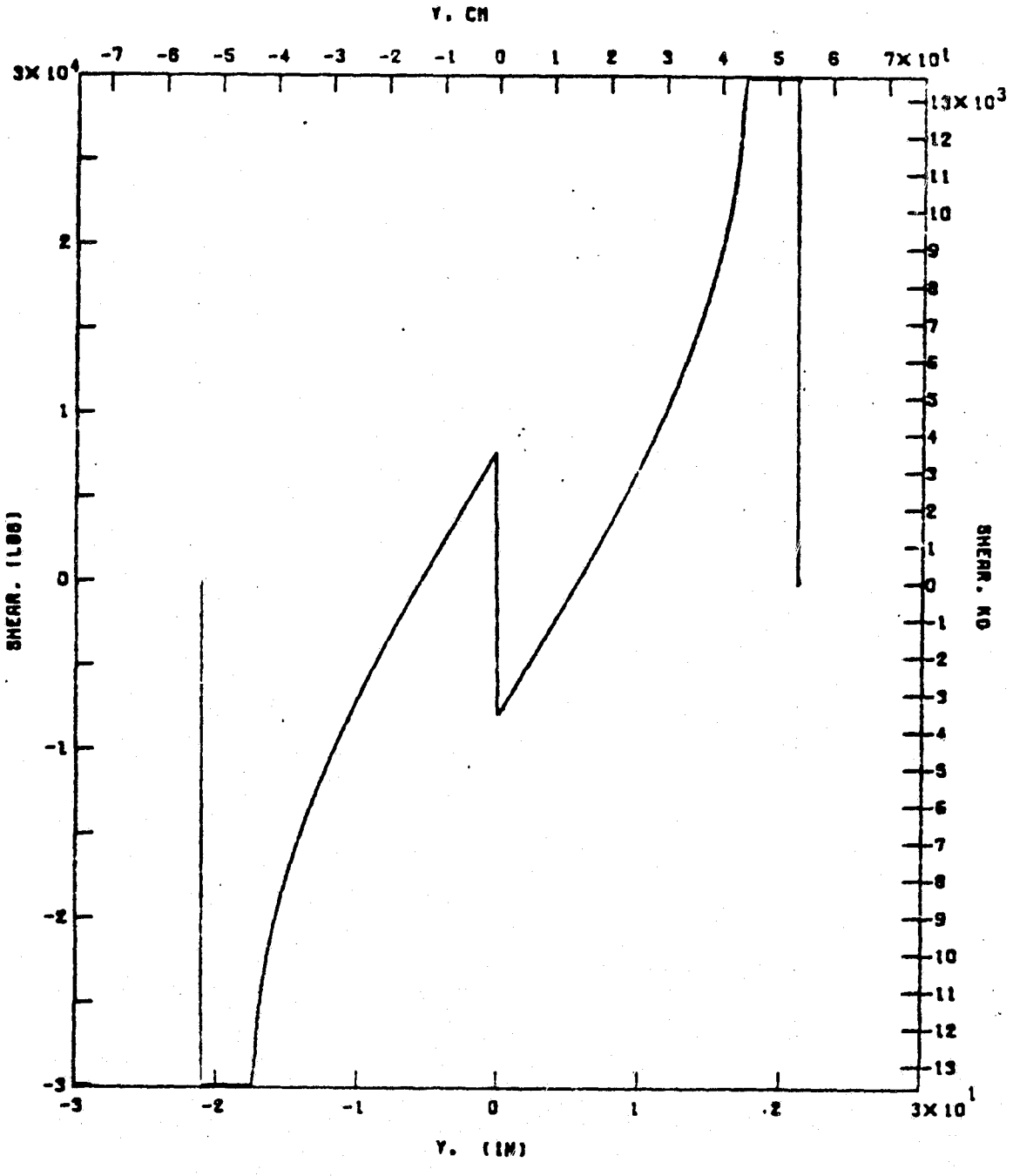

FIGURE 4.4-19 - Shear Distribution in the Wing Support Structure for the 3g Symmetric Condition.

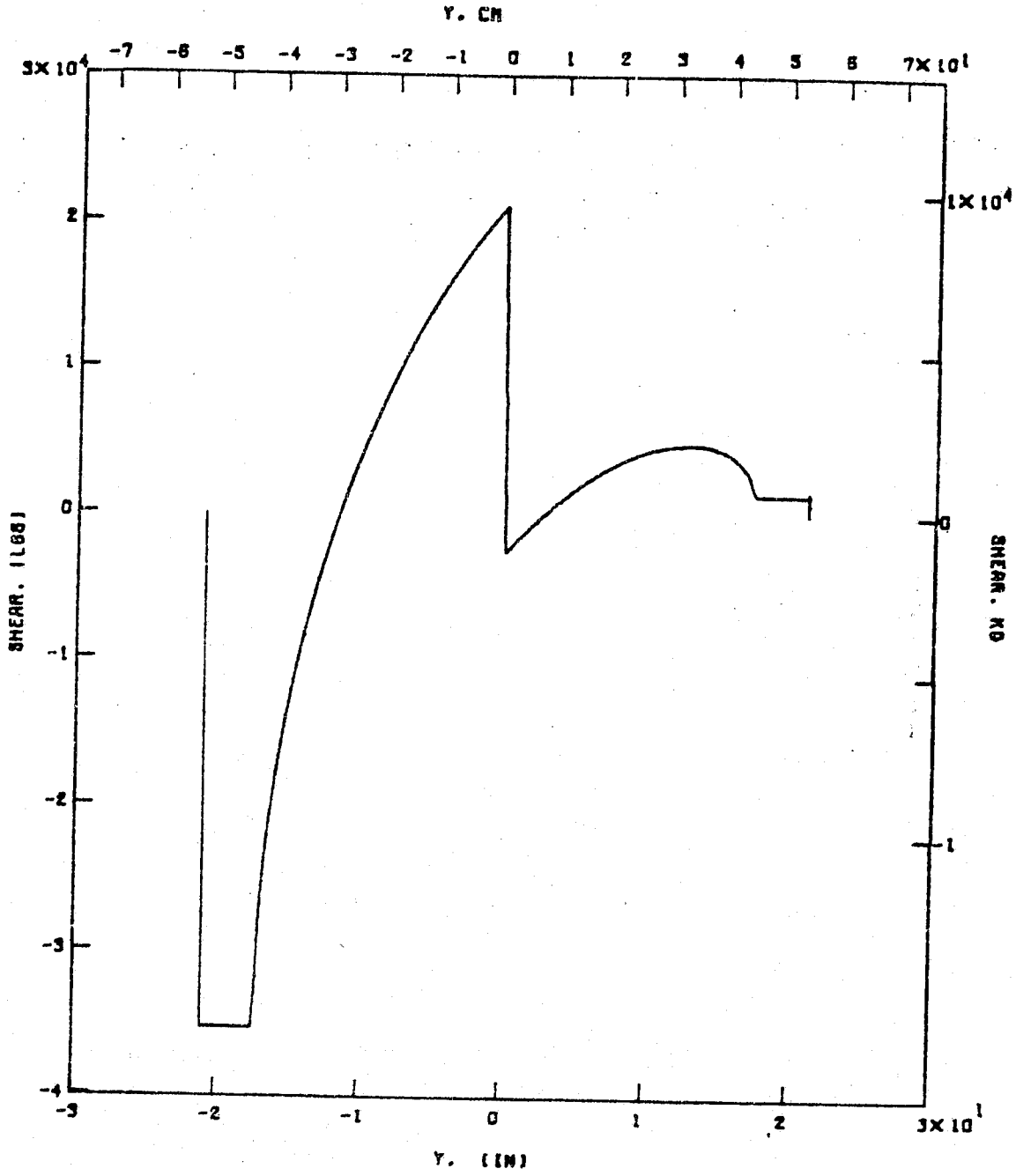

FIGURE 4.4-20 - Shear Distribution in the Wing Support Structure for the 2.4g maximum roll acceleration Condition.

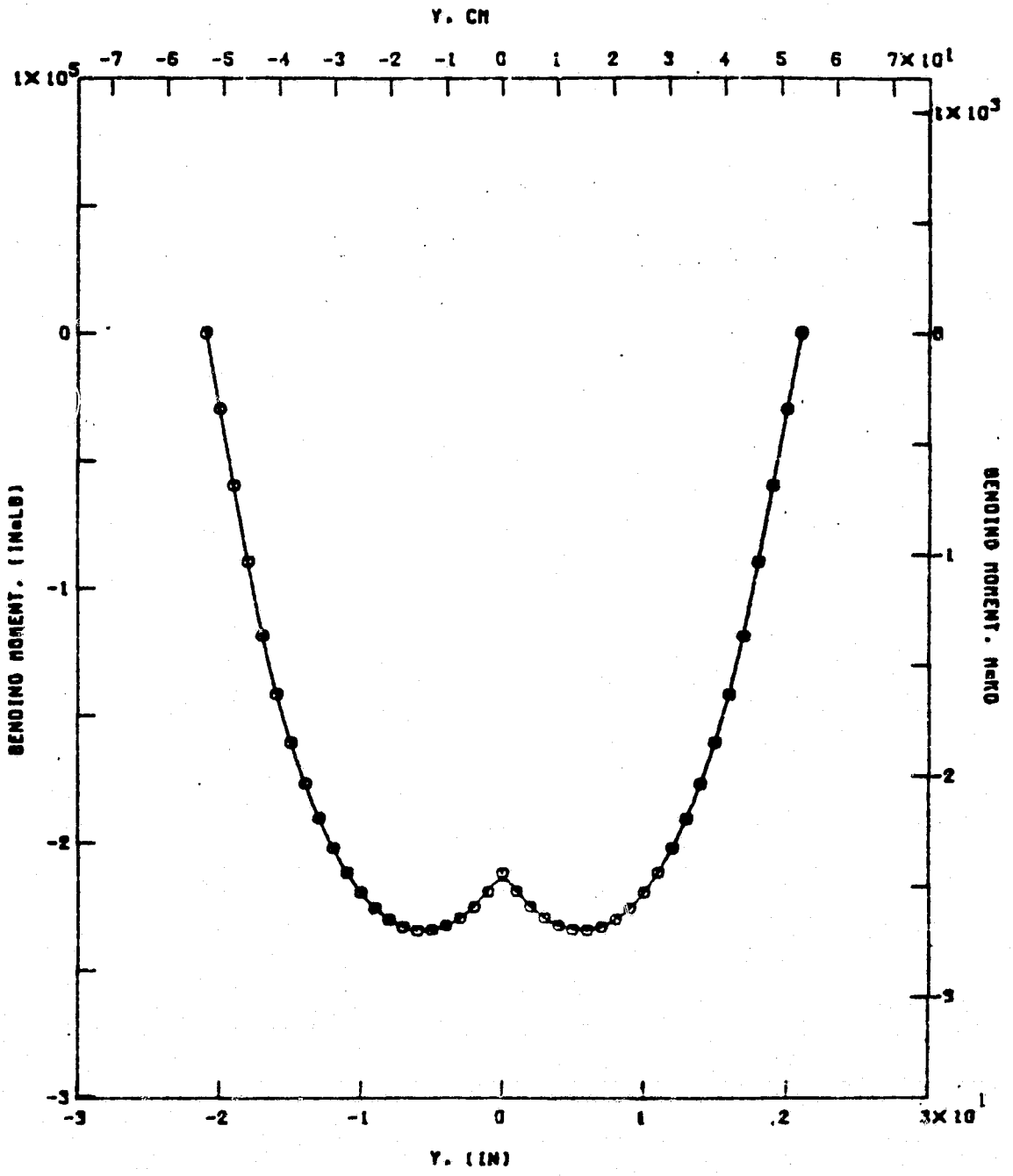

FIGURE 4.4-21 - Bending Distribution in the Wing Support Structure for the 3g Symmetric Condition.

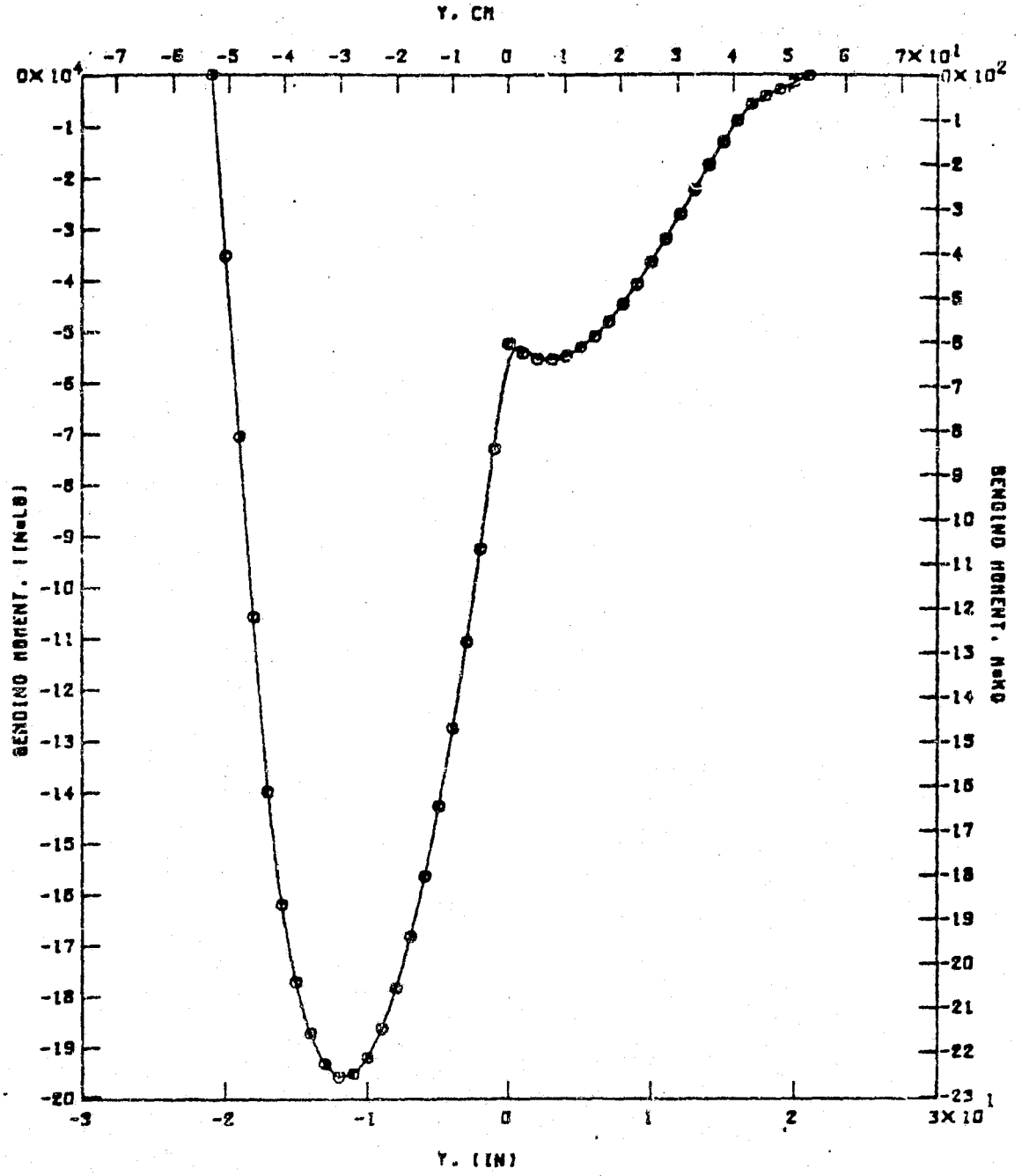

FIGURE 4.4-22 - Bending Distribution in the Wing Support Structure for the 2.4g maximum roll acceleration condition.

TABLE 4.4-13 - Bending Distribution in the Wing Support Structure for the 3g symmetric Condition

Location, y cm	(in.)	Bending Moment m kg	(in lb)
-53.34	(-21.00)	0.	(0.)
-50.80	(-20.00)	-.344E+03	(-.299E+05)
-48.26	(-19.00)	-.689E+03	(-.598E+05)
-45.72	(-18.00)	-.103E+04	(-.897E+05)
-43.18	(-17.00)	-.137E+04	(-.119E+06)
-40.64	(-16.00)	-.163E+04	(-.142E+06)
-38.10	(-15.00)	-.185E+04	(-.161E+06)
-35.56	(-14.00)	-.204E+04	(-.177E+06)
-33.02	(-13.00)	-.220E+04	(-.191E+06)
-30.48	(-12.00)	-.233E+04	(-.202E+06)
-27.94	(-11.00)	-.244E+04	(-.212E+06)
-25.40	(-10.00)	-.253E+04	(-.220E+06)
-22.86	(-9.00)	-.260E+04	(-.226E+06)
-20.32	(-8.00)	-.265E+04	(-.230E+06)
-17.78	(-7.00)	-.268E+04	(-.233E+06)
-15.24	(-6.00)	-.270E+04	(-.234E+06)
-12.70	(-5.00)	-.270E+04	(-.234E+06)
-10.16	(-4.00)	-.268E+04	(-.233E+06)
-7.62	(-3.00)	-.264E+04	(-.230E+06)
-5.08	(-2.00)	-.259E+04	(-.225E+06)
-2.54	(-1.00)	-.253E+04	(-.219E+06)
0.00	(0.00)	-.244E+04	(-.212E+06)
2.54	(1.00)	-.253E+04	(-.219E+06)
5.08	(2.00)	-.259E+04	(-.225E+06)
7.62	(3.00)	-.264E+04	(-.230E+06)
10.16	(4.00)	-.268E+04	(-.233E+06)
12.70	(5.00)	-.270E+04	(-.234E+06)
15.24	(6.00)	-.270E+04	(-.234E+06)
17.78	(7.00)	-.268E+04	(-.233E+06)
20.32	(8.00)	-.265E+04	(-.230E+06)
22.86	(9.00)	-.260E+04	(-.226E+06)
25.40	(10.00)	-.253E+04	(-.220E+06)
27.94	(11.00)	-.244E+04	(-.212E+06)
30.48	(12.00)	-.233E+04	(-.202E+06)
33.02	(13.00)	-.220E+04	(-.191E+06)
35.56	(14.00)	-.204E+04	(-.177E+06)
38.10	(15.00)	-.185E+04	(-.161E+06)
40.64	(16.00)	-.163E+04	(-.142E+06)
43.18	(17.00)	-.137E+04	(-.119E+06)
45.72	(18.00)	-.103E+04	(-.897E+05)
48.26	(19.00)	-.689E+03	(-.598E+05)
50.80	(20.00)	-.344E+03	(-.299E+05)
53.34	(21.00)	.170E-09	(.148E-07)

TABLE 4.4-14 - Bending Distribution in the Wing Support Structure for the 2.4g maximum roll acceleration Condition.

Location, y cm	(in.)	Bending Moment m kg	(in lb)
-53.34	(-21.00)	0.	(0.)
-50.80	(-20.00)	-.407E+03	(-.353E+05)
-48.26	(-19.00)	-.813E+03	(-.706E+05)
-45.72	(-18.00)	-.122E+04	(-.106E+06)
-43.18	(-17.00)	-.161E+04	(-.140E+06)
-40.64	(-16.00)	-.187E+04	(-.162E+06)
-38.10	(-15.00)	-.204E+04	(-.177E+06)
-35.56	(-14.00)	-.216E+04	(-.187E+06)
-33.02	(-13.00)	-.223E+04	(-.193E+06)
-30.48	(-12.00)	-.226E+04	(-.196E+06)
-27.94	(-11.00)	-.225E+04	(-.195E+06)
-25.40	(-10.00)	-.221E+04	(-.192E+06)
-22.86	(-9.00)	-.215E+04	(-.186E+06)
-20.32	(-8.00)	-.206E+04	(-.178E+06)
-17.78	(-7.00)	-.194E+04	(-.168E+06)
-15.24	(-6.00)	-.180E+04	(-.156E+06)
-12.70	(-5.00)	-.165E+04	(-.143E+06)
-10.16	(-4.00)	-.147E+04	(-.128E+06)
-7.62	(-3.00)	-.128E+04	(-.111E+06)
-5.08	(-2.00)	-.107E+04	(-.925E+05)
-2.54	(-1.00)	-.841E+03	(-.730E+05)
0.00	(0.00)	-.602E+03	(-.523E+05)
2.54	(1.00)	-.626E+03	(-.544E+05)
5.08	(2.00)	-.638E+03	(-.554E+05)
7.62	(3.00)	-.640E+03	(-.555E+05)
10.16	(4.00)	-.631E+03	(-.548E+05)
12.70	(5.00)	-.613E+03	(-.532E+05)
15.24	(6.00)	-.587E+03	(-.510E+05)
17.78	(7.00)	-.554E+03	(-.481E+05)
20.32	(8.00)	-.514E+03	(-.447E+05)
22.86	(9.00)	-.470E+03	(-.408E+05)
25.40	(10.00)	-.421E+03	(-.365E+05)
27.94	(11.00)	-.368E+03	(-.320E+05)
30.48	(12.00)	-.314E+03	(-.272E+05)
33.02	(13.00)	-.258E+03	(-.224E+05)
35.56	(14.00)	-.203E+03	(-.176E+05)
38.10	(15.00)	-.151E+03	(-.131E+05)
40.64	(16.00)	-.103E+03	(-.898E+04)
43.18	(17.00)	-.659E+02	(-.572E+04)
45.72	(18.00)	-.482E+02	(-.418E+04)
48.26	(19.00)	-.327E+02	(-.284E+04)
50.80	(20.00)	-.173E+02	(-.150E+04)
53.34	(21.00)	-.187E+01	(-.162E+03)

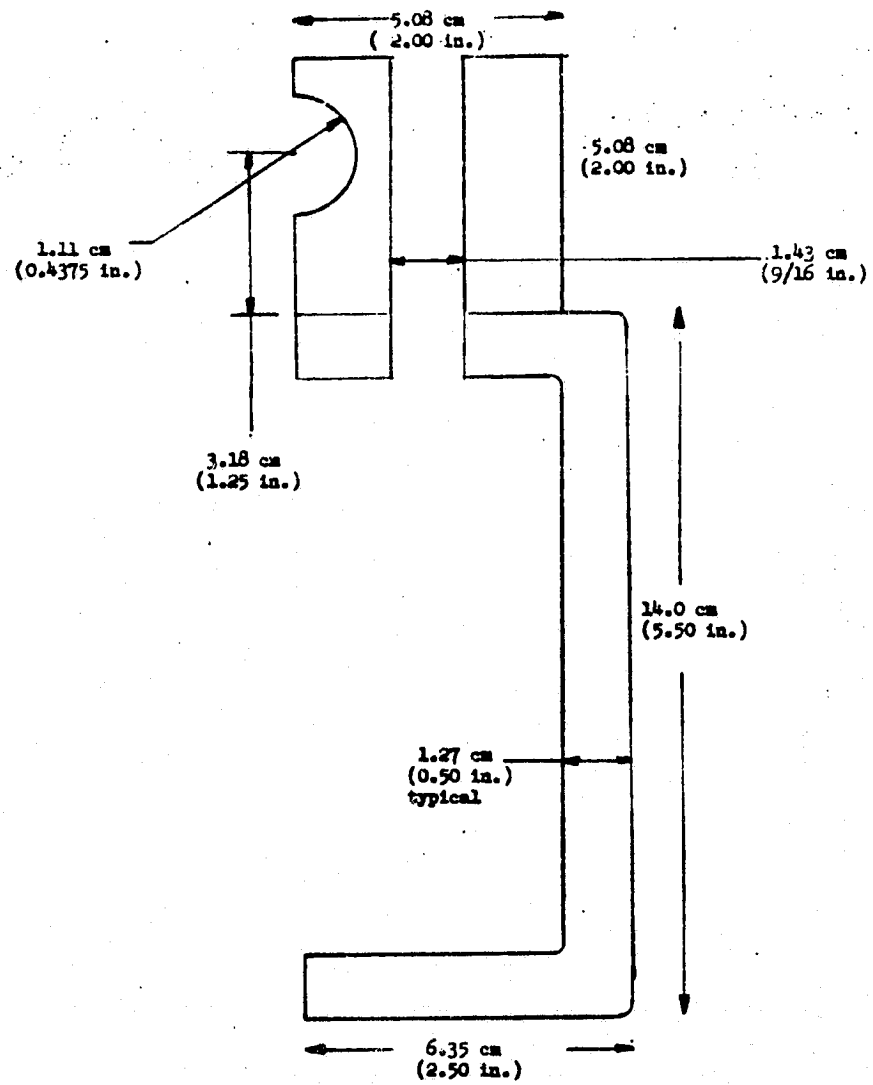

FIGURE 4.4-23 - Section through Wing Support Structure along centerline (aft side shown, forward side opposite.)

4.4.3.3 Forward Arm

Bending Due to Vertical Load

The vertical (design limit) load on the end of the forward arm is 10.9×10^3 kg (24.0×10^3 lb) and the arm is 1.16 m (46 in). The resulting moment at the root of the arm is $M = 12.7 \times 10^4$ m kg (1.10×10^6 in lb).

The section of the arm at the root is 14.0 cm x 36.8 cm (5.5 in. x 14.5 in.) and 1.27 cm (1/2 in.) thick.

$$I = 1/12\ (36.8 \times 14.0^3 - 34.26 \times 11.46^3) = 4120\ cm^4\ (98.5\ in^4),$$

$$c = 6.99\ cm\ (2.75\ in).$$

The bending stress is $Mc/I = 21.6 \times 10^6$ kg/m^2 (30.7×10^3 psi)

The margin of safety is $\frac{127}{2 \times 21.6} - 1 = 1.94$

Buckling of Upper Plate of Arm

The upper plate of the arm is conservatively considered as a rectangular panel 36.8 cm x 116 cm (14.5 in x 46 in) in compression in the amount determined above. The buckling stress of the plate (K = 3.6) is

$$KE\left(\frac{t}{b}\right)^2 = 3.6 \times 20.4 \times 10^9 \times \left(\frac{1.27}{36.8}\right)^2 = 87.5 \times 10^6\ kg/m^2$$

(124×10^3 psi)

The margin of safety is $\frac{124}{2 \times 21.6} - 1 = 1.87$.

Loads Due to Wing Rotation Actuator

The wing rotation actuator piston area is assumed to be 36.8 cm^2 (5.7 in^2). With a hydraulic pressure of 210 kg/cm^2(3000 psi) the maximum output of the actuator is

$$P = 210\ kg/cm^2 \times 36.8\ cm^2 = 7.73 \times 10^3\ kg\ (17.0 \times 10^3\ lb)$$

This load is applied to the actuator attach fitting on the forward arm. The actuator attach point is situated δx behind the forward end of the arm, δy to the right and δz below the centerline of the arm, where:

$$\delta x = 33.0\ cm\ (13\ in),$$

$$\delta y = 18.0\ cm\ (7.1\ in),$$

$$\delta z = 7.6\ cm\ (3\ in).$$

The section of the arm at this point is 10.2 cm x 14.6 cm (4 in x 5.75 in) with a typical wall thickness of 1.27 cm (1/2 in). The section properties are

$$I_{yy} = \frac{1}{12}(14.6 \times 10.2^3 - 12.06 \times 7.66^3) = 839 \text{ cm}^4 \ (20.0 \text{ in}^4)$$

$$c_y = 5.1 \text{ cm } (2 \text{ in})$$

$$I_{zz} = \frac{1}{12}(10.2 \times 14.6^3 - 7.66 \times 12.06^3) = 1526 \text{ cm}^4 \ (36.6 \text{ in}^4)$$

$$c_z = 7.30 \text{ cm } (2.88 \text{ in})$$

The moments due to both the actuator load and the arm load are

$$M_y = 10.9 \times 10^3 \text{ kg} \times 0.330 \text{ m} + 7.73 \times 10^3 \text{ kg} \times 0.076 \text{ m} =$$

$$4.18 \times 10^3 \text{ m kg } (363 \times 10^3 \text{ in lb})$$

$$M_z = 7.73 \times 10^3 \text{ kg} \times 0.180 \text{ m} = 1.39 \times 10^3 \text{ m kg } (121 \times 10^3 \text{ in lb})$$

The stress at the critical corner of the section is

$$\frac{M_z c_z}{I_{zz}} + \frac{M_y c_y}{I_{yy}} = 32.1 \times 10^6 \text{ kg/m}^2 \ (45.6 \times 10^3 \text{ psi})$$

The margin of safety is $\frac{127}{2 \times 32.1} - 1 = 0.98$.

4.4.3.4 Truss Assembly

Loads

The function of the A-frame truss is to distribute the load to the two forward fuselage points. The forward arm attaches to the A-frame through a universal joint and passes only vertical load. The truss is shown in Figure 3.4-1. Upload puts the diagonal members in tension and the cross member in compression. The loads for the 2.4g maximum roll acceleration condition are (design limit loads):

Upload	10.8×10^3 kg	$(23.9 \times 10^3$ lb)
Diagonal member	9.0×10^3 kg	$(19.9 \times 10^3$ lb)
Cross member	-7.2×10^3 kg	$(-15.9 \times 10^3$ lb)

Static Margin

The A-frame is constructed of steel tubes of outer diameter 3.81 cm (1.5 in) and inner diameter of 2.54 cm (1 in). The sectional area of the tubes is 6.33 cm^2 (0.98 in^2). The stresses are:

Diagonal member 22×10^6 kg/m^2 (31.0×10^3 psi)

Cross member -77×10^6 kg/m^2 (-24.8×10^3 psi)

With a factor of safety of 2.0 and ultimate allowable of steel equal to 127×10^6 kg/m^2 (180×10^3 psi) the margins of safety for both members are high.

Column Buckling of Cross Member

The moment of inertia of the cross member is

$$I = \frac{\pi}{64} (3.81^4 - 2.54^4) = 8.30 \text{ cm}^4 \ (0.199 \text{ in}^4),$$

and its length L = 1.054 m (41.5 in). Using $E = 20.4 \times 10^9$ kg/m^2 (29×10^6 psi) the pinned buckling load of the member becomes

$$P = \frac{\pi^2}{L^2} EI = 15.0 \times 10^3 \text{ kg } (33.2 \times 10^3 \text{ lb}).$$

Using the design limit load of subsection 4.4.3.4 and a factor of safety of 2, the margin of safety is

$$\frac{15.0}{2 \times 7.2} - 1 = 0.04$$

4.4.4 Existing F-8 Structure

The loads on existing F-8 structures are given in Table 4.4-10, Section 4.4.3.1 These design loads are converted to ultimate loads by use of a factor of safety of 1.5. Figure 4.4-23 compares the ultimate loads of this study with the F-8 ultimate loads for which existing F-8 structures is good as substantiated by test. It is seen that the oblique wing loads are lower than original F-8 loads. The margins of safety of forward and aft points are:

Aft (wing attach lug) $\frac{66.8}{24.0} - 1 = 1.78$

Fwd $\frac{11.8}{8.1} - 1 = 0.46$

4.5 Weight

The mass properties analysis was performed using the F-8J as a base, since this data was readily available. Mass properties on the two place F-8 (a prototype development) was not documented to the proper detailed level to allow its use as a data base for a "put and take" derivation. However, comparing the configuration differences between the F-8J and the NTF-8A, it was concluded that the NTF-8A mass properties would not be significantly different from the F-8J, with guns removed.

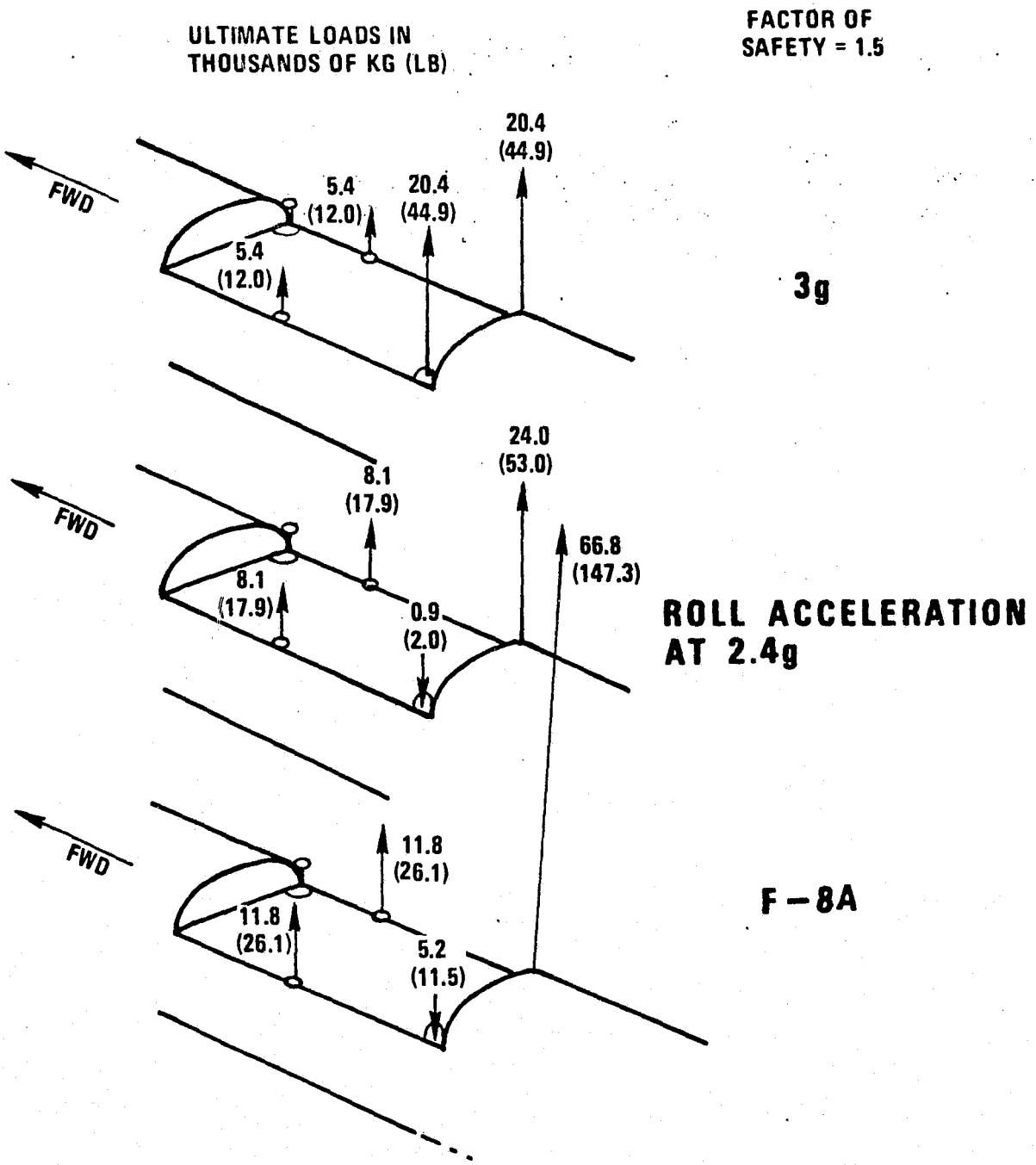

FIGURE 4.4-24 – Loads in F-8 Fuselage Attach Points

4.5.1 Take-Off Gross Weight

A take-off gross weight for the oblique wing airplane is derived as follows:

	kg	(lb)
F-8J - 4 gun fighter - take-off	13720	(30248)
Remove: Wing and wing installed systems	-1872	(-4128)
Wing fuel	-1767	(-3895)
Guns ammo and provisions	-440	(-969)
Add: Turntable bearing	109	(240)
Turntable support assembly	145	(320)
Truss fitting	14	(30)
Wing pivot actuator assembly	43	(95)
Fuselage/wing fairings	34	(75)
New wing consisting of:		
Torque box skins	1084	(2390)
Torque box spars	136	(300)
Torque box ribs	63	(140)
Pivot attach fitting	227	(500)
Fixed leading edge	51	(112)
Fixed trailing edge	65	(144)
Ailerons	29	(64)
Flaps	23	(50)
Attachments and misc.	227	(500)
Non structural fairing and systems	229	(504)
Take-off gross weight	12120	(26720)

4.5.2 Mass Properties

The following mass properties were derived for use in the structural, dynamics, and loads analyses:

Total airplane - zero sweep - Take-off weight

Weight = 12120 kg (26720 lbs)

Centroid = $\overline{X}$ = F.S. 456.2 (28.9% MAC)
$\overline{Y}$ = B.L. 0
$\overline{Z}$ = W.L. 104.7

$I_{xx} = 27.5 \times 10^3$ kg m^2 (94.0×10^6 lb in^2)

$I_{yy} = 126.3 \times 10^3$ kg m^2 (431.7×10^6 lb in^2)

$I_{zz} = 142.1 \times 10^3$ kg m^2 (485.8×10^6 lb in^2)

$P_{xy} = 0$

$P_{yz} = 0$

P_{zx} = 4.4 x 10^3 kg m^2 (14.9 x 10^6 lb in^2)

Total airplane - $\frac{\pi}{4}$ (45°) skew - Take-off weight

C.G. shift is negligible

I_{xx} = 12.8 x 10^3 kg m^2 (43.7 x 10^6 lb in^2)

I_{yy} = 141.0 x 10^3 kg m^2 (482.0 x 10^6 lb in^2)

I_{zz} = 142.1 x 10^3 kg m^2 (485.8 x 10^6 lb in^2)

P_{xy} = 9.8 x 10^3 kg m^2 (33.5 x 10^6 lb in^2)

P_{yz} = 0

P_{zx} = 4.4 x 10^3 kg m^2 (14.9 x 10^6 lb in^2)

Total airplane less wing and contents - take-off

Weight = 9986 kg (22016 lbs)

Centroid = $\overline{X}$ = F.S. 454.4
$\overline{Y}$ = B.L. 0
$\overline{Z}$ = W.L. 96.4

I_{xx} = 5.2 x 10^3 kg m^2 (17.8 x 10^6 lb in^2)

I_{yy} = 123.7 x 10^3 kg m^2 (442.8 x 10^6 lb in^2)

I_{zz} = 122.1 x 10^3 kg m^2 (417.3 x 10^6 lb in^2)

P_{xy} = 0

P_{yz} = 0

P_{zx} = 3.8 x 10^3 kg m^2 (13.0 x 10^6 lb in^2)

Wing and Contents only

Weight = 2134 kg (4704 lbs)

Centroid = $\overline{X}$ = 2.63 cm aft of pivot
$\overline{Y}$ = Centerline of wing
$\overline{Z}$ = Center of airfoil

I_{xx} = 19.8 x 10^3 kg m^2 (67.6 x 10^6 lb in^2)

I_{yy} = 0.18 x 10^3 kg m^2 (0.60 x 10^6 lb in^2)

I_{zz} = 19.9 x 10^3 kg m^2 (68.1 x 10^6 lb in^2)

Wing and contents mass distribution 10 equal slices taken along the 40% chord line).

Bay B.L. Sta Inch	Weight Per Side kg (lbs)	Centoirds (Wing System) cm (in) y	x	z	I_{yy}	I_{xx}	Inertia kg cm^2 (lb in^2) I_{zz}
0-30	297.2	36.09	2.26	0	294 836	170 799	409 319
	(655.3)	(14.21)	(0.89)	(0)	(100 754)	(58 367)	(139 876)
30-60	174.5	110.85	3.12	0	182 142	106 406	254 492
	(384.7)	(43.64)	(1.23)	(0)	(62 243)	(36 362)	(86 967)
60-90	136.8	189.46	3.18	0	132 412	77 679	186 844
	(301.5)	(74.59)	(1.25)	(0)	(45 249)	(26 545)	(63 850)
90-120	115.4	265.58	2.95	0	95 959	63 694	143 693
	(254.4)	(104.56)	(1.16)	(0)	(32 792)	(21 766)	(49 104)
120-150	95.8	341.66	2.74	0	67 585	51 494	108 548
	(211.2)	(134.51)	(1.08)	(0)	(23 096)	(17 597)	(37 094)
150-180	78.0	417.73	2.51	0	45 996	40 916	80 295
	(171.9)	(164.46)	(0.99)	(0)	(15 718)	(13 982)	(27 439)
180-210	61.9	493.75	2.29	0	30 015	31 791	57 973
	(136.5)	(194.39)	(0.90)	(0)	(10 257)	(10 864)	(19 811)
210-240	47.7	569.72	2.06	0	18 582	23 996	40 459
	(105.1)	(224.30)	(0.81)	(0)	(6 350)	(8 200)	(13 826)
240-270	35.1	645.59	1.83	0	10 742	17 397	27 188
	(77.5)	(254.17)	(0.72)	(0)	(3 671)	(5 945)	(9267)
270-300	24.4	721.33	1.60	0	5 659	11 904	17 145
	(53.9)	(283.99)	(0.63)	(0)	(1 934)	(4 068)	(5 859
TOTAL	1066.8	234.32	2.62	0	883 806	40.320 709	41 050 660
	(2352.0)	(92.25)	(1.03)	(0)	(302 022)	(13 778 734)	(14 028 179)

4.5.3 Balance

There is no unsolvable balance problem with the wing pivot located at F.S. 463.53. The take-off center of gravity is calculated to be F.S. 456.2 or 28.9% MAC. Fuel burn will vary the C.G. between 27.3% MAC and 38.7%. The take-off C.G. may also be moved anywhere between 24.4% and 33.0% MAC by adding up to 136 Kilograms (300 pounds) of ballast.

5.0 PROPOSED FOLLOW ON PROGRAM

5.1 Introduction

The completed study establishes the structural feasibility of an oblique wing for the F-8 aircraft. A follow-on program is recommended herein to exploit the feasibility study and extend it into a hardware program. The proposed follow-on program effort is presented in three phases as follows:

Phase I - Engineering Validation
Phase II - Engineering Design
Phase III - Tooling and Manufacturing

The Engineering Validation phase is necessary as an extension to the completed study. This phase will encompass problems of stability and control, define control surfaces, investigate the aerodynamic fairing of the pivot, establish seal requirements for wing/fairing interface and prepare analytic tools for handling supersonic loads on a flexible oblique wing. The majority of effort in this phase will have to be completed prior to initiation of Phase II.

A statement-of-work is presented in the following pages to define in some detail the various tasks associated with each phase of the overall program. These tasks are generally listed under the various disciplines, or associated departmental functions, to provide the basis for estimating costs for the various phases. The Tooling and Manufacturing policies are defined in order to establish the requirements for completing the prototype hardware, quantity of one, and for modifying the aircraft to accept the oblique wing hardware. The Quality and Materials Department tasks are not separately defined as they are an integral part of the Tooling and Manufacturing phase.

A proposed program schedule is presented to illustrate the time span for the three phases. This schedule shows the anticipated start date, the phase relationship or overlapping time span for program continuity, the basic program milestones, and the completion date for the installation and basic checkout of the aircraft at NASA-FRC Edwards, California. Subsequent ground and flight tests are not included as part of this program.

5.2 Statement of Work

5.2.1 Phase I: Engineering Validation Program

5.2.1.1 Aerodynamics Tasks

Airplane configuration will be established:

(a) Wing planform.

(b) Airfoil section (tip thickness ratio may be influenced by space requirements of controls mechanism).

(c) Wing location.

(d) Wing incidence.

Flying Qualities and performance of the configuration will be investigated and the following defined:

(a) Control surface geometry.

(b) Control deflections and interconnections required for landing, cruise, and wing skew positions (based on flexible aerodynamic data).

(c) Stabilization systems, control authority for different flight conditions, coupling between lateral and longitudinal systems.

Wind tunnel tests will be conducted to establish:

(a) Wing/fuselage fairing contour.

(b) Surface pressure data on the wing, fuselage and UHT (data to be used for rigid load distributions and verification of local panel design loads).

(c) Force data for evaluation of flying qualities, performance, and airplane balance for structural analysis.

5.2.1.2 Structural Dynamics Tasks

Modify completed flutter analysis to include effects of:

(a) Wing control surfaces (rigid).

(b) Flexible fuselage to include realistic wing-fuselage interface (but not to include fuselage aerodynamics).

(c) Empennage unsteady aerodynamics (rigid empennage).

Refine current wing stiffness requirements based on above results.

5.2.1.3 Loads Tasks

Develop new methods and computer programs to handle oblique wing for the following conditions:

(a) Modify existing roll analysis program.

(b) Modify existing VSD routine to perform a supersonic static aerolastic solution for oblique wing panel point flexible airload.

Improve existing NASA subsonic oblique wing routine to include the following:

(a) Input-output format revision.

(b) Symmetric balance equations added.

(c) Capability to include camber.

Define design criteria to include the following:

(a) Maneuvering V-n diagrams.

(b) Gust V-n diagrams.

(c) Pitching acceleration.

(d) Rolling.

(e) Yawing.

(f) Unsymmetrical and lateral gusts.

5.2.1.4 Structures Design Tasks

Investigate allowables of vendor's turntable bearing.

Support wing, fuselage and systems design in iterations of control surface geometry and wing stiffness requirements.

5.2.1.5 Weights Tasks

Support team by supplying weight balance and inertia data.

Construct mass properties data on NFT-8A aircraft.

5.2.1.6 Wing Design Tasks

Support team in iteration of wing geometry and wing control surface geometry.

Support Aerodynamics on wing fairing interface with wing.

5.2.1.7 Fuselage Design Tasks

Support team in iterations of wing location.

Support Aerodynamics on wing fairing interface with fuselage.

Master Dimensions Group generate lofted lines for the wing/wing cavity fairing.

5.2.1.8 Systems Design Tasks

Support team in iterations of control surface geometry by determining applicable actuator placement and control routing.

5.2.1.9 Avionics Tasks

Study the power control servo requirements for the wing control surfaces. Perform preliminary analysis to get a first cut at power servo sizing to meet realistic performance criteria.

Study and define modifications required in the longitudinal and directional control systems to achieve compatibility with the lateral control system.

5.2.2 Phase II: Engineering Design

5.2.2.1 Aerodynamics Tasks

Wing

(a) Establish spanwise and chordwise rigid load distributions for previously established critical design conditions.

(b) Establish wing skew actuator loads over the speed range for operational and holding functions.

Fuselage

(a) Establish aerodynamic load distributions for selected critical design conditions.

(b) Establish pressure differentials for design of the wing/fuselage fairing.

Horizontal Tail

(a) Establish spanwise and chordwise rigid load distributions for previously selected critical design conditions.

(b) Establish actuator hinge moment requirements for the flight design envelope.

Wing Control Surfaces

(a) Establish hinge moment requirements over the normal operating range of speed and deflection for:

(1) Trailing edge flap.
(2) Aileron.

5.2.2.2 Structural Dynamics Tasks

Perform complete flutter analysis for the airplane configuration of Phase I (i.e., flexible wing with rigid control surfaces, flexible fuselage without aerodynamics, rigid empennage with aerodynamics).

Design, fabricate and test flutter models. Models are to include dynamically similar wings to be attached to existing F-8 flutter model flexible fuselage/sting mounts. Tests to be conducted in High Speed Wing Tunnel to Mach 1.4. Test to design points in Para. 5.2.1 above. Wings are to include rigid, adjustable, control surfaces.

5.2.2.3 Loads Tasks

Critical flight loads to be determined for wing, fuselage and tail. At least three sweep angles will be investigated, 0^{o}, 45^{o}, and 60^{o}. For each sweep angle, the following conditions will be studied.

(a) Maneuvering V-n diagrams.

(b) Gust V-n diagrams.

(c) Pitching acceleration.

(d) Rolling conditions.

(e) Yawing conditions.

(f) Unsymmetrical and lateral gusts.

Ground loads and landing response loads (wing down bending) to be determined.

Control surface loads to be determined.

5.2.2.4 Structures Design Tasks

Structures Development (or Structures Design) will support Wing Design and Fuselage Design by detailed stress analysis to ensure that:

Stiffness requirements on wing and attach fitting are met.

The ground rules of Section 3.1.3 regarding static safety and fatigue life are complied with.

To achieve the preceding objectives, stress analysis will be performed as follows:

PART	METHOD
Wing Main Box	Box beam analysis
Wing Fairings	Box beam analysis
Wing Control Surfaces	Box beam analysis
Wing Bearing Fitting	Finite element (NASTRAN)
Fuselage Bearing and Fitting and Adapter	Finite element (NASTRAN)
Existing F-8 Structure	Compare loads to F-8 allowables as reflected in F-8 stress reports and F-8 tests reports

Structural influence coefficients will be produced by finite element modeling (NASTRAN) to support loads in their work on supersonic flexible aerodynamics.

5.2.2.5 Weights Tasks

Weight tracking and reporting.

Update mass properties distributions in support of team.

5.2.2.6 Design Tasks

Engineering drawings of wing (Section 3.3), wing support structure (Section 3.4), and systems (Section 3.5) will be prepared and released to Manufacturing. Military drawing specifications will not apply.

5.2.2.7 Avionics Tasks

Define the stability augmentation and trim system requirements.

Establish the sensor requirements (types and locations) for the flight control system.

Establish the requirements for interfacing systems, such as the electrical and hydraulic systems, and for the feel system.

5.2.3 Phase III: Tooling and Manufacturing

Vought's Production Development Manufacturing organization will have the responsibility for the modification of the two-place F-8 airplane and for the fabrication of the newly designed oblique wing assembly on a one-shot prototype basis. The existing Production Development shops, under the Production Development Director, will be responsible for detail fabrication, tool fabrication, fuselage modification, assembly, and installation operations both at Vought and off-site. The Director of Production Development will report to the Program Management Office. His prime objective is to achieve transformation of engineering data into prototype hardware at the least cost and shortest time span possible.

The F-8 two-place airplane will be modified, both structure and controls, to receive the new oblique wing. The new wing will be of one piece construction with a 50 foot span, welded and bolted steel torque box, aluminum fixed leading and trailing edges, and aluminum constructed ailerons and flaps. It will attach to the fuselage with a large diameter ball bearing turntable and will pivot through $\frac{\pi}{3}$ (60°) by means of a hydraulic actuator controlled from both cockpits.

5.2.3.1 Tooling Policy

Tooling for the wing and for the fuselage modification will be built for a one-shot prototype article. Subassembly fixtures, such as weld tools, will be built by using engineering metal drawings attached to plywood bases utilizing angle iron locators bolted to the base. Necessary form blocks, etc., will be one-shot tools made of less expensive type materials such as compreg and will be fabricated only where necessary to produce a part. Manufacturing Engineering will design and fabricate all required major assembly fixtures, handling slings and required stretch form tools. All other tools found to be necessary will be fabricated by Production Development or off-loaded by Production Development to the tool shops as required. Only those tools built by Manufacturing Engineering will require identification and accountability per standard operating procedures. Tool proofing and/or tool tryout will not be required. Tool Inspection will consist of dimensional inspection only. Mylar layout templates (MLOT) will be supplied in lieu of templates where possible. MLOT's will be supplied by Manufacturing Engineering.

All planning will be accomplished by the Production Development Planning organization.

5.2.3.2 Make-Or-Buy

The large diameter turntable ball bearing will be purchased from Keene Corp., Kaydon Bearing Division, Muskegon, Michigan. The wing pivot and flap hydraulic actuators, with an electric motor and clutch back-up, will be purchased. All raw materials, flex hoses, standard hardware, equipment, and rubber seals will be purchased. All other items are in-house make.

5.2.3.3 Scheduling

The Master Schedule, Figure 5.2-1, is the vehicle for integration of all departmental tasks to ensure program milestones. Upon establishment of the mechanical sequence of assembly by the Manufacturing Plan, each functional area has developed time spans for the accomplishment of its tasks which have been integrated by Scheduling into a Master Schedule. Analysis was then made to disclose any incompatibilities in time phasing which may have existed and negotiations conducted to resolve these differences. After contract go-ahead no change to this Master Schedule will occur without Customer/Vought management approval.

5.2.3.4 Manufacturing

This manufacturing plan has been developed utilizing the total resources and best expertise available at Vought to provide NASA the most cost effective approach to manufacture reliable, quality hardware for the F-8 Oblique Wing program. We will establish a manufacturing program control center and a system of tracking manufacturing performance, both schedule and cost. Total program visibility will be provided of all manufacturing program objectives and initiation of problem corrective action will be accomplished at periodic working level meetings attended by Manufacturing supervision and top management.

Detail parts and assembly fabrication will be the total responsibility of the Production Development Manufacturing organization. However, the entire Manufacturing organization and shops will be available to assist the Production Development organization as required.

5.2.3.5 Wing Fabrication

The wing will be built in one piece having a 50 foot span, Figure 5.2-2.

The wing assembly fixture, Figure 5.2-3, will be a vertical picture frame type fixture with T.E. up and will be designed to build the torque box, fixed trailing edge and fixed leading edge. The fixture will locate the center bearing support ring, torque box spars, torque box ribs, and the upper and lower torque box skins. Attach holes through the torque box skins, spars, and ribs will be drilled using a controlled speed, power feed drill such as a Quackenbush. The torque box skins will be bolted to the structure utilizing nut plates and/or gang channels on one surface. The ribs will be bolted to the spars and the spars bolted to the bearing support ring. Remove the jig locators for the ribs and spars and add locators to hold the fixed trailing edge spars, trailing edge ribs, trailing edge skins, fixed leading edge ribs and skins as shown in Figure 5.2-4. Drill and rivet all parts together. The jig will also contain a removable locator simulating a portion of the fuselage with provisions for attaching all flex hydraulic hoses between the fuselage and wing and an inclinometer for rigging the pivot actuator throws. See Figure 5.2-5.

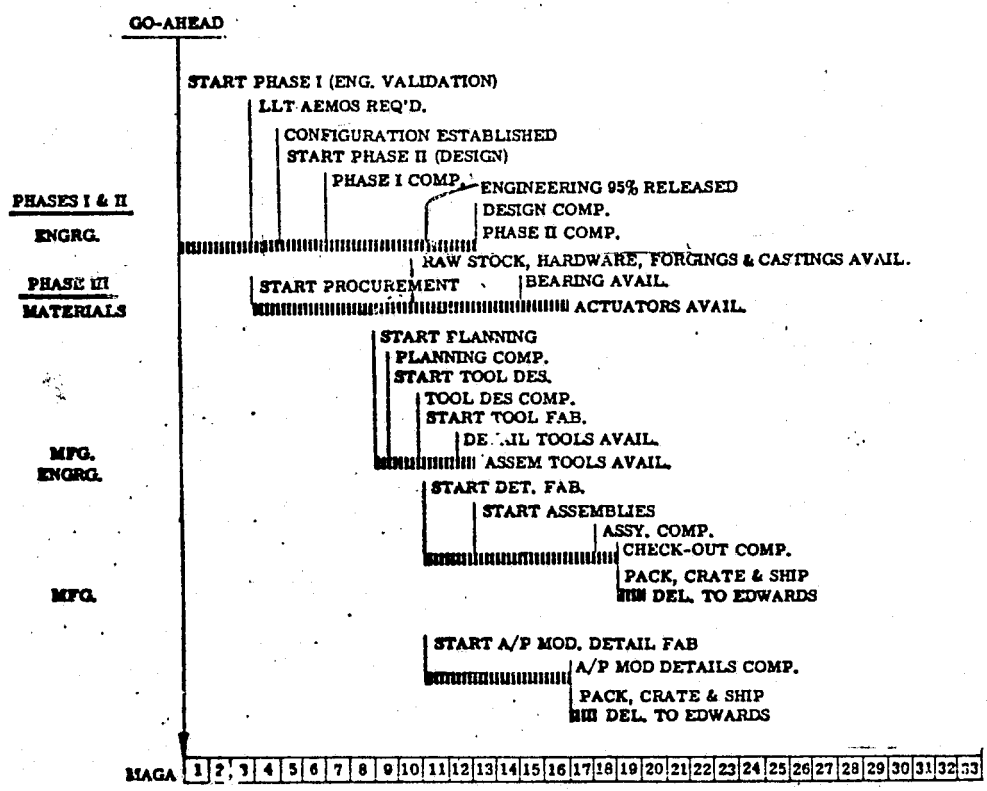

Figure 5.2-1 Fabrication Schedule

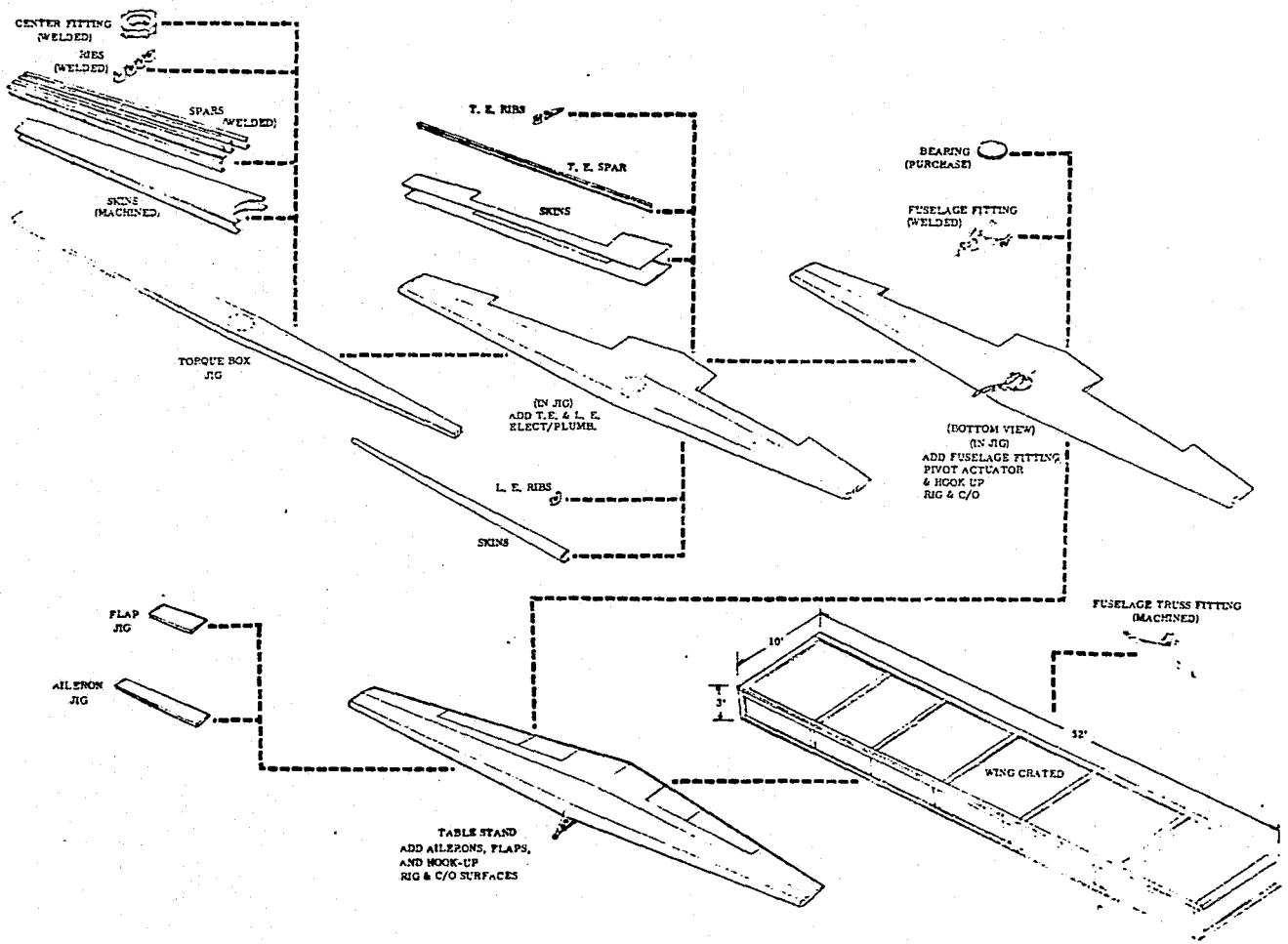

Figure 5.2-2 Wing Fabrication Flow Plan

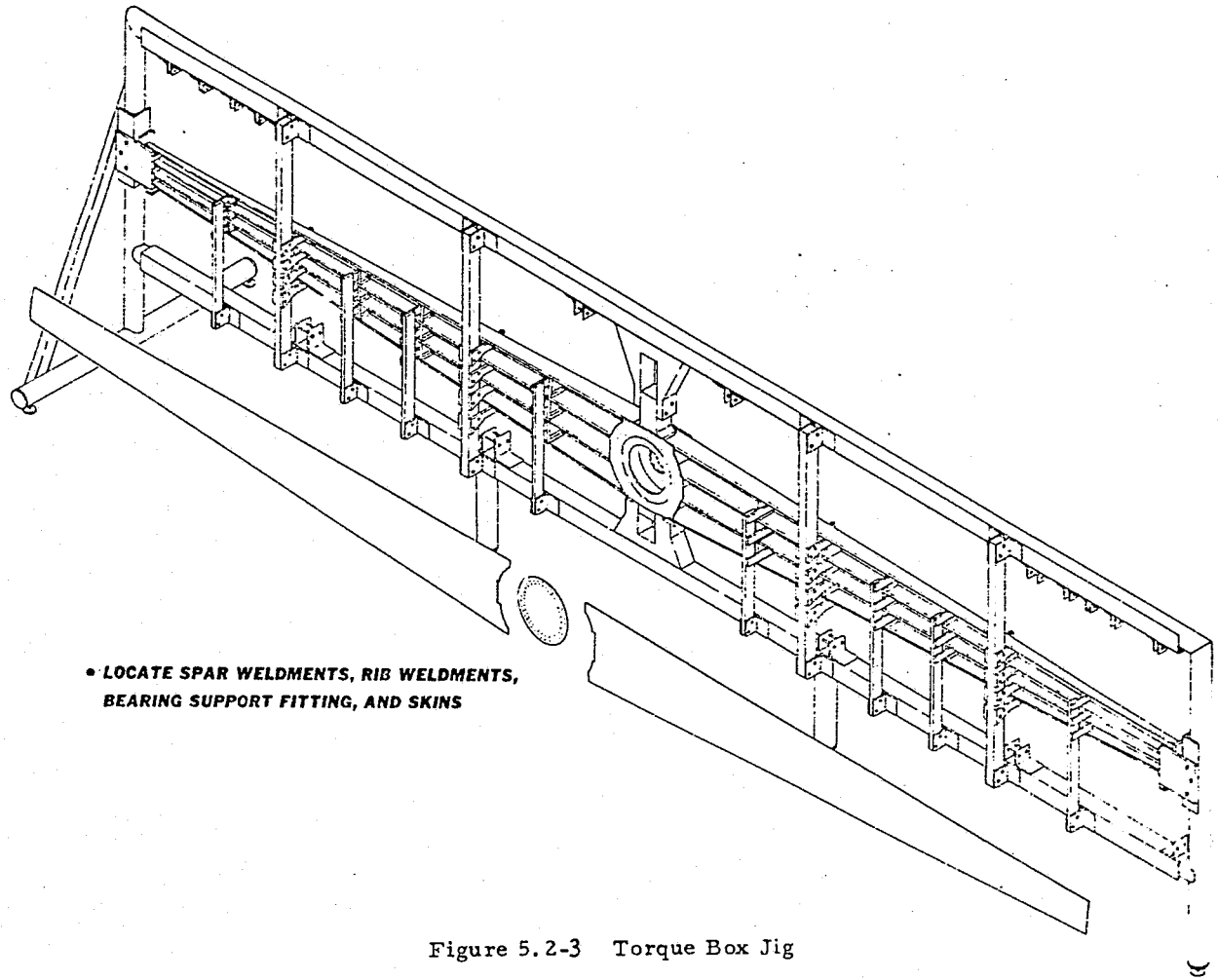

Figure 5.2-3 Torque Box Jig

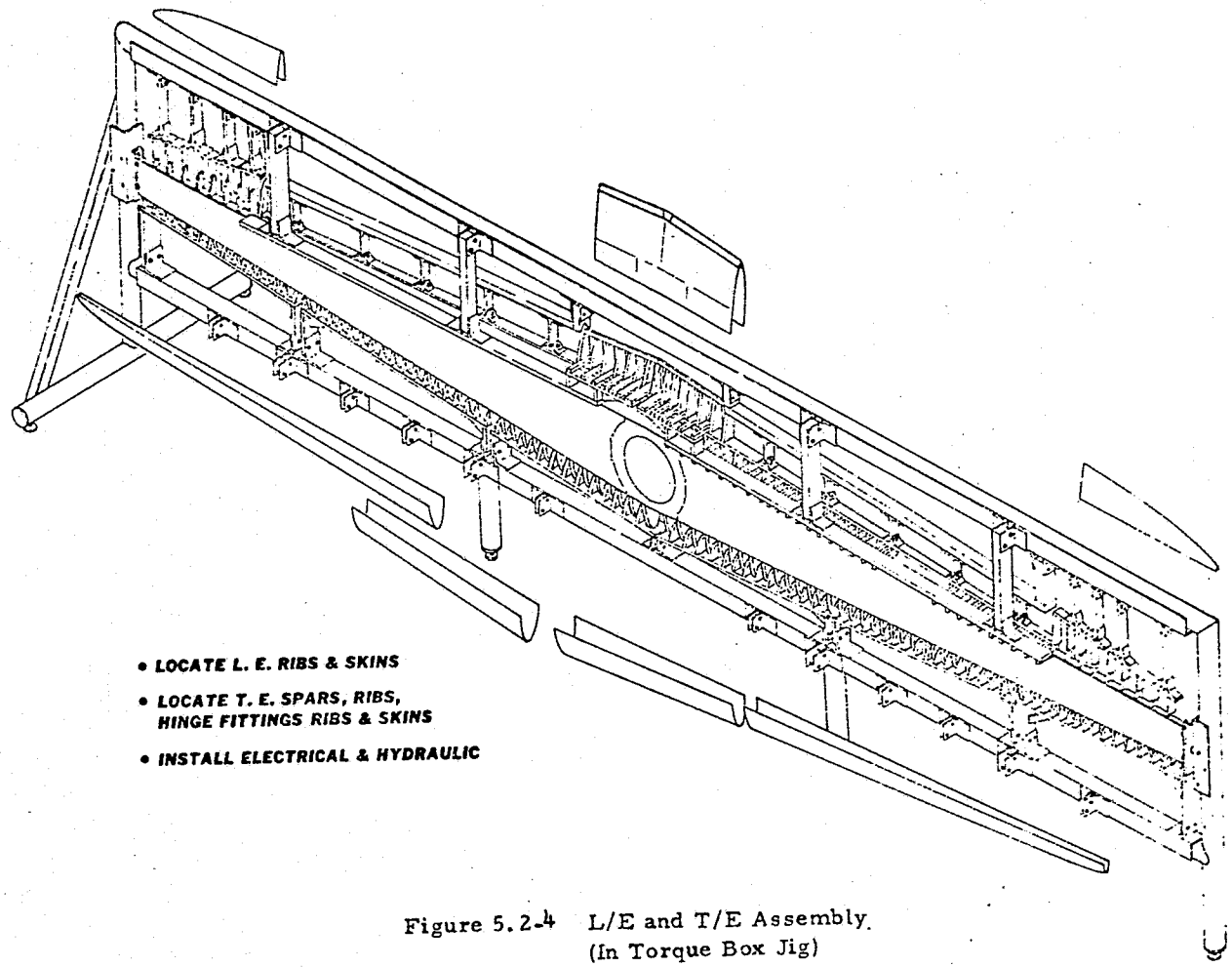

Figure 5.2-4 L/E and T/E Assembly (In Torque Box Jig)

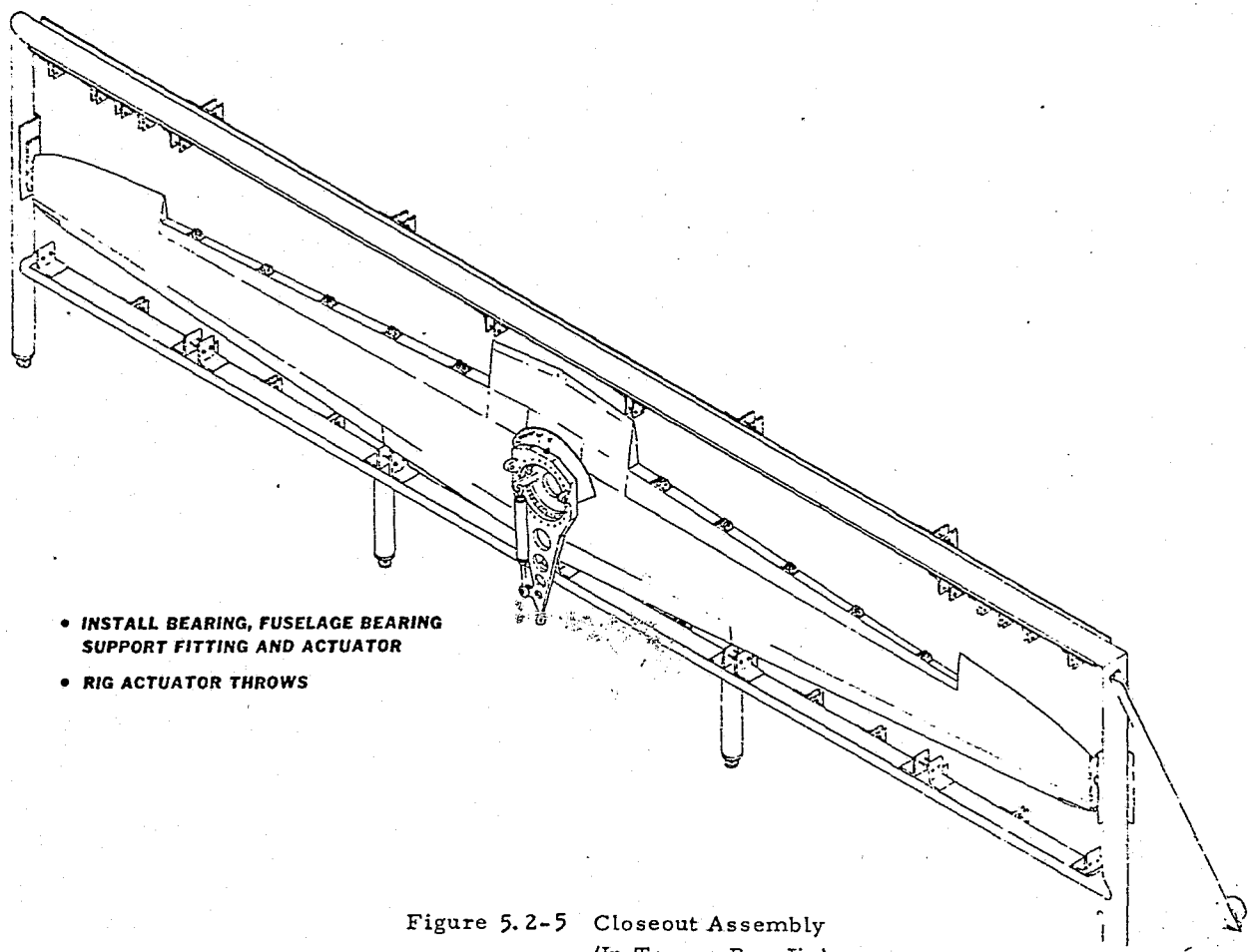

Figure 5.2-5 Closeout Assembly
(In Torque Box Jig)

With the wing assembly still held in the wing assembly jig, install the turntable bearing to the wing bearing fitting. Install the wing support structure assembly to the bearing outer race. Attach the wing pivot actuator to the fitting on the wing support structure and to a fitting bolted onto the bearing inner race. Install the jig detail simulating the fuselage structure on the jig and hook up all flex hydraulic hoses between the jig and the wing. Attach hydraulic power (hand pump) to the pivot actuator, and electrical power to the actuator electric motor. Rig and check out the actuator throw by actuating the turntable on the wing and checking to the inclinometer on the jig. Check out the electrical motor backup of the actuator by disconnecting hydraulic power. Check flex hose clearances as the turntable actuates. Remove flex hoses, hydraulic and electrical connections, and the jig detail. Remove the wing from the jig and place on padded saw-horse stands, Figure 5.2.6.

Install the flaps, ailerons and wing tip and hook-up actuators. Apply hydraulic power to actuators and rig the ailerons and flaps using contour boards. Check flap and aileron travel using inclinometers attached to the wing fixed trailing edges. Fasten the flaps and ailerons in a stationary neutral position and send wing to shipping for packing and crating.

5.2.3.6 Wing Components

Torque Box Skins

Machining will be accomplished on the horizontal five axis profiler.

Torque Box Spars and Ribs

Prototype weld tools required for spars and 12 ribs. Rubber form blocks will be used for the tip ribs.

Access Panel

No fixtures required.

Wing Bearing Fitting

A weld fixture is required.

Fixed Leading Edge

Ribs will be jig located in the wing assembly jig and riveted to the front spar. The rib locators will then be removed, and the skins located to jig contour locators and installed. The skins and ribs will be drilled and riveted together.

Fixed Trailing Edge

Jig locate the spars and ribs in the wing assembly fixture and rivet ribs to spars. Remove the locators and position the skins. Drill and rivet the skins to the ribs and spars. Prior to riveting the trailing

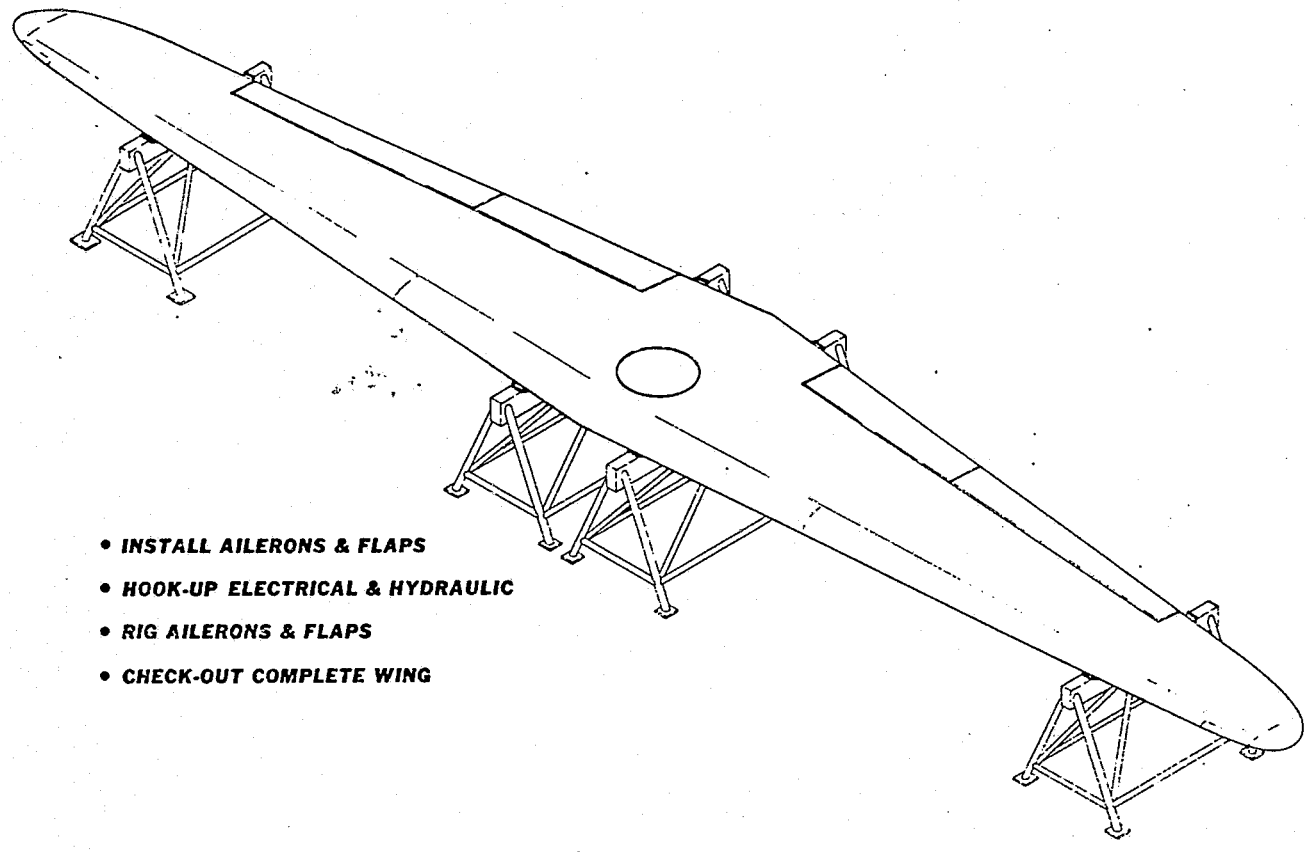

Figure 5.2-6 Pick-up/Rig/Checkout

edge skins to the structure, install the brackets and fittings for the control surfaces actuators, the hydraulic lines and electrical wiring.

Wing Tip

A left hand and a right hand wing tip will be required. It will be a one-piece fiberglass layup.

Wing Support Structure

A weld fixture will be required to control the upper plate of the wing support flat and parallel to the holes in the wing pivot bulkhead lugs and to control the length in relation to the pivot bulkhead lugs. After welding of the bearing support assembly, check the upper surface for flatness. Machining of the upper surface adjacent to the bearing may be required. After checking and/or machining, drill the holes in the lugs for attaching to the wing pivot bulkhead lugs in relation to the upper surface.

Truss Assembly

The tubes will be cut to length and welded and the fittings inserted into the tube ends and welded. No tools are required. The truss fittings will be shipped to Edwards AFB as a loose part and installed to the fuselage bearing support fitting prior to wing installation.

Fuselage to Wing Dorsal Fairing

The fairings will be made of 1 mm (0.04 in.) thick fiberglass in two pieces, split around the fuselage contour (station plane) at approximately the center of the bearing turntable.

Aileron Assembly (1 LH and 1 RH Required)

A left hand and a right hand assembly jig will be required. The aileron will contain a brake formed sheet metal buildup jig located spar, three machined hinge fittings bolted to the spar, formed sheet metal jig located ribs, an upper and a lower flat aluminum skin with a filler between the skins at the trailing edge. A roll formed leading edge skin will be attached to the spar and supported by formed aluminum jig located gussets.

Flaps Assembly (1 LH and 1 RH Required)

A left hand and a right hand assembly jig will be required. The flap will contain a 1.3 mm (0.05 in.) 2024 aluminum brake formed built up spar with two machined hinge fittings bolted to the spar. Formed aluminum ribs and the spar will be jig located. The trailing edge skin will be a one piece brake formed wrap around skin attached with standard flush and blind rivets. The leading edge skin will be roll formed 1.3 mm (0.05 in) 2024 aluminum attached to the spar and rubber formed L.E. jig located gussets.

5.2.3.7 Packing and Shipping

The wing assembly with the ailerons and flaps installed will be packed, along with all other loose components, in a wooden crate approximately 3m (10 ft) wide by 16m (52 ft) long by 1m (3 ft) deep with the wing in flight position and protected from shipping damage. Shipment to Edwards AFB will be by rail.

5.2.3.8 Fuselage Modification

The modification to the F-8 two-place airplane, Figure 5.2-7 Flow Plan, will be accomplished at Edwards AFB by Vought personnel. All new parts/assemblies required for the modification will be made at Vought and shipped as a kit to Edwards AFB. Hand tools required will be supplied by each individual mechanic. Vought assumes that portable/durable tools, electrical tools, tube benders, etc., can be made available by NASA. Perishable tools will be supplied by Vought.

Upon receipt of the airplane at Edwards, Vought personnel will:

Drain and purge

Disarm

Remove the wing (storage area will be required).

Remove the wing incidence hydraulic actuator and the two wing incidence stop fittings on each side of the wing cavity at F.S. 397.5. (Ref. CV15-410563-1 LH and CV15-410658-1 RH.) Replace the stop fittings with two new fittings similar in design except beefier and with double lugs for bolting on the truss fitting. Attachments for these fittings penetrate into a fuel cell cavity which must be sealed after installation.

Deactivate the wing hinge pin lock, wing fold, wing down lock, wing incidence, emergency wing incidence/droop, and the wing leading edge droop control systems.

Modify the existing rudder control system.

Install new wing controls systems for a two-position LH and RH trailing edge flap and an F-8 type LH and RH drooping aileron, and modify the existing lateral control system in fuselage.

Install new aileron - rudder - wing position with UHT - wing position interconnect provisions.

Remove the two wing island fairings on the top-side of the fuselage and patch the opening with an aluminum sheet metal skin having four (4) formed stiffeners, two (2) on each side.

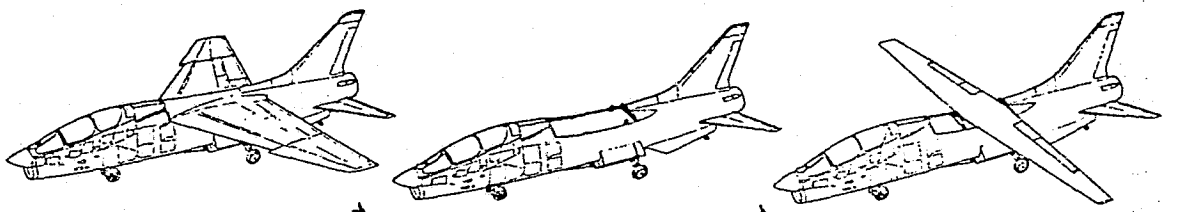

- RECEIVE F-8 2-PLACE AIRPLANE
- DRAIN – PURGE – DISARM
- REMOVE WING
- DEACTIVATE SYSTEMS
  - HINGEPIN LOCK
  - WING FOLD
  - WING DOWN LOCK
  - WING INCIDENCE
- MODIFY SYSTEMS
  - RUDDER CONTROL SYSTEM
  - FUSELAGE LATERAL CONTROL SYSTEM
  - WING SURFACE CONTROLS
  - AUTOMATIC AILERON – RUDDER – WING POSITION INTERCONNECT
  - UHT – WING POSITION INTERCONNECT
  - WING DOWN LOCK CONTROL SYSTEM INTO FLAP CONTROL SYSTEM
  - WING INCIDENCE CONTROL SYSTEM INTO WING PIVOT CONTROL SYSTEM

- REMOVE WING ISLAND FAIRINGS
- INSTALL SKIN PATCH BOTH SIDES
- REPLACE WING INCIDENCE STOP FITTINGS (L AND R) WITH NEW FITTINGS

- INSTALL WING (WITH FUSELAGE TRUSS FITTING)
- HOOKUP WIRING
- HOOKUP TUBING
- INSTALL FAIRING

Figure 5.2-7 Fuselage Modification F-8 Two Place Airplane Flow Plan (VSD Modify At Edwards AFB)

Modify the existing wing down lock and wing incidence control systems into flap and wing pivot control systems respectively. New cockpit control handles will be required.

NOTE: All wiring and tubing changes required will be accomplished by hand wiring and plumbing to fit on the airplane.

5.2.3.9 Wing Installation

Vought personnel at Edwards will install the wing to the F-8 two-place fuselage by pinning the fuselage bearing support fitting to the fuselage wing pivot bulkhead lugs. Place wing jacks on each side of the fuselage under the L.E. of the wing for support. These wing jacks must have a padded 2 x 4 wooden cradle between the wing surface and the jacks. Install "A" frame truss fitting to the forward arm of the wing support structure by bolting through the spherical bearing and bolt the two new fuselage attach fittings to the truss fitting. Jack the wing up or down as required to optically locate the forward arm on required plane. Using flat and/or tapered shims (make on assembly) as required, attach the two new fuselage fittings on either side of the wing cavity by bolting to the fuselage longeron using shims for alignment. Reseal the fitting bolts in the fuel cell cavity. Remove the wing jacks. Make all hydraulic and electrical connections. Install fairings between fuselage and wing. Rig and operate all control surfaces and wing pivot actuation. Turn airplane over to NASA for flight test.

5.3 Program Schedule

The schedule for the three phase program is presented in Figure 5.3-1. A twenty-one month program is proposed, with a go-ahead date of 1 October 1977. All hardware will be delivered to NASA-FRC by the end of the nineteenth month, with installation and system checkout by the end of the twenty-first month.

The three program phases are presented to show overlapping activities necessary to provide program continuity, as each phase is dependent upon successful completion of the preceeding phase. Additional details presented in Figure 5.2-1 show anticipated long lead time materials requirements, tooling and manufacturing tasks and hardware completion and delivery dates (months after go-ahead).

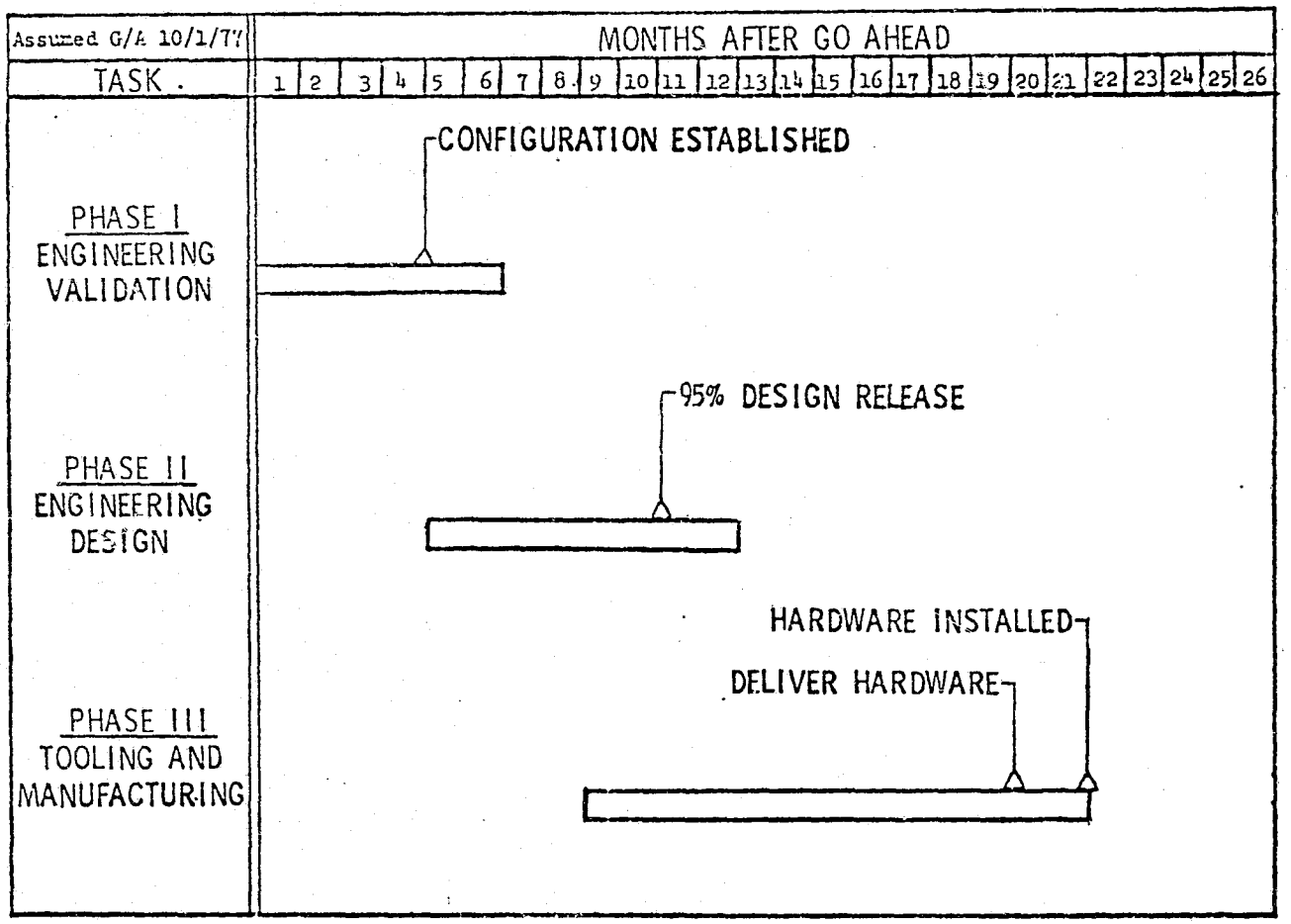

FIGURE 5.3-1 PROGRAM SCHEDULE

6.0 CONCLUSIONS

The oblique wing concept on an F-8 aircraft is structurally feasible. The technology required to design and fabricate the wing and pivot hardware is within the state-of-the-art.

The turntable pivot concept utilizing a large diameter steel bearing, readily available in industry, is the recommended concept when compared initially to a cantilivered post concept. The cantilivered post concept would require numerous highly loaded machined parts, new and unproven designs requiring costly structural testing, and would provide very limited access for hydraulic lines and control mechanisms.

The F-8 aircraft can readily be modified to accept the fuselage pivot support structure without major fuselage modification. The cavity available when the regular F-8 wing and mechanisms are removed provides adequate space for the new structure and control mechanisms.

A study program to determine the flying qualities of the F-8 with the wing and pivot hardware concept should be conducted as the next step of the total oblique wing program. This study program is described as Phase I and would be required prior to the initiation of the design effort. The design effort is described as Phase II, with the tooling and manufacturing effort described as Phase III. The Phase III effort would be concluded upon the installation and initial functional check-out of the airplane at the NASA-FRC facility.

The ground test and flight test program for the F-8 aircraft with an oblique wing was not defined or priced in this study program. This demonstration program should be considered as Phase IV and should be undertaken as a joint NASA-Contractor Program in order to provide maximum benefits to government and industry.

APPENDIX A

LOADS AND STRESS DISTRIBUTIONS FOR THE n_z=3 CONDITION

This appendix contains the data displayed in Figures 4.4-1, 4.4-2, and 4.4-5 through 4.4-12 in the form of numerical tables. The figures are part of Section 4.4 of the report.

TABLE A-1 - EI Distribution

Wing y		EI	
m	(in.)	kg m^2	(lb in^2)
-7.62	(-300.00)	.172E+05	(.588E+08)
-6.86	(-270.00)	.547E+05	(.187E+09)
-6.10	(-240.00)	.131E+06	(.448E+09)
-5.33	(-210.00)	.265E+06	(.907E+09)
-4.57	(-180.00)	.481E+06	(.164E+10)
-3.81	(-150.00)	.806E+06	(.275E+10)
-3.05	(-120.00)	.127E+07	(.434E+10)
-2.29	(-90.00)	.191E+07	(.652E+10)
-1.52	(-60.00)	.276E+07	(.942E+10)
-.76	(-30.00)	.386E+07	(.132E+11)
0.00	(0.00)	.527E+07	(.180E+11)
.76	(30.00)	.386E+07	(.132E+11)
1.52	(60.00)	.276E+07	(.942E+10)
2.29	(90.00)	.191E+07	(.652E+10)
3.05	(120.00)	.127E+07	(.434E+10)
3.81	(150.00)	.806E+06	(.275E+10)
4.57	(180.00)	.481E+06	(.164E+10)
5.33	(210.00)	.265E+06	(.907E+09)
6.10	(240.00)	.131E+06	(.448E+09)
6.86	(270.00)	.547E+05	(.187E+09)
7.62	(300.00)	.172E+05	(.588E+08)

(See Figure 4.4-1)

TABLE A-2 - GJ Distribution

Wing y		GJ	
m	(in.)	kg m^2	(lb in^2)
-7.62	(-300.00)	.198E+05	(.676E+08)
-6.86	(-270.00)	.629E+05	(.215E+09)
-6.10	(-240.00)	.151E+06	(.515E+09)
-5.33	(-210.00)	.305E+06	(.104E+10)
-4.57	(-180.00)	.554E+06	(.189E+10)
-3.81	(-150.00)	.926E+06	(.317E+10)
-3.05	(-120.00)	.146E+07	(.499E+10)
-2.29	(-90.00)	.219E+07	(.749E+10)
-1.52	(-60.00)	.317E+07	(.108E+11)
-.76	(-30.00)	.444E+07	(.152E+11)
0.00	(0.00)	.606E+07	(.207E+11)
.76	(30.00)	.444E+07	(.152E+11)
1.52	(60.00)	.317E+07	(.108E+11)
2.29	(90.00)	.219E+07	(.749E+10)
3.05	(120.00)	.146E+07	(.499E+10)
3.81	(150.00)	.926E+06	(.317E+10)
4.57	(180.00)	.554E+06	(.189E+10)
5.33	(210.00)	.305E+06	(.104E+10)
6.10	(240.00)	.151E+06	(.515E+09)
6.86	(270.00)	.629E+05	(.215E+09)
7.62	(300.00)	.198E+05	(.676E+08)

(See Figure 4.4-2)

TABLE A-3 - Distribution of Net Running Load

(Design Limit Load)

Wing y		Local Load	
m	(in.)	kg/m	(lb/in)
-7.62	(-300.00)	.632E+03	(.354E+02)
-6.86	(-270.00)	.168E+04	(.939E+02)
-6.10	(-240.00)	.214E+04	(.120E+03)
-5.33	(-210.00)	.242E+04	(.135E+03)
-4.57	(-180.00)	.264E+04	(.148E+03)
-3.81	(-150.00)	.276E+04	(.155E+03)
-3.05	(-120.00)	.285E+04	(.160E+03)
-2.29	(-90.00)	.294E+04	(.165E+03)
-1.52	(-60.00)	.291E+04	(.163E+03)
-.76	(-30.00)	.258E+04	(.145E+03)
0.00	(0.00)	.217E+04	(.122E+03)
.76	(30.00)	.235E+04	(.132E+03)
1.52	(60.00)	.254E+04	(.142E+03)
2.29	(90.00)	.258E+04	(.145E+03)
3.05	(120.00)	.256E+04	(.144E+03)
3.81	(150.00)	.235E+04	(.132E+03)
4.57	(180.00)	.214E+04	(.120E+03)
5.33	(210.00)	.193E+04	(.108E+03)
6.10	(240.00)	.168E+04	(.939E+02)
6.86	(270.00)	.123E+04	(.686E+02)
7.62	(300.00)	-.610E+02	(-.342E+01)

(See Figure 4.4-5)

TABLE A-4 - Shear Distribution

(Design Limit Load)

Wing y		Shear	
m	(in.)	kg	lb
-7.62	(-300.00)	-.190E-05	(-.419E-05)
-6.86	(-270.00)	.885E+03	(.195E+04)
-6.10	(-240.00)	.237E+04	(.523E+04)
-5.33	(-210.00)	.412E+04	(.907E+04)
-4.57	(-180.00)	.605E+04	(.133E+05)
-3.81	(-150.00)	.811E+04	(.179E+05)
-3.05	(-120.00)	.102E+05	(.226E+05)
-2.29	(-90.00)	.125E+05	(.275E+05)
-1.52	(-60.00)	.147E+05	(.324E+05)
-.76	(-30.00)	.168E+05	(.371E+05)
0.00	(0.00)	.186E+05	(.410E+05)
.76	(30.00)	-.140E+05	(-.309E+05)
1.52	(60.00)	-.121E+05	(-.267E+05)
2.29	(90.00)	-.102E+05	(-.224E+05)
3.05	(120.00)	-.819E+04	(-.181E+05)
3.81	(150.00)	-.632E+04	(-.139E+05)
4.57	(180.00)	-.461E+04	(-.102E+05)
5.33	(210.00)	-.305E+04	(-.673E+04)
6.10	(240.00)	-.167E+04	(-.369E+04)
6.86	(270.00)	-.544E+03	(-.120E+04)
7.62	(300.00)	-.688E-06	(-.152E-05)

(See Figure 4.4-6)

TABLE A-5 - Shear Flow

(Design Limit Load)

Wing y		Shear Flow	
m	(in.)	kg/m	(lb/in)
-7.62	(-300.00)	-.452E-04	(-.253E-05)
-6.86	(-270.00)	.141E+05	(.792E+03)
-6.10	(-240.00)	.285E+05	(.159E+04)
-5.33	(-210.00)	.396E+05	(.222E+04)
-4.57	(-180.00)	.485E+05	(.272E+04)
-3.81	(-150.00)	.558E+05	(.313E+04)
-3.05	(-120.00)	.618E+05	(.346E+04)
-2.29	(-90.00)	.668E+05	(.374E+04)
-1.52	(-60.00)	.709E+05	(.397E+04)
-.76	(-30.00)	.738E+05	(.413E+04)
0.00	(0.00)	.749E+05	(.419E+04)
.76	(30.00)	-.615E+05	(-.344E+04)
1.52	(60.00)	-.585E+05	(-.328E+04)
2.29	(90.00)	-.545E+05	(-.305E+04)
3.05	(120.00)	-.494E+05	(-.277E+04)
3.81	(150.00)	-.435E+05	(-.244E+04)
4.57	(180.00)	-.370E+05	(-.207E+04)
5.33	(210.00)	-.294E+05	(-.165E+04)
6.10	(240.00)	-.201E+05	(-.113E+04)
6.86	(270.00)	-.868E+04	(-.486E+03)
7.62	(300.00)	-.164E-04	(-.918E-06)

(See Figure 4.4-7)

TABLE A-6 - Bending Distribution

(Design Limit Load)

Wing 2y/b	Bending Moment	
	m kg	(in lb)
-1.00	0.	(0.)
-.90	.279E+03	(.242E+05)
-.80	.150E+04	(.130E+06)
-.70	.396E+04	(.343E+06)
-.60	.782E+04	(.679E+06)
-.50	.132E+05	(.115E+07)
-.40	.202E+05	(.175E+07)
-.30	.288E+05	(.250E+07)
-.20	.392E+05	(.340E+07)
-.10	.512E+05	(.444E+07)
-.00	.639E+05	(.554E+07)
.00	.521E+05	(.453E+07)
.10	.408E+05	(.354E+07)
.20	.308E+05	(.258E+07)
.30	.223E+05	(.194E+07)
.40	.153E+05	(.133E+07)
.50	.982E+04	(.853E+06)
.60	.567E+04	(.492E+06)
.70	.276E+04	(.240E+06)
.80	.973E+03	(.844E+05)
.90	.150E+03	(.130E+05)
1.00	0.	(0.)

(See Figure 4.4-8)

TABLE A-7 - Spanwise Distribution of Mc/I

(Design Limit Stress)

Wing 2y/b	Mc/I	
	kg/m^2	(psi)
-1.00	0.	(0.)
-.90	.180E+06	(.256E+03)
-.80	.946E+06	(.135E+04)
-.70	.244E+07	(.347E+04)
-.60	.472E+07	(.671E+04)
-.50	.779E+07	(.111E+05)
-.40	.117E+08	(.166E+05)
-.30	.163E+08	(.232E+05)
-.20	.216E+08	(.308E+05)
-.10	.277E+08	(.394E+05)
-.00	.338E+08	(.480E+05)
.00	.276E+08	(.392E+05)
.10	.221E+08	(.314E+05)
.20	.170E+08	(.242E+05)
.30	.126E+08	(.179E+05)
.40	.886E+07	(.126E+05)
.50	.580E+07	(.825E+04)
.60	.342E+07	(.487E+04)
.70	.171E+07	(.243E+04)
.80	.615E+06	(.874E+03)
.90	.972E+05	(.138E+03)
1.00	0.	(0.)

(See Figure 4.4-9)

TABLE A-8 - Running Torque

(Design Limit Load)

Wing y		Running Torque	
m	(in.)	kg	(in lb/in)
-7.62	(-300.00)	.255E+03	(.562E+03)
-6.86	(-270.00)	.626E+03	(.138E+04)
-6.10	(-240.00)	.948E+03	(.209E+04)
-5.33	(-210.00)	.136E+04	(.299E+04)
-4.57	(-180.00)	.160E+04	(.354E+04)
-3.81	(-150.00)	.898E+03	(.198E+04)
-3.05	(-120.00)	.387E+03	(.853E+03)
-2.29	(-90.00)	.475E+03	(.105E+04)
-1.52	(-60.00)	.534E+03	(.118E+04)
-.76	(-30.00)	.744E+03	(.164E+04)
0.00	(0.00)	.118E+04	(.259E+04)
.76	(30.00)	.108E+04	(.239E+04)
1.52	(60.00)	.505E+03	(.111E+04)
2.29	(90.00)	-.859E+03	(-.189E+04)
3.05	(120.00)	-.197E+04	(-.434E+04)
3.81	(150.00)	-.119E+04	(-.263E+04)
4.57	(180.00)	-.610E+03	(-.134E+04)
5.33	(210.00)	-.298E+03	(-.658E+03)
6.10	(240.00)	-.696E+02	(-.153E+03)
6.86	(270.00)	.171E+03	(.377E+03)
7.62	(300.00)	-.590E+01	(-.130E+02)

(See Figure 4.4-10)

TABLE A-9 - Torsion

(Design Limit Load)

Wing 2y/b	Torque	
	m kg	(in lb)
-1.00	0.	(0.)
-.90	.326E+03	(.283E+05)
-.80	.927E+03	(.804E+05)
-.70	.180E+04	(.156E+06)
-.60	.296E+04	(.257E+06)
-.50	.392E+04	(.340E+06)
-.40	.475E+04	(.378E+06)
-.30	.467E+04	(.406E+06)
-.20	.506E+04	(.439E+06)
-.10	.552E+04	(.479E+06)
-.00	.626E+04	(.544E+06)
.00	.203E+04	(.176E+06)
.10	.292E+04	(.253E+06)
.20	.360E+04	(.313E+06)
.30	.343E+04	(.298E+06)
.40	.219E+04	(.190E+06)
.50	.976E+03	(.847E+05)
.60	.320E+03	(.278E+05)
.70	-.163E+02	(-.141E+04)
.80	-.156E+03	(-.135E+05)
.90	-.115E+03	(-.994E+04)
1.00	0.	(0.)

(See Figure 4.4-11)

TABLE A-10 - Spanwise Distribution of Tr/J

(Design Limit Stress)

Wing 2y/b	Shear Stress	
	kg/m^2	(psi)
-1.00	0.	(0.)
-.90	.588E+06	(.836E+03)
-.80	.163E+07	(.232E+04)
-.70	.309E+07	(.439E+04)
-.60	.497E+07	(.707E+04)
-.50	.641E+07	(.912E+04)
-.40	.696E+07	(.989E+04)
-.30	.729E+07	(.104E+05)
-.20	.771E+07	(.110E+05)
-.10	.822E+07	(.117E+05)
-.00	.911E+07	(.130E+05)
.00	.295E+07	(.419E+04)
.10	.435E+07	(.618E+04)
.20	.549E+07	(.781E+04)
.30	.536E+07	(.762E+04)
.40	.350E+07	(.498E+04)
.50	.160E+07	(.227E+04)
.60	.537E+06	(.764E+03)
.70	-.279E+05	(-.397E+02)
.80	-.275E+06	(-.391E+03)
.90	-.207E+06	(-.294E+03)
1.00	0.	(0.)

(See Figure 4.4-12)

REFERENCES

1. Keene Corporation, Kaydon Bearing Division; Kaydon Standard Bearing Selection Guide, Bulletin #304, May 1975.

2. Jones, R. T. and Nisbet, J. W.; Aeroelastic Characteristics of an Oblique Wing, to be published.

3. Weisshaar, Terrence A. and Ashley, Holt; Static Aeroelasticity and the Flying Wing, Revisited. J. of Aircraft, Vol. 11, No. 11, 1974, pp 718-720.

4. Weisshaar, Terrence A.; The AIRLOD Computer Code, Static Aeroelastic Characteristics of Oblique Swept Wings. Virginia Polytechnic Institute.

5. Military Standarization Handbook, Metallic Materials and Elements for Aerospace Vehicle Structures (MIL-HDBK-5B), 1971.

6. Roark, Raymond J.; Formulas for Stress and Strain. Fourth Ed. McGraw Hill Book Co., 1965.

EXHIBIT A

ENGINEERING DRAWINGS

TITLE	VSD NUMBER
General Arrangement, Basic F-8, Oblique Wing Study	78-002817 Sheet 1 and 2
General Arrangement, Two-Place F-8, Oblique Wing Study	78-002818 Sheet 1 and 2
Wing Basic Geometry Data, Oblique Wing Study	78-002819
Wing Structural Arrangement, Oblique Wing Study	78-002820
Support Assembly, Oblique Wing Study, F-8 2 Place	78-002821
NTF-8A Control System Rework, Fuselage Mid-Section and Wing, Oblique Wing Study	78-002822